5 Results and Discussion

5.1 Preformulation studies

5.1.1 Analytical method development for estimation of TNZ by UV-Visible spectroscopy

5.1.1.1 Identification of λ_{max}

TNZ at a concentration of 8 µg/ml was scanned in double beam UV-Visible spectrophotometer in water and McIlvaine buffer (pH 6.6) between the scanning range of 200-400 nm to determine the λ_{max}. UV-Visible spectrums of TNZ in water and McIlvaine buffer are depicted in Figure 5.1 and Figure 5.2, respectively. TNZ showed two absorption maxima at 225 nm and 319 nm, in both the media. The absorption maximum at 319 nm was distinctly separated from the other with comparatively high intensity, and hence, it was chosen for the TNZ estimation during further studies.

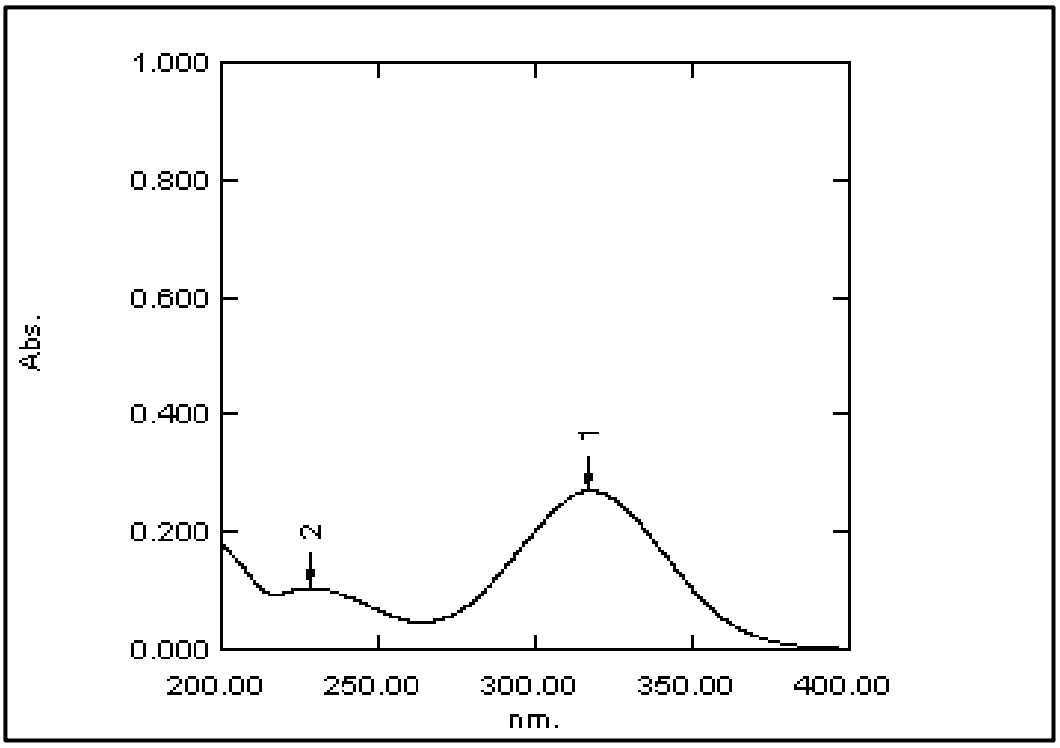

Figure 5.1 UV-Visible absorbance spectra of pure TNZ in water

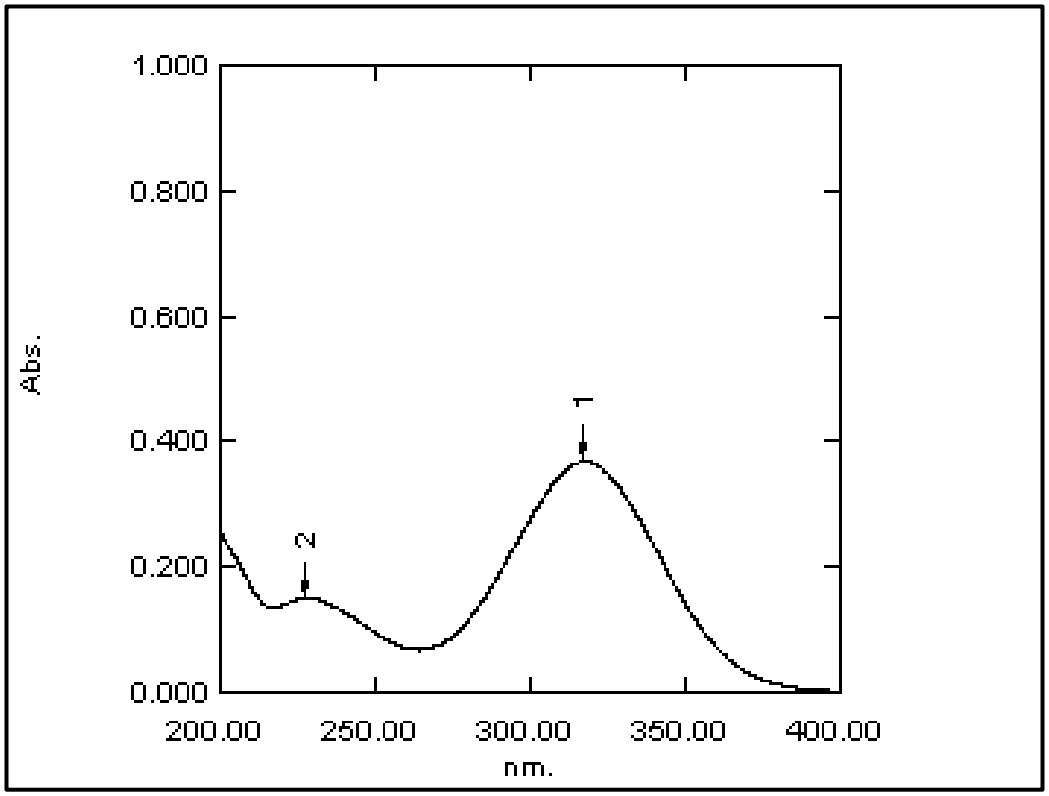

Figure 5.2 UV-Visible absorbance spectra of pure TNZ in McIlvaine buffer (pH 6.6)

5.1.1.2 Calibration curve

Standard calibration curve of TNZ in water and McIlvaine buffer was prepared by plotting of TNZ concentrations versus absorbance at λ_{max} (319 nm) and shown in Figure 5.3 and Figure 5.4, respectively. Beer-Lambert's law was found to be followed in the concentration range of 4-20 µg/ml in water and McIlvaine buffer. All the calibration curves were obtained as straight lines with high regression coefficients (> 0.99).

The straight line regression equation obtained by linear regression analysis can be represented as $y = 0.0553X - 0.003$ and $y = 0.0551X - 0.0041$ for water and McIlvaine buffer, respectively. The value of regression coefficient (R^2) was found to be more than 0.99 in both media, indicating the presence of high linearity between absorbance and concentration in the range of 4-20 µg/ml.

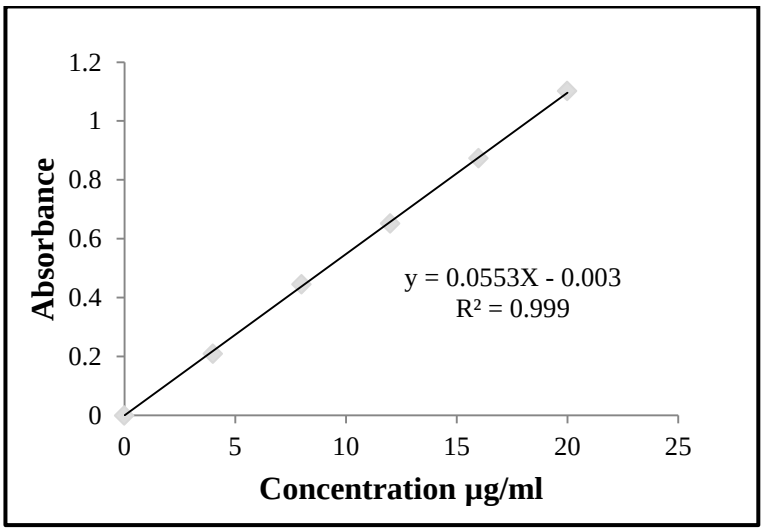

Figure 5.3 Calibration curve of TNZ by UV-Visible spectroscopy in water

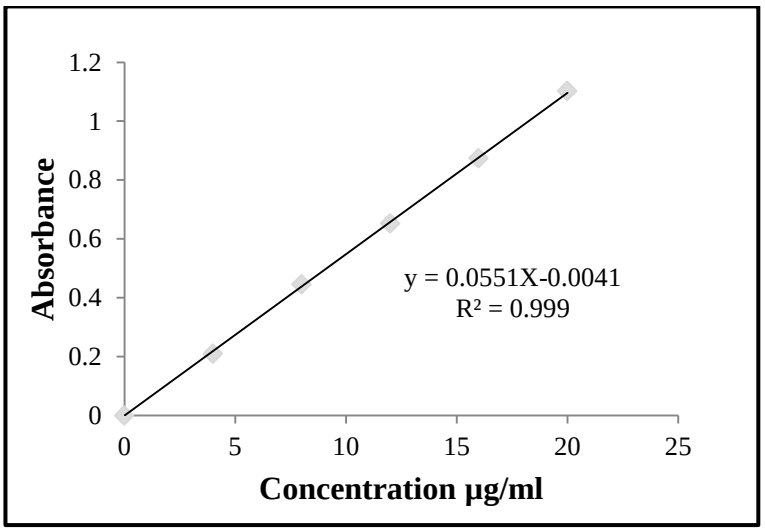

Figure 5.4 Calibration curve of TNZ by UV-Visible spectroscopy in McIlvaine buffer pH 6.6

For accurate determination of the developed method for the estimation of TNZ in water and McIlvaine buffer recovery study was performed. The variability associated with the developed analytical method in different media was measured by determining precision (intra-day and inter-day). Three different concentrations of TNZ namely low (4 µg/ml), medium (8 µg/ml) and high (12 µg/ml) were selected. Each sample was scanned in UV-Visible spectrophotometer at the same day (n = 3) and over three consecutive days (n = 3) to access intra-day and inter-day variation, respectively. The results of intra-day and inter-day variability in water, as well as McIlvaine buffer, are summarized in Table

5.1 and Table 5.2, respectively. Results were within the specified limits of less than 15% for all the three different concentrations [Bressolle et al. 1996, Shah et al. 1991].

The consistency of results on the same day as well as on different days confirmed that the developed analytical method is accurate and reproducible for the measurement of TNZ in water and McIlvaine buffer. The low variability in the results indicated the suitability of the analytical method for consistent and efficient analysis during the *in vitro* studies in different media, water and McIlvaine buffer. LOD and LOQ for the developed analytical method in water were found to be 0.25 µg/ml and 0.76 µg/ml, respectively. Whereas, LOD and LOQ for the developed analytical method in McIlvaine buffer pH 6.6 were found to be 0.19 µg/ml and 0.58 µg/ml, respectively.

Table 5.1 The intra-day and inter-day variability of the analytical method in water

Actual Concentration (µg/ml)	4	8	12
	Intra-day variation		
*Calculated Concentration	3.94±0.064	7.75±0.04	11.68±0.028
*Recovery (%)	98.34±1.57	95.71±0.78	96.41±0.73
% RSD	1.274	0.653	0.697
% Bias	-1.64	-3.715	-3.417
	Inter-day variation		
*Calculated Concentration	3.96±0.088	7.83±0.62	11.94±0.228
*Recovery (%)	98.59±1.87	98.61±1.78	98.68±1.75
% RSD	2.34	1.85	1.79
% Bias	-1.45	-1.28	-1.36

*Values represent mean±SD; n = 3

Table 5.2 The intra-day and inter-day variability of the analytical method in McIlvaine buffer (pH 6.6)

Actual Concentration (µg/ml)	4	8	12
Intra-day variation			
*Calculated Concentration	4.06±0.088	8.19±0.062	12.04±0.228
*Recovery (%)	100.82±0.57	101.17±1.78	100.64±0.80
% RSD	2.16	2.53	1.05
% Bias	0.82	1.17	0.64
Inter-day variation			
*Calculated Concentration	4.18±0.168	8.13±02.172	12.14±0.225
*Recovery (%)	104.06±0.57	102.12±1.78	101.24±0.80
% RSD	4.13	2.61	2.67
% Bias	4.06	2.12	1.24

*Values represent mean±SD; n = 3

5.1.1.3 Solubility Studies

Solubility was determined by shake-flask-method. The results of solubility of TNZ in water, as well as McIlvaine buffer, are summarized in Table 5.3.

Table 5.3 Solubility of TNZ in different medium

S. No.	Solvent system	TNZ (mean±SD, n = 3) (mg/ml)
1	Water	11.5±0.52
2	McIlvaine Buffer	13.4±0.35

Formulation development, *in vitro* and *in vivo* characterizations of different nanofiber-based drug delivery systems

In the current research work, three novel drug delivery formulations loaded with TNZ were developed for the treatment of periodontitis. TNZ encapsulated PCL electrospun nanofiber membrane (TNZ-PCLNF), TNZ loaded GE/PCL hybrid nanofiber membrane (TNZ-PGHNF), and TNZ loaded CH/PCL hybrid nanofiber membrane (TNZ-PCHNF)

were developed and extensively evaluated for *in vitro* as well as *in vivo* characterizations. The study was divided into three parts as stated below:

5.2 Preparation, optimization, *in vitro* and *in vivo* characterization of TNZ encapsulated PCL nanofiber membrane (TNZ-PCLNF)

For the preparation of PCL, nanofiber membrane electrospinning technique was used because it is a simple, continuous and reproducible method for the preparation of nanofiber. For intermediate polarity of solvent which produces stable tailor cone, continuous and homogeneous formation of nanofiber, mixture of formic acid and acetic acid was used since formic acid has high dielectric constant (57.2 at 25 °C) and acetic acid has relatively low dielectric constant (6.6 at 25 °C) hence mixture gives an optimum or moderate conductivity to the solvent system. Formulation (TNZ-PCLNF) was optimized by using "Quality by Design" approach to meet the critical quality attributes of the final product.

5.2.1 Experimental design

A total of 17 batches of TNZ-PCLNF membrane were fabricated in accordance with the design matrix of BBD generated by the Design-Expert software, by altering the independent variables, i.e., polymer concentration (X_1), drug concentration (X_2), and the solvent ratio (X_3) in three defined levels. Two dependent responses were analyzed, i.e., nanofiber diameter (Y_1) and EE (Y_2). The results for different experimental runs are summarized in Table 5.4. In the polynomial equation, a direct relationship between the independent variables and dependent responses is denoted by a positive coefficient, whereas an inverse relation is denoted by negative coefficient. Figure 5.5, shows three-dimensional surface plots, which delineate the interaction of any two independent variables on the dependent variable, by keeping the third at a constant level. Further, the utility of "Quality by Design" approach in performing experiments was confirmed by

the statistical data analysis and statistical optimization [Patel et al. 2014b, Solanki et al. 2007]. The useful results obtained by statistical analysis of data as shown in Table 5.5 reaffirmed the utility of "Quality by Design" approach in performing experiments.

Table 5.4 Box–Behnken experimental design representing experimental runs with independent variables and dependent responses of TNZ-PCL nanofiber[a]

Run No.	Independent Variables			Dependent Variables	
	X_1	X_2	X_3	Y_1	Y_2
Factorial Points					
1	-1	-1	0	142.7±12.4	78.8±0.8
2	1	-1	0	174±10.5	88.2± 1.2
3	-1	1	0	138±11.9	70.8±2.4
4	1	1	0	171.5±9.25	72.4±1.8
5	-1	0	-1	174.6±10.4	76.7±0.9
6	1	0	-1	198.3±12.2	84.5±0.6
7	-1	0	1	138.2±8.5	74.2±1.3
8	1	0	1	172.9±9.8	73.6±0.8
9	0	-1	-1	178.4±11.6	86.8±0.7
10	0	1	-1	176.3±11.2	72.5±1.4
11	0	-1	1	148.4±9.3	85.6±0.6
12	0	1	1	139.2±14.7	70.4±1.2
Centre Points					
13	0	0	0	152.7±12.5	80±0.9
14	0	0	0	150.8±10.8	82.3±0.7
15	0	0	0	152±13.4	81.2±1.0
16	0	0	0	151.5±10.7	80.8±0.8
17	0	0	0	150.4±11.4	80.4±1.4

[a]All data are shown as mean ±S.D.; n = 3

Table 5.5 Statistical analysis results for lack of fit test and model summary for diameter and entrapment efficiency of nanofiber

Model	Lack of fit test					Model summary statistics					Remark
	SS	df	MS	F-Value	p-Value prob >F	SD	R^2	Adjusted R^2	Predicted R^2	PRESS	
Diameter											
Linear	944.68	9	104.96	123.92	0.0002	8.54	0.8091	0.7650	0.6620	1678.38	
2FI	900.62	6	150.10	177.22	< 0.0001	9.51	0.8179	0.7087	0.3209	3371.81	
Quadratic	10.73	3	3.58	4.22	0.0989	1.42	0.9972	0.9935	0.9643	177.01	Suggested
Cubic	0.000	0	-	-	-	0.92	0.9993	0.9973	-	+	Aliased
Pure error	3.39	4	0.85	-	-	-	-	-	-	-	-
Entrapment Efficiency											
Linear	81.42	9	9.05	11.63	0.0154	2.55	0.8289	0.7895	0.6843	156.01	
2FI	46.47	6	7.74	9.95	0.0217	2.23	0.8997	0.8395	0.6606	167.72	
Quadratic	4.27	3	1.42	1.83	0.2821	1.03	0.9851	0.9659	0.8520	73.14	Suggested
Cubic	0.000	0	-	-	-	0.88	0.9937	0.9748		+	Aliased
Pure error	3.11	4	0.78	-	-						

SS: sum of squares, df: degree of freedom, MS: mean square, SD: standard deviation, PRESS: Predicted Residual Error Sum of Squares; 2FI: two-factor interaction, +: PRESS statistic not defined, p-value < 0.05 was considered as statistically significant.

5.2.1.1 Influence of independent variables on diameter (Y_1)

Diameter is one of the critical factors for achieving desired drug release profile from nanofiber-based drug delivery systems. The Smaller diameter is preferable for nanofibers as it provides shorter diffusion passage length for effective mass transfer along with greater surface area. The diameter of prepared batches varied from a minimum of 138±11.9 nm to a maximum of 198.3±12.2 nm. The observed wide variation recommended that the nanofiber diameter was strongly affected by the selected independent formulation variables. Based on the lack of fit test and model summary statistics, the quadratic model was selected for the analysis of influence of variables on diameter. The relationship between the diameter of nanofibers and independent variables was derived by following polynomial equation.

$$\text{Diameter} = 151.48 + 15.40X_1 - 2.31X_2 - 16.11X_3 + 0.55X_1X_2 + 2.75X_1X_3 - 1.78X_2X_3 + 7.75X_{12} - 2.68X_{22} + 11.77X_{32}$$

The quadratic model was found to be significant as it had F value of 272.70 ($p < 0.0001$) and best suited for establishing a relation between the diameter of nanofibers and independent variables. The higher value of R^2 coefficient (0.9972) indicates the existence of a good correlation between predicted values and experimental values. The lack of fit data was found to be non-significant with F-value 4.22 and p values 0.0989, inferring the adequate fitting of data. Moreover, a lower value for the coefficient of variation (0.89%) confirmed the reliability of the quadratic model with a higher degree of precision. The difference between the predicted R^2 (0.9643) value and adjusted R^2 (0.9935) value was very less, which indicated the suitability of the selected model for prediction of responses. Therefore, the present quadratic model can be used to navigate the design space.

Statistical analysis revealed that polymer concentration (X_1) exhibited direct relationship with the diameter of TNZ-PCLNF membrane owing to its direct impact on the viscosity, shown in Figure 5.5(I). At higher polymer concentration, the viscosity of the electrospinning solution increases, which ultimately impacts resistance of jet. This, in turn, forms thicker fibers due to bending instability and a faster solidification of the polymer jet [De Vrieze et al. 2007, Jacobs et al. 2010]. Contrarily, drug concentration and FA/AA ratio have an inverse impact on the diameter as depicted in Figure 5.5 (II & III). Reduction in viscosity was found at a higher amount of TNZ, which might be due to TNZ molecules acting as a plasticizer for polymer chains. Simultaneously, the conductivity of electrospinning solution was increased as a consequence of the enhanced polarity. Therefore, both, reduced viscosity with an increased conductivity would have decreased diameter of nanofibers by the addition of TNZ [Zamani et al. 2010].

Likewise, on increasing the FA/AA ratio (X_3) conductivity of the electrospinning solution increases (dielectric constant 57.2 for FA and 6.2 for AA at 25 ºC) and thereby, the diameter of nanofiber decreases. When the conductivity of solution increases, the electric charges carried by the electrospinning jet also increases, this, in turn, enforces generation of higher elongation forces to the jet under applied electrical field [Ramakrishna et al. 2005]. Bending instability also increases at higher solution conductivity and thereby, causes elongation of the jet path with higher stretching of the solution, leading to a reduction in nanofiber diameter.

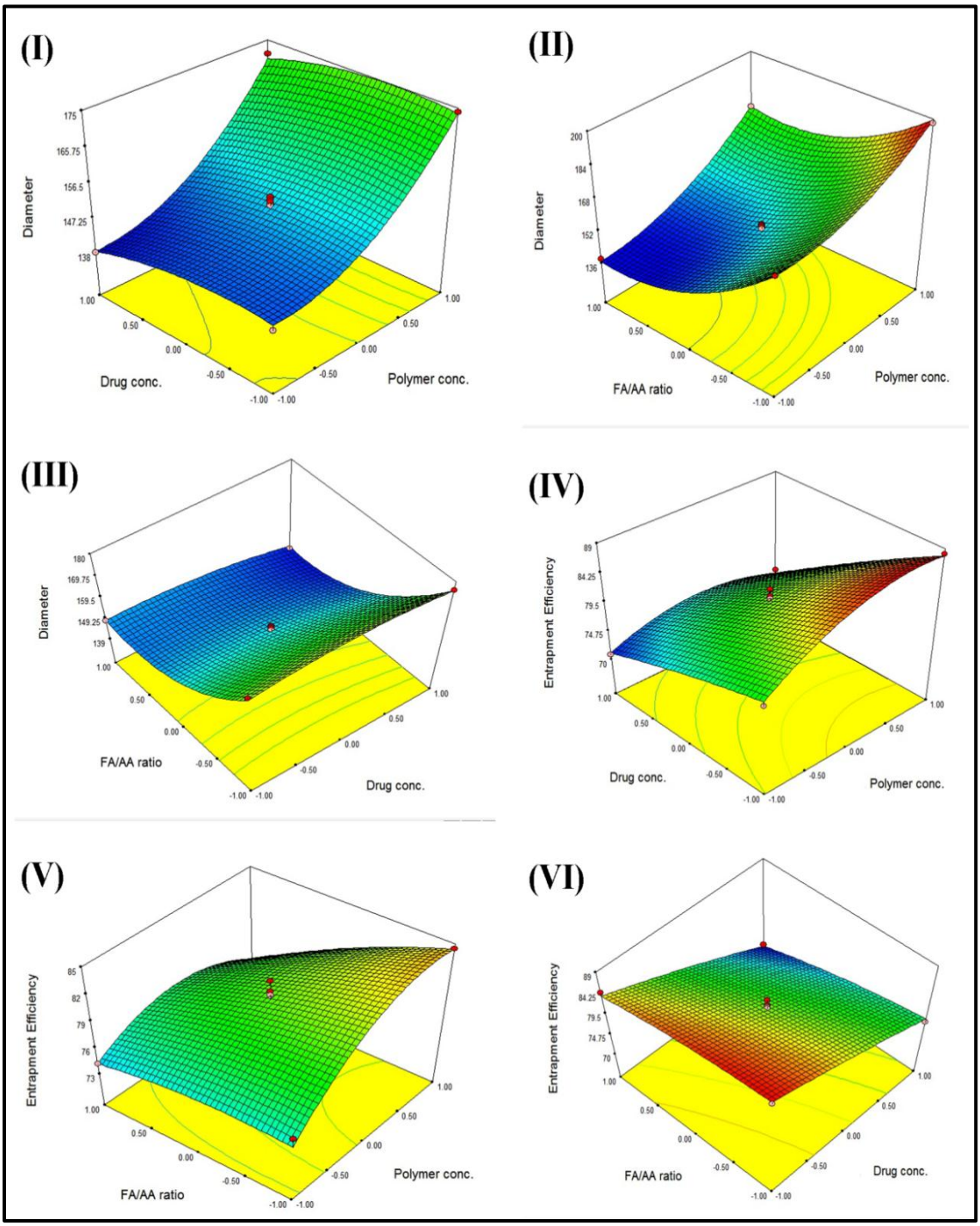

Figure 5.5 Three-dimensional response surface plots showing the effect of independent variables (concentration of polymer, concentration of drug and FA/AA ratio on response variables: diameter of nanofiber (I-III) and entrapment efficiency (IV - VI).

5.2.1.2 Influence of independent variables on entrapment efficiency (Y_2)

The Entrapment Efficiency of TNZ-PCLNF membrane was found to be varying between a minimum of 70.4% to a maximum of 88.2% for different experimental runs.

The second order polynomial equation which illustrated the effect of independent variable on EE (Y_2) can be written in terms of coded significant model terms as:

$$EE = 80.94 + 2.28X_1 - 6.16X_2 - 2.84X_3 - 1.95X_1X_2 - 2.10X_1X_3 - 2.98X_{12}$$

The quadratic model was analysed to be significant with the Model F value of 51.30 ($p < 0.0001$) as indicated by model summary statistics. A good correlation between the predicted and the experimental values was indicated by the high value of R^2 coefficient (0.9851). The model also revealed an adequate fitting to the data which was indicated by a non-significant lack of fit, having p values of 0.2821 ($p < 0.05$). The difference between predicted R^2 (0.8520) and adjusted R^2 (0.9659) value is very less, which indicated the adequacy of the selected model for prediction of responses. Thus, this model was selected for the analysis of the effect of independent variables on EE. ANOVA analysis showed that X_1, X_2, X_3, X_1X_2, X_1X_3, X_{12} were the significant model terms.

The influence of the independent variables on entrapment efficiency can be evaluated by observing the Figure 5.5(IV-VI). As depicted in Figure 5.5(IV & V) concentration of polymer (X_1) had a significant positive effect on EE whereas drug concentration and FA/AA ratio affected inversely. Also, higher coefficient value (6.16) of the concentration of drug (X_2) suggested that it had more significant effect on EE followed by the concentration of polymer (X_1) and FA/AA ratio (X_3). Though, the effect of independent variables on EE was lower than the effect on particle size. This was because of the lower coefficient value of the main effects and interaction terms in the polynomial equation of EE compared with the polynomial equation of nanofiber diameter.

A significant increase in the EE of formulated TNZ-PCLNF membrane was observed with an increase in the polymer concentration. The higher polymer concentration conferred a diffusional barrier due to increased viscosity of the solution and hence hindered the outward movement of TNZ, ultimately enhancing the EE. Increased diffusional path length owing to increased diameter at higher polymer concentration might also be one of the plausible reasons for higher EE [Budhian et al. 2007]. Conversely, a significant reduction in the EE was observed at higher concentrations of the drug. The probable reason might be the presence of the solubilized drug in the polymeric solution, which might have enhanced the migration of dissolved drug towards the surface of the nanofiber membrane during the electrospinning process. Similarly, reduced EE with an increase in FA/AA ratio (X_3) was noticed due to a substantial reduction in the diameter of the nanofiber.

5.2.1.3 Optimization of TNZ-PCLNF membrane

The formulation was statistically optimized by using the desirability based numerical optimization technique. Different constraints were fixed for all three independent variables in the Design Expert® Software to achieve maximized EE with minimum diameter. Predicted levels of independent variables X_1, X_2 and X_3 were found to be 9.8% w/v, 10% w/w and 0.25, respectively, with diameter of 146.98 nm, EE of 85.78% and desirability of 0.858. After that, the optimized TNZ-PCLNF membrane was formulated with predicted levels of independent variables to establish the validity as well as the predictability of BBD. The optimized experimental TNZ-PCLNF membrane exhibited a diameter of 147.6±7.6 nm and EE of 84.36±1.5%. The lower value of bias between the predicted values and the experimental values indicated that results were in good agreement with observed values and thereby, confirmed the reliability of BBD for statistical optimization to develop nanofiber system for TNZ delivery aimed towards

the treatment of periodontitis [Chaubey et al. 2014]. Optimized TNZ-PCLNF membranes were further selected for various *in vitro* and *in vivo* characterizations.

Table 5.6 Comparison of experimental and predicted values of optimized TNZ-PCLNF with its desirability

Independent Variables		**Levels**	
X_1 = Concentration of polymer (%w/v)		9.8	
X_2 = Concentration of drug (%w/w)		10	
X_3 = FA/AA ratio (v/v)		0.25	
Validation			
	Experimental values	Predicted values	% Bias*
Diameter (nm)	147.6±7.6	146.98	- 0.421
Encapsulation efficiency (%)	84.36±1.5	85.78	1.6
Overall Desirability		0.858	

*Bias was calculated as [(predicted value-experimental value)/predicted value] × 100; All results are shown as mean±S.D; n = 3

5.2.2 Solid state characterization of TNZ-PCLNF by FTIR, DSC and PXRD

5.2.2.1 Fourier transform infrared spectroscopy (FTIR) study

FTIR was performed to confirm the interaction between drug and polymer as well as to ensure the effectiveness of the electrospinning process on the available functional groups present in the resulting structure. FTIR spectra of TNZ, PCL, PM and optimized nanofiber membrane are depicted in Figure 5.6.

TNZ spectrum showed characteristic peaks at 1265, 1301 and 1367 cm^{-1}, which were assigned to stretching vibration of C-O, the asymmetric stretching vibration of S=O and symmetric stretching vibration of N=O respectively. The FTIR peaks appeared at 1492, 1521 and 2914-3001 cm^{-1} attributed to asymmetric stretching vibration of N=O (NO_2), C=N (imidazole ring) and C-H respectively. PCL related stretching vibrations were represented by the characteristic peak at 1733 cm^{-1} (C=O stretching), 2853 cm^{-1}

(symmetric CH_2 stretching) and 2948 cm^{-1} (asymmetric CH_2 stretching). The FTIR spectra of PM of PCL and TNZ showed characteristic peaks of all the excipients, and no new bands or shifts in characteristic peaks appeared, thus indicated the absence of any possible interaction between the drug and polymer. FTIR spectrum of nanofiber membrane exhibited all the characteristic peaks of TNZ and PCL with little variation in frequencies similar to its pure form which confirms that electrospinning process did not adversely affect the molecular structure of TNZ present in the resulting structure. Therefore, it can be confirmed that the drugs and polymers are compatible and can be formulated into nanofiber.

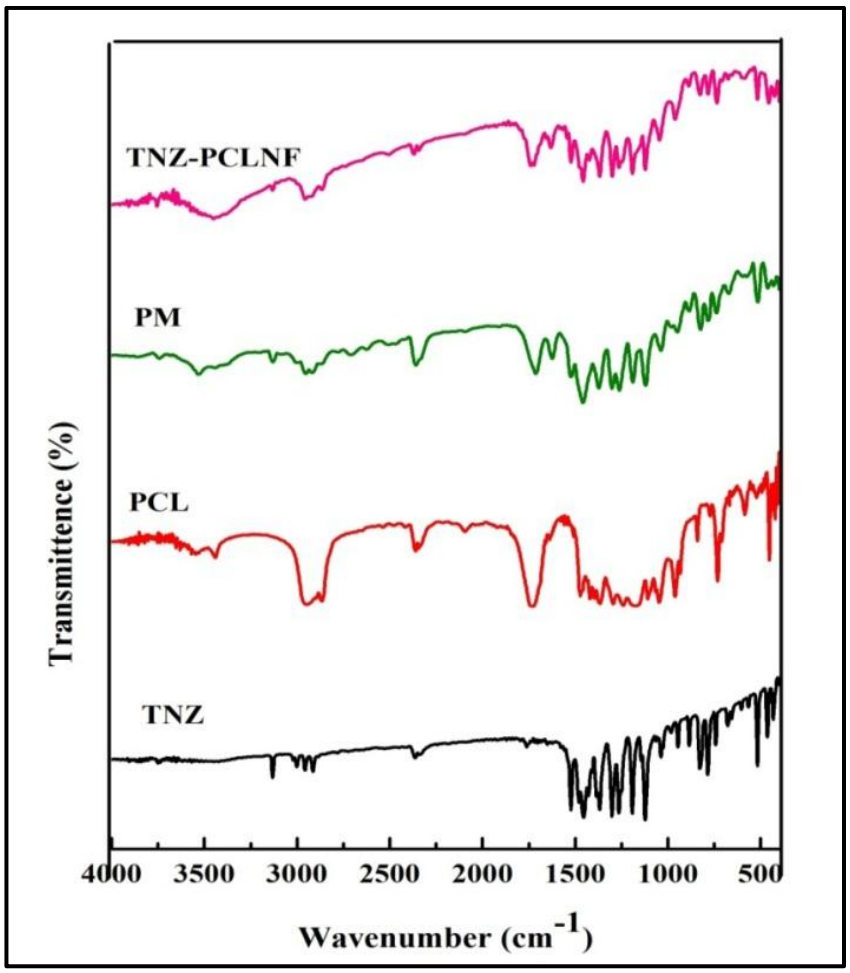

Figure 5.6 FTIR spectra of TNZ, PCL, PM of TNZ with excipients and optimized formulation (TNZ-PCLNF)

5.2.2.2 Differential scanning calorimetry (DSC) study

DSC studies were performed to characterize the solid state of drugs and polymers. Further, compatibility between drug and excipients can be evaluated by observing the thermal behaviour of compounds such as appearance or disappearance of an endothermic or exothermic peak. If all the peaks remain the same, compatibility can be expected. DSC thermogram of TNZ, PCL, their PM and optimized nanofiber membrane are depicted in Figure 5.7. DSC thermogram of TNZ showed a sharp endothermic peak at 128.5 ºC which is attributed to its melting point. The sharp melting peaks exhibited by TNZ confirmed their existence as a crystalline form. Thermogram of PCL exhibited a characteristic peak at 60 ºC due to its semi-crystalline nature. The PM also exhibited characteristic peaks of all components indicating physical compatibility between excipients and drug. Whereas, optimized TNZ-PCLNF membrane showed flat curve without sharp endothermic or exothermic peaks of drug. This indicates that transformation of phase i.e. crystalline state to amorphous state has taken place, during the entrapment process. This might be due to shear stress provided by the stirrer and electrospinning during the fabrication process of nanofiber which may prevent the recrystallization of TNZ, leaving TNZ in molecular dispersion form inside the TNZ-PCLNF membrane.

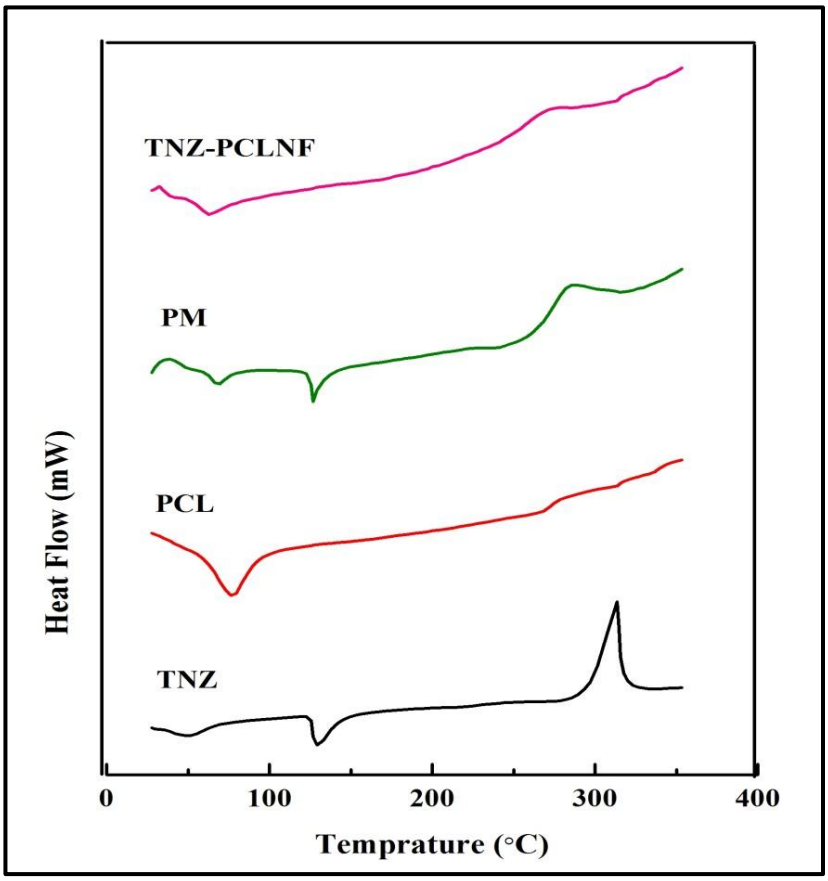

Figure 5.7 DSC Thermograms of TNZ, PCL, PM of TNZ with excipients and optimized formulation (TNZ-PCLNF)

5.2.2.3 Powder X-ray diffractometry (PXRD) study

To understand the crystallinity of the drug in the nanofiber membrane, PXRD pattern of pure drug, PCL, their PM and optimized TNZ-PCLNF membrane were recorded. The PXRD pattern of TNZ, as shown in Figure 5.8, exhibited four characteristic peaks at 2θ of 12.2º, 17.9º, 22.7º and 33.8º which demonstrates crystalline nature of the drug. PCL showed two peaks in the diffractogram at a diffraction angle of 22.4º and 24.6º indicates semi-crystalline nature of PCL. The crystalline peaks of the TNZ were retained in the diffractogram of PM of TNZ along with PCL, which indicated TNZ holding their crystalline nature in the PM without any interactions. Whereas, XRD pattern of TNZ-PCLNF membrane exhibited more of an amorphous nature as compared to pure TNZ due to shifting of its diffraction intensity, conforming TNZ physical state transformed

from crystalline state to amorphous state during the entrapment process in the nanofiber membrane [Natarajan et al. 2011].

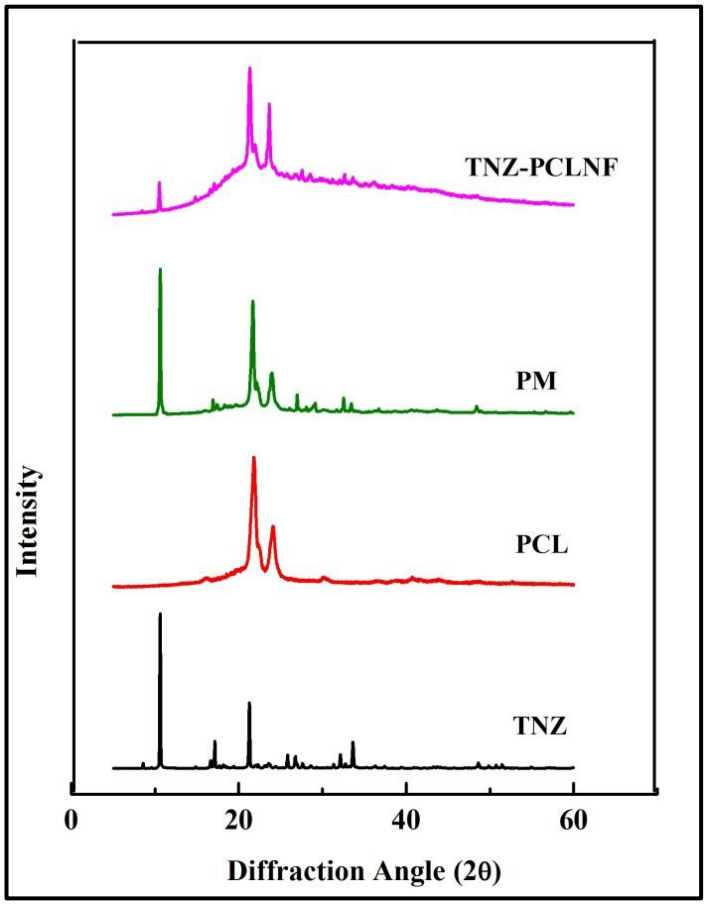

Figure 5.8 Overlay of PXRD patterns of (a) TNZ (b) PCL (C) PM of TNZ with excipients and (d) TNZ-PCLNF.

5.2.3 Shape and surface morphology

Figure 5.9 shows SEM micrographs of TNZ-PCLNF membrane of the optimized batch at different magnification. As can be seen from the figure, uniform and smooth nanofibers were formed with minimal bead defects. The diameters of the nanofiber with different concentration of the drug were in the range of a minimum of 138±11.9 nm to a maximum of 198.3±12.2 nm and shown in the Table 5.4. Porosities of the nanofiber membranes were found in the in the range 65% to 82%. It had been reported by Chong et al, that porosities within the range of 60-90% are essential for the exchange of gas and nutrient. Moreover, smaller pore size of membrane than the size of fibroblast is

beneficial because it prevents ingrowths of fibroblasts into the tissue defect [Chong et al. 2007]. Hence, we successfully fabricated TNZ loaded PCL nanofiber membrane.

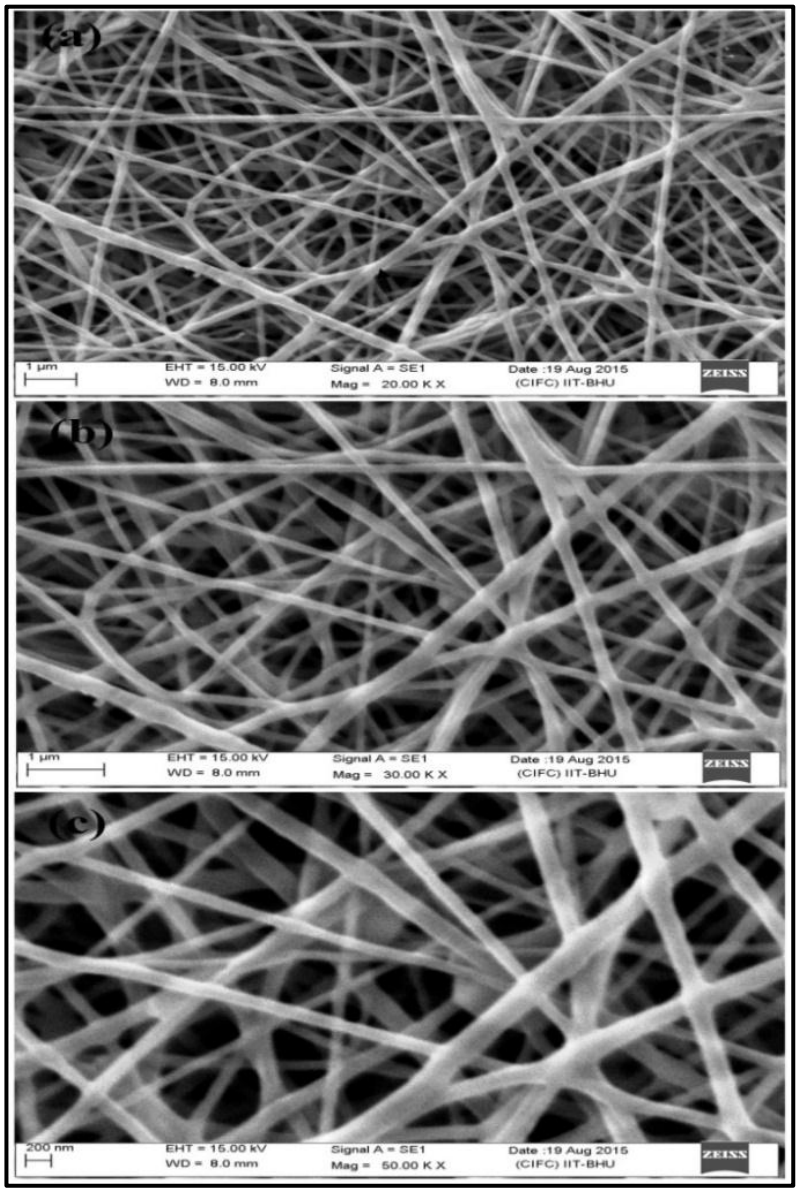

Figure 5.9 Scanning electron microscopic images of optimized nanofiber membrane at different resolutions

AFM study was further used to study more detailed structure, surface morphology and diameter of electrospun nanofiber membrane. The topographic as well as 3D AFM images of nanofiber membrane, generated by atomic level interaction between surfaces of electrospun nanofiber and the sharp tip of scanner are depicted in Figure 5.10. The fiber diameters were measured from the height and were found in accordance with SEM

study. AFM micrographs showed an arbitrarily interconnected structure, smooth morphology and uniform distribution of electrospun nanofiber with rare bead defect. The possible reason for smooth surface could be attributed to uniform mixing of drug and polymer in the combined solvent system of FA/AA.

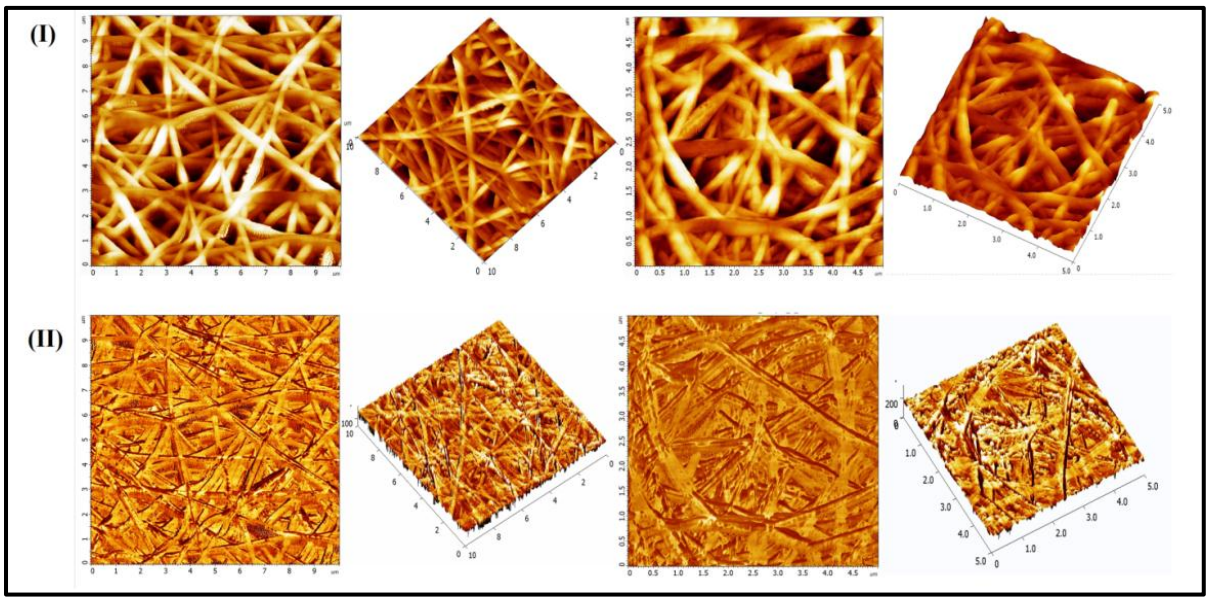

Figure 5.10 Surface morphology of optimized nanofiber membrane at different resolutions (I) 2D and 3D-atomic force microscopic images showing smooth and bead free surface of nanofiber membrane, (II) corresponding phase image

5.2.4 Surface pH and Drug Content Uniformity

Surface pH of nanofiber membrane was taken into consideration because too much acidic or basic pH affects the area of application and causes irritation to oral mucosal membrane leading to patient discomfort [Ahuja et al. 2006]. Also, acidic pH leads to the dissolution of enamel and demineralisation of teeth. To overcome these problems, the pH of the nanofiber membrane must be nearer to pH of the GCF (pH 6.6). Surface pH of all the batches ranged from 6 to 7.5 demonstrating the acceptability of formulation for pocket insertion. In fact, formulations with pH 6.5 to 7 are more preferred because of the closeness of pH values to neutrality. Further, content uniformity studies of the nanofiber showed that the drug was uniformly distributed and recovery was found to be in the range of 82.2% to 86.5% for all the batches.

Table 5.7 Physicochemical characteristics of different batches of TNZ-PCLNF membrane

Run No.	Total drug Content* (%)	Surface pH
1	82.2±2.45	6.5
2	84.5±2.87	6.5
3	82.3±3.25	7.5
4	85.4±2.45	7.5
5	84.6±3.77	7.0
6	86.6±2.25	6.0
7	85.2±2.67	6.5
8	84.5±2.65	7.5
9	86.2±2.58	6.0
10	82.6±3.45	7.5
11	86.8±2.47	7.0
12	84.7±3.67	7.5
13	86.5±3.27	7.0
14	84.3±2.55	6.5
15	85.7±2.25	7.0
16	86.5±2.70	7.0
17	85.0±2.35	7.0
Optimized TNZ-PCLNF	87.8±2.32	6.5

*Result are presented as mean±SD, (n = 3)

5.2.5 Contact angle

Contact angle impersonates the wettability or hydrophilicity of the nanofiber membrane, which influences attachment and proliferation of cells. In spite of the excellent biocompatibility of PCL, the real confinement of this material is its hydrophobicity. Subsequently, contact angle estimations were done to explore the impacts of TNZ on the hydrophilicity of the nanofiber membrane. The results are represented in Figure 5.11. It was demonstrated that placebo nanofiber membrane has the higher contact angle (123.6±2.8)° as compared to drug-loaded optimized nanofiber membrane, indicating that some improvement in hydrophilicity was observed in case of

drug loaded nanofiber membrane. This improvement was attributed to the sulfonyl and polar imidazole ring functional groups on the TNZ molecule [Xue et al. 2014b].

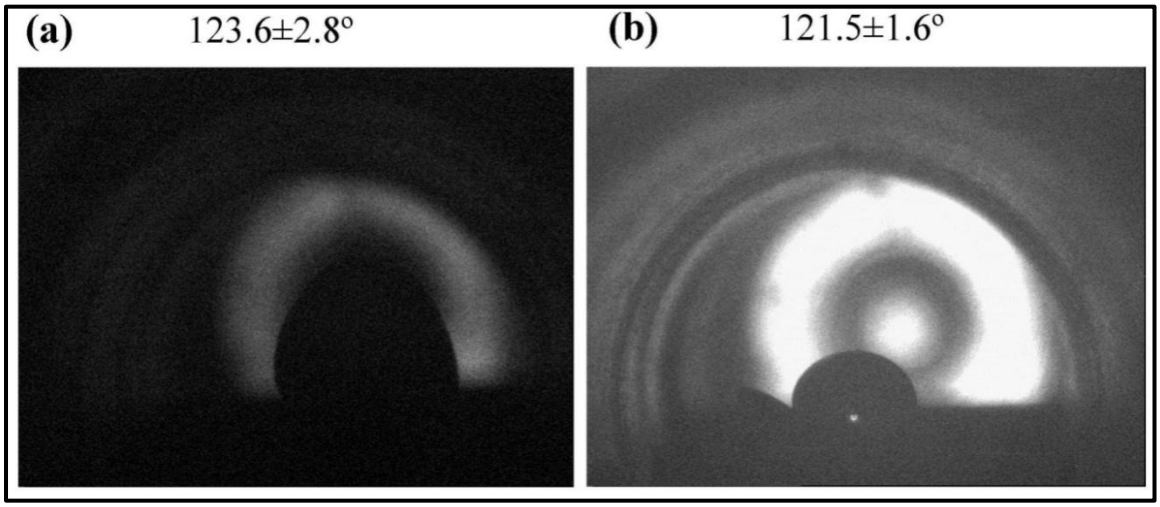

Figure 5.11 Contact angle of TNZ-PCLNF membrane: (a) Placebo nanofiber; (b) TNZ loaded optimized nanofiber; Images suggesting that PCL nanofiber is hydrophobic with a contact angle of 123.6°.

5.2.6 Entrapment efficiency

The EE of different batches of TNZ-PCLNF membrane was found to be in the range of 70.4±1.4% to 88.2±2.7% which is presented in Table 5.4. The outcomes revealed a precise dependence of the entrapment efficiency on the concentration of incorporated drug. It was observed that EE decreased at higher drug concentration; which might be due to the inclination of the dissolved drug molecules in the polymer solution to relocate to the surface or close to the surface of nanofiber during electrospinning procedure. Another reason could be the loss of a part of the aggregated drug, which might not have been entrapped into the nanofiber membrane. Moreover, the entrapment of TNZ into nanofiber membrane also depends on the factors such as effective hydrogen bonding of TNZ with PCL and homogenous mixing of TNZ and PCL in the solvent. [Xue et al. 2014c].

5.2.7 *In vitro* release study

The drug release profiles of the nanofiber membrane and pure drug suspension are shown in Figure 5.12, Table 5.8 and Table 5.9. Drug release from nanofiber as well as drug suspension was evaluated in McIlvaine buffer pH 6.6 by the static method as described earlier. As illustrated in the Figure 5.12, TNZ-PCL nanofiber exhibited a significant 22% burst within 8 hr of release whereas almost 90% TNZ released within first 8 hr from TNZ drug suspension. Thus, TNZ-PCL nanofiber membrane as compared to drug suspension greatly reduced burst effect and achieved sustained release of TNZ over 20 days. A similar explanation was also reported previously that the drug release from PCL nanofiber was ideally prolonged in comparison with various controlled drug release systems for periodontal diseases [Mundargi et al. 2007, Reise et al. 2012, Zamani et al. 2010]. The nanofiber membrane released the drug in a biphasic manner with an initial burst release followed by sustained release. The immediate burst release was contributed by the leaching of free drug particles on the superficial layer of the membrane which was in immediate access to the dissolution media. On account of the presence of the bacterial load in pockets and to provide immediate effect as well as achieve MIC, burst release of antibiotics is useful for antimicrobial therapy [Khan et al. 2016b]. Since TNZ is highly soluble in AA, which was the main portion of the solvent mixture, the solution remains homogeneous during the electrospinning process without separation of drug crystals. Therefore, the affinity and compatibility between the drug and polymer were vital to achieve perfect entrapment of the drug inside the electrospun nanofiber during the rapid stretching and quick solvent evaporation throughout the process of electrospinning [Zeng et al. 2005]. The kinetic data of the optimized batch with r^2 values obtained for different models are shown in Results are shown as mean ±SD; n = 3

Table 5.10 The release kinetic modelling showed that the drug release pattern from TNZ-PCL was best explained by Korsmeyer-Peppas equation than other models, with the highest value of linearity ($r^2 > 0.9$). Additionally, the diffusion coefficient (n) value for Korsemeyer-Peppas equation for all batches was less than 0.5 which showed drug released by the diffusion mechanism [Costa and Lobo 2001]. This was expected as there was no biodegradation of PCL during the first two weeks.

Table 5.8 *In vitro* drug release data of the optimized TNZ-PCLNF membrane in McIlvaine buffer pH 6.6.

Time (hr)	Cumulative % drug release
1	7.4±3.62
2	11.3±3.27
4	15.6±3.22
6	19.4±2.34
8	22.6±4.16
12	27.6±4.56
24	34.3±3.67
48	41.5±3.92
72	48.7±3.88
96	54±3.85
120	57.8±3.65
144	61.5±2.87
168	64.4±3.27
192	67.8±3.45
216	71.5±4.18
240	74.2±2.92
264	77.5±2.28
288	80.3±3.75
312	82.8±4.8
336	86.5±2.87
360	88.8±2.46
384	90.6±2.48
408	92.8±3.65
432	93.3±4.76
456	94.6±3.39
480	95.4±2.47

Results are shown as mean ±SD; n = 3

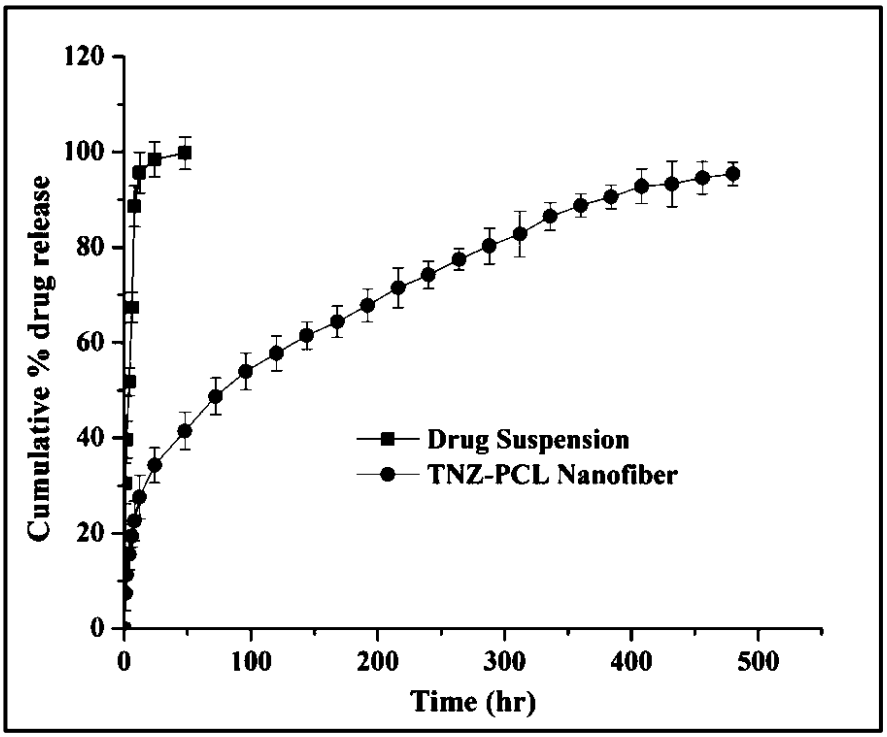

Figure 5.12 *In vitro* drug release profile of optimized TNZ-PCL nanofiber and drug suspension in McIlvaine buffer pH 6.6 (vertical bars represent SD, results are shown as mean ±SD; n = 3)

Table 5.9 *In vitro* drug release data of the TNZ suspension in McIlvaine buffer pH 6.6

Time (hr)	Cumulative % drug release
1	30.5±4.50
2	39.7±3.64
4	51.8±2.65
6	67.4±3.25
8	88.6±3.55
12	95.7±4.35
24	98.5±2.57
48	99.8±3.45

Results are shown as mean ±SD; n = 3

Table 5.10 Release kinetic modelling for optimized batch of TNZ-PCL in McIlvaine buffer pH 6.6

Batch	Zero-order	First order	Higuchi model	Korsmeyer-Peppas model
TNZ-PCL	$r^2 = 0.806$	$r^2 = 0.612$	$r^2 = 0.941$	$r^2 = 0.960$ $n = 0.271$

5.2.8 *In vitro* antibacterial study

The *in vitro* antibacterial activity of the electrospun nanofiber membrane was evaluated using well diffusion method in which the zone of inhibition against *S. aureus* was measured (MTCC1303). It was observed that all the drug-loaded nanofiber membranes exhibited a prolonged antibacterial activity over a period of 21 days, whereas placebo membrane showed non-significant antibacterial activity (Figure 5.13). The mean inhibition zone was observed to be 32.25±0.75 mm, 34.6±1.2 mm and 40.65±1.38 mm on the first day for TNZ-PCLNF (10%), TNZ-PCLNF (20%) and TNZ-PCLNF (30%) membrane, respectively. After that, the inhibition zone slowly decreased to 13.6±0.95 mm, 15.74±0.82 mm and 18.5±1.2 mm at the end of 21 days of incubation, Figure 5.13 (I & II), which was calculated to be equivalent to 4.75, 5.5, and 7.0 µg/ml of TNZ.

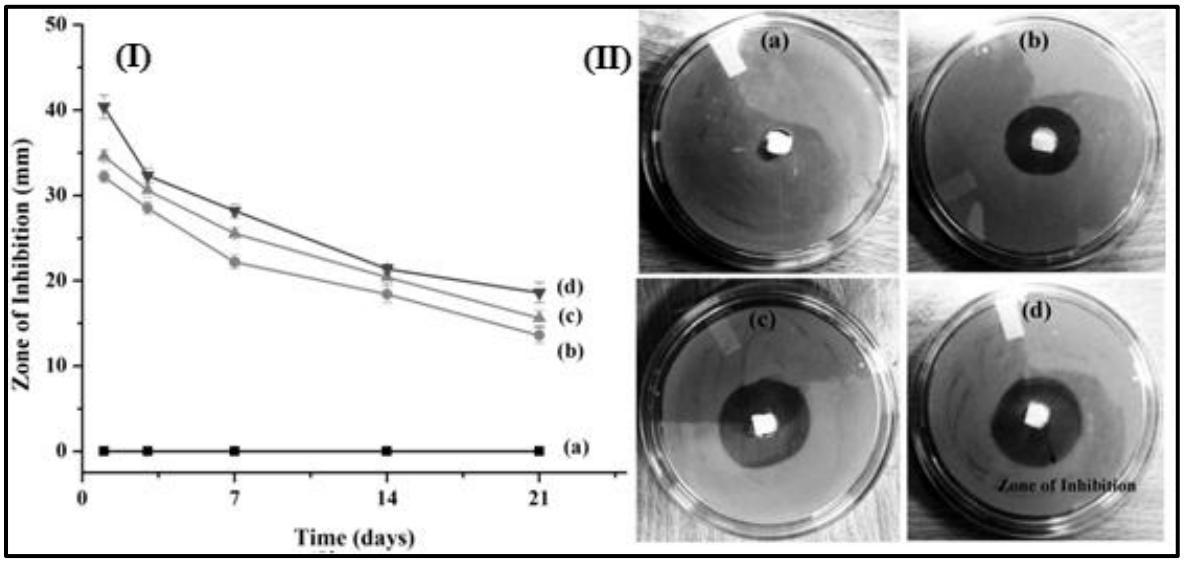

Figure 5.13 (I) Graphical illustration representing inhibition zone diameter versus incubation time for TNZ-PCL nanofiber membrane containing w/w percentages of TNZ: (a) 0%; (b) 10% (c) 20% and (d) 30% against *S. aureus*. (II) Inhibition of bacterial growth on agar plate against *S. aureus.*

Since the MIC of TNZ against periodontal pathogen was reported as 2.4 µg/ml [Alou et al. 2009, Nagaraju et al. 2003]. Therefore, we can come to the conclusion that TNZ is released from nanofiber membrane at a constant rate and is effective against these bacterial strains over 21 days [Kassem et al. 2015]. Similarly, a prolonged antibacterial

activity for 30 days against *Fusobacterium nucleatum* of sustained release nanofiber membrane, based on PCL containing metronidazole, was observed by Xue et al. [Xue et al. 2014c].

5.2.9 Cytocompatibility Study

Figure 5.14 shows the cell viabilities of mouse fibroblast (L-929 cell lines) treated with different aliquots of DMEM taken from media incubated with nanofiber from 1-21 days. The percentage cell viability values near to 100 indicated that the nanofiber membrane were not cytotoxic to the cells. Figure 5.15 shows images from the microscopic analysis of the L-929 cells that were exposed directly on the surface of the drug-loaded nanofiber membrane with different concentrations of TNZ and coloured with FDA and EtBr.

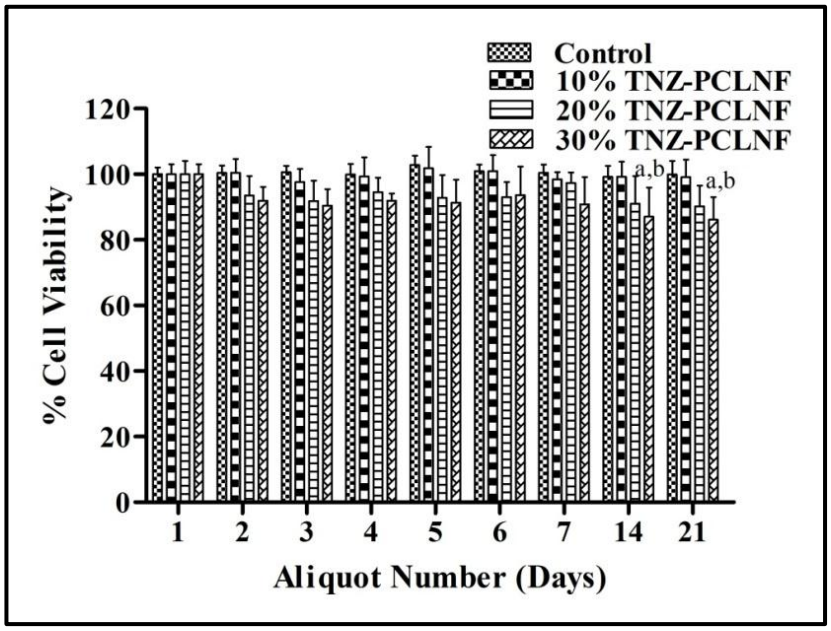

Figure 5.14 Graphics illustrating L-929 cell viability (%), measured by MTT assay, after exposure to aliquots of DMEM media. DMEM aliquots were taken from the nanofiber membrane on successive days (1–7) and then for a week (days 14-21).

The fibroblasts were observed as green coloured due to staining by FDA and exhibit their typical structure. This clearly suggested the biocompatibility of the nanofiber membrane. Thus, it was concluded that the TNZ-PCLNF membrane would not cause

any toxicity to the periodontal tissues during its use. Reise et al. also reported such explanation while studying the release of metronidazole from electrospun poly (l-lactide-co-d/l-lactide) nanofiber for local periodontitis treatment [Reise et al. 2012].

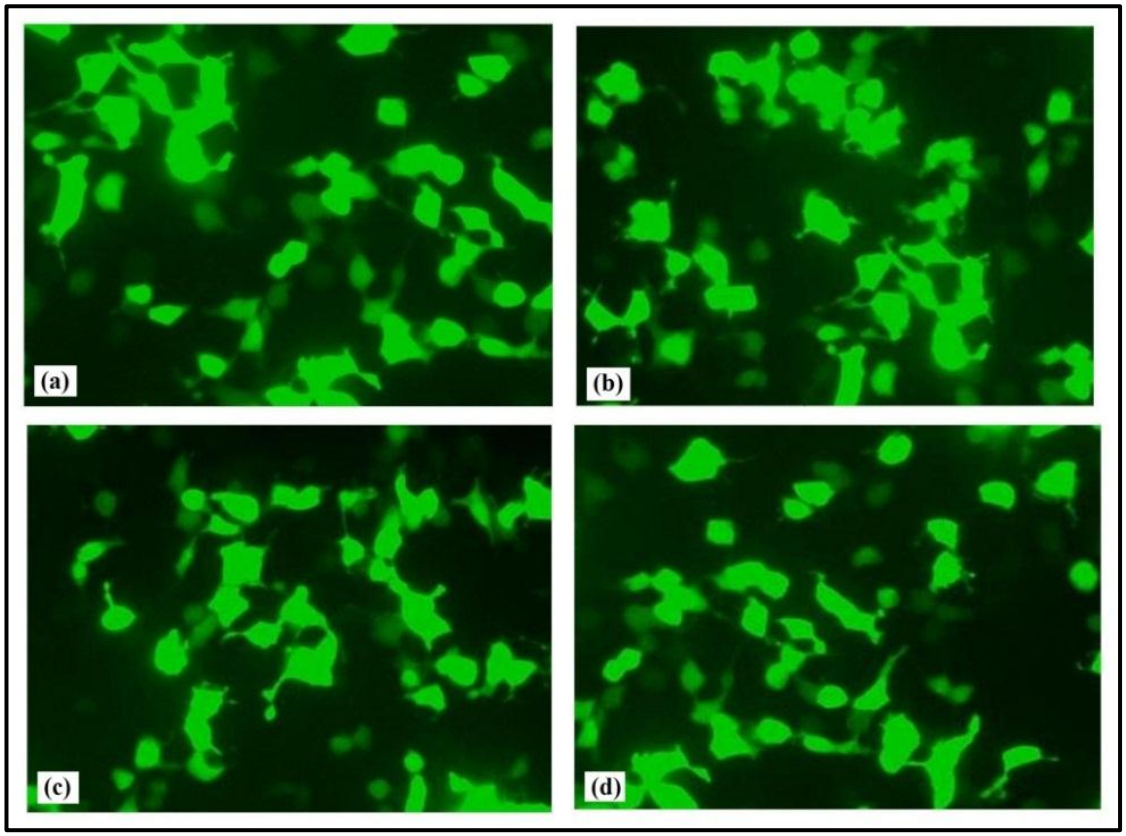

Figure 5.15 Image shows cytocompatibility of nanofiber membrane with mouse fibroblasts (L-929 cell lines) after direct exposure to the surface of TNZ-PCLNF membrane containing w/w percentages of TNZ: (A) 0%; (B) 10.0%; (C) 20.0%; (D) 30.0%; typical healthy structures are apparent in all cases

5.2.10 Haemocompatibility of TNZ-PCLNF membrane

Biocompatibility of developed drug delivery device is essential because some polymer in contact with the living body tissue causes various critical reactions, such as thrombosis. Along these lines, haemocompatibility of TNZ-PCLNF membrane was determined by haemolysis method. The degree of red blood cells broken by the test sample in contact with blood denotes as haemolysis percentage (HP). HP consequences of ACD blood with nanofiber membrane loaded with different concentration of TNZ (0%, 10%, 20%, and 30%) are shown in Figure 5.16. Results exhibited that the HP was

under 3% for 0%,10% and 20% TNZ loaded nanofiber membrane, demonstrating the good character of anti-haemolysis among all the TNZ-PCLNF membrane [Dey and Ray 2003]. However, nanofiber membrane loaded with 30% TNZ showed maximum HP viz. 3.75±0.50%. This might be attributed to the expanded surface roughness of TNZ-PCLNF (30%) membrane because of higher concentration of the drug, so a shear stress induced the red blood cells to crack and carried about haemolysis when blood contact with the rough surface of nanofiber [Meng et al. 2010].

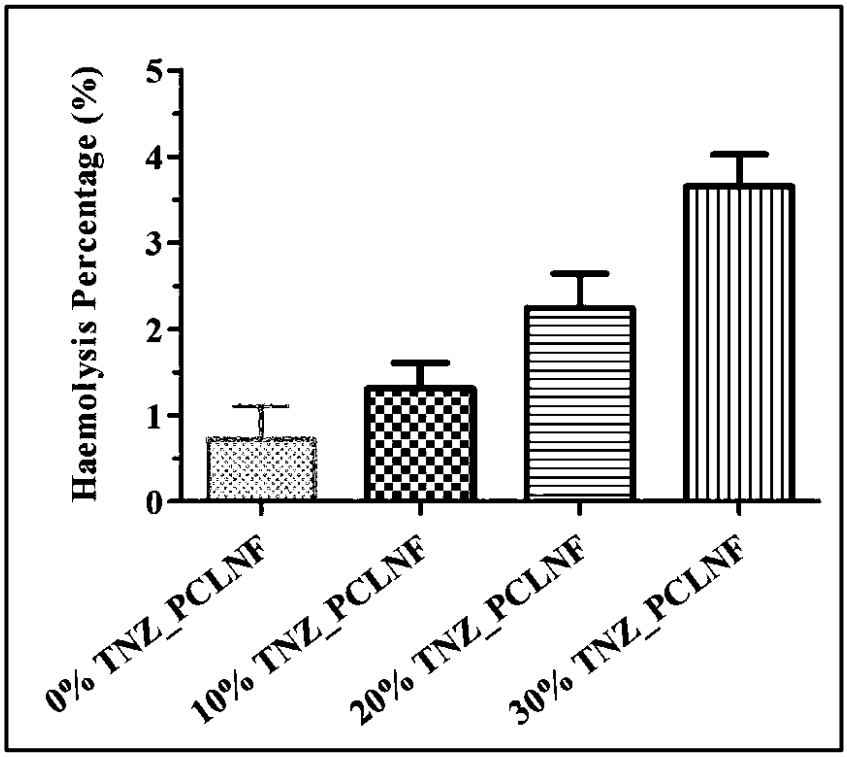

Figure 5.16 Haemolysis percentage of electrospun TNZ-PCLNF membrane containing w/w percentages of TNZ: (a) 0%; (b) 10.0%; (c) 20.0%; (d) 30.0%. Vertical bars in Figure represents SD; results are shown as mean±S.D.; (n = 3).

5.2.11 Storage stability study

The ability of nanofiber membrane to remain stable against environmental changes is of the prime requirement to ensure its final *in vivo* performance. The change in properties of TNZ-PCLNF like diameter and EE during stability study over 6 months at room temperature (30±2 ºC), refrigerated condition (4±1 ºC), and accelerated condition

(40±2 ºC/75±5% RH) is depicted in Figure 5.17. There was no any significant noticeable change in the physical appearance (i.e., colour change and change in pH) observed at different environmental condition during the study. Similarly, insignificant ($p > 0.05$) change in the diameter and EE of TNZ-PCLNF was observed during the storage at room temperature (30±2 ºC) and refrigerated condition (4±1 ºC). Whereas, a significant change was observed in all above parameters accelerated condition (40±2 ºC/75±5% RH) suggesting instability due to degradation of polymer which would have expelled the drug molecule from nanofiber hence, it was strongly recommended that the nanofiber membrane should be stored at room temperature (30±2 °C) as well as refrigerated condition (4±1 °C), to hold the pharmaceutical properties for safe and effective long-term use.

The shelf-life of optimized nanofiber membrane was found to be 21.01, 20.83 and 12.07 months when stored at refrigeration, room temperature and high-temperature storage, respectively (Figure 5.18). This indicated high stability of nanofiber membrane for longer period especially if stored refrigerated and room temperature condition.

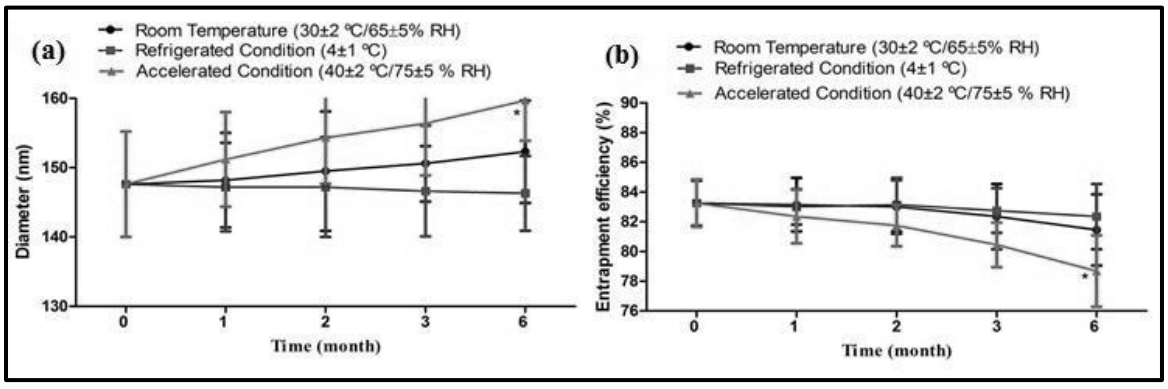

Figure 5.17 Effect on (a) diameter and (b) entrapment efficiency of TNZ-PCLNF stored at different environmental conditions over a different time interval (vertical bars represent ±SD; n = 3). *significant values at $p < 0.05$ compared with zero time (One-way ANOVA; Dunnett's multiple comparison test).

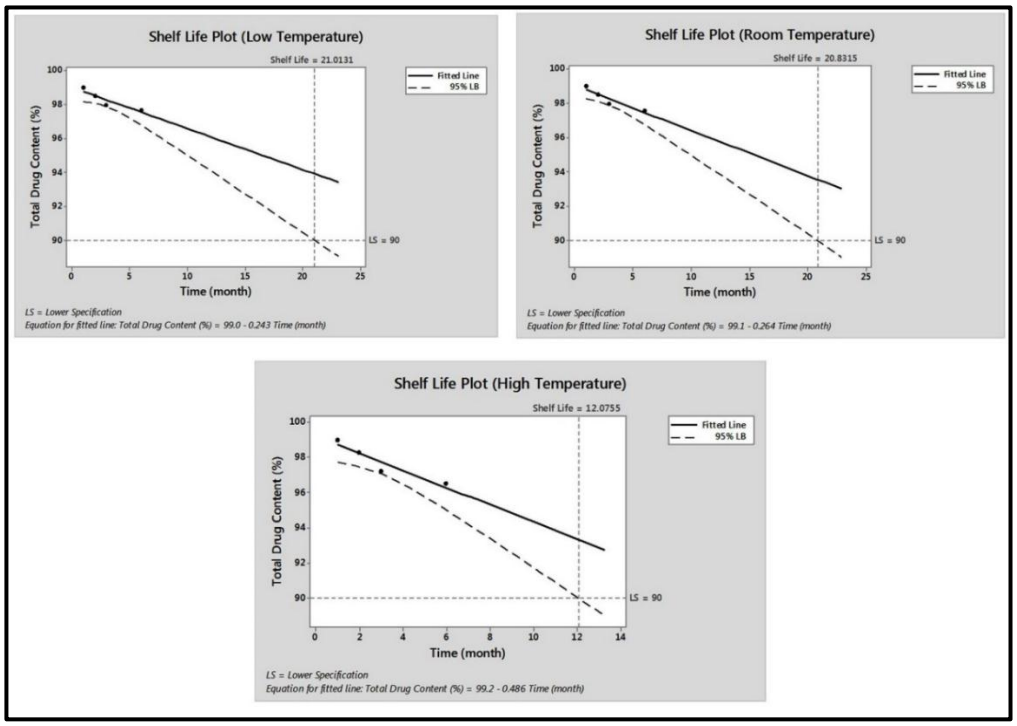

Figure 5.18 Shelf-life plots of optimized batch of TNZ-PCLNF membrane at different storage conditions, viz. Storage 1 (refrigeration), Storage 2 (room temperature) and Storage 3 (high temperature) LS: lower specification (90%).

5.2.12 *In vivo* study (Ligature-induced periodontitis in rats)

It had been reported that the structure of the periodontal tissue in rats is very similar to that of humans [Souza et al. 2006]. It had also been reported that the ligature-induced periodontitis model in rats presents various bacterial species, which are hybridized to probe of commonly observed periodontal bacterial species of humans. Therefore, Ligature-induced periodontitis in rats was used to study the progression of periodontitis and to test the effect of the developed TNZ-PCLNF membrane.

Figure 5.19 illustrates non-absorbable suture placed around the incisor teeth for induction of periodontitis in rats. Whereas, Figure 5.20(a) represents the graded response for continuity of epithelium and Figure 5.20(b) represents graded response for continuity of transseptal fibers of the interdental papilla respectively. It was observed that the group C rats showed significant improvement in the continuity of the epithelium of the Interdental papilla in comparison to the group A and group B

($p < 0.05$). The group C retained the continuity of epithelium of the Interdental papilla up to a large extent. The response of the group B regarding the continuity of epithelium was non-significant in comparison to the group A ($p > 0.05$). Further, in case of transseptal fibres of interdental papilla, a significant improvement was found in group C, compared to group A and group B ($p < 0.05$).

Figure 5.19 Image illustrating non-absorbable suture placed around the upper incisor teeth for induction of periodontitis in rats

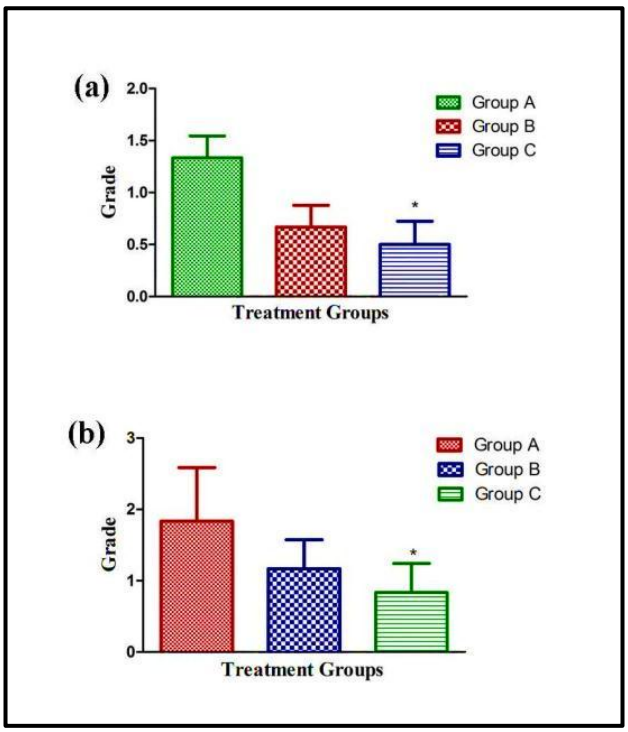

Figure 5.20 Graph represents (a) Graded response for continuity of epithelium in the interdental papilla and (b) Graded response for continuity of transseptal fibers in the interdental papilla. *$p < 0.05$, n.s. = not significant, compared to control group by one-way (ANOVA) followed by Tukey's multiple comparison test, $n = 6$.

Figure 5.21 shows the histo-micrograph of the periodontium of rats in different treatment groups subjected to ligature-induced periodontitis. The cementoenamel junction (CEJ)-bone distance, alveolar bone resorption and periodontal ligament degeneration could be used to assess periodontitis [Xie et al. 2011]. It can be observed from the Figure 5.21, that there was a clear demarcation of degeneration of ligament tissue in the different groups. It could be noticed that TNZ loaded nanofiber treated group showed minimal degeneration of periodontal ligament and cementoenamel junction (CEJ)-bone distance in comparison with the TNZ gel treated group.

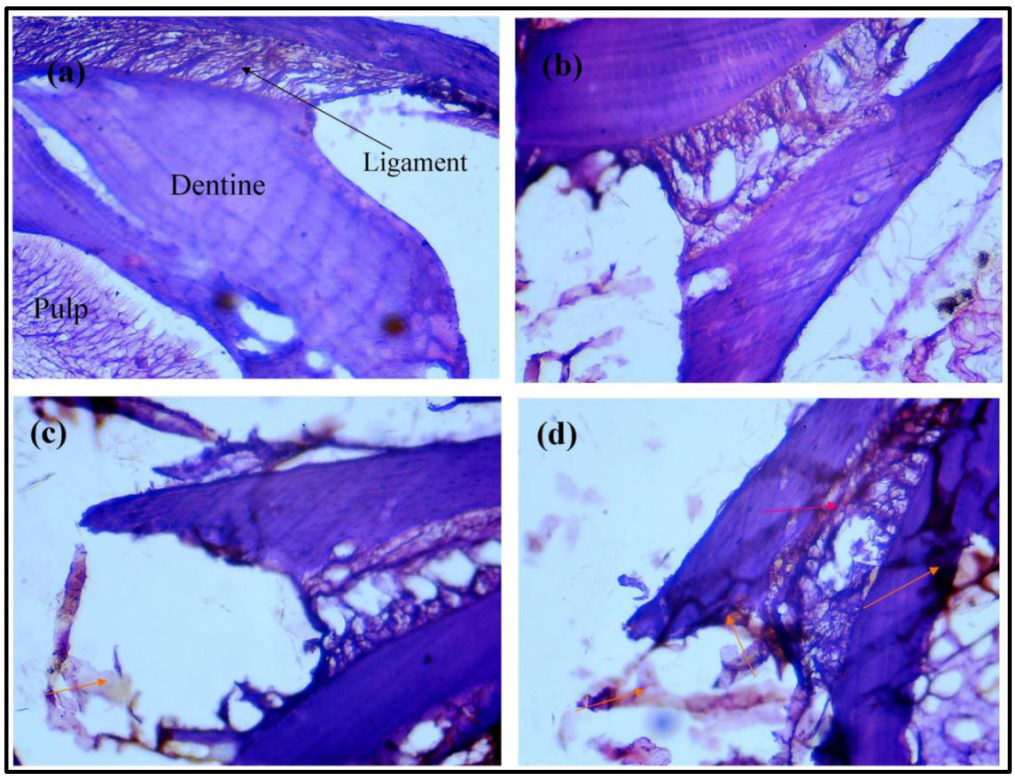

Figure 5.21 Histological results of the periodontium of rats in different treatment groups subjected to ligature-induced periodontitis (a) healthy periodontium (b) periodontitis induced periodontium showing disrupted ligament tissue structure and (c & d) treated with TNZ gel and TNZ-PCL nanofiber membrane respectively, arrow indicate the formation of ligament tissue.

5.3 Preparation, optimization, *in vitro* and *in vivo* characterization of TNZ encapsulated GE/PCL hybrid nanofiber membrane (TNZ-PGHNF)

In the first part of the study, the potential of PCL nanofiber loaded with TNZ against periodontal disease was proved. Although, the studied PCL nanofiber membrane had

certain limitations viz. interference with tissue regeneration owing to characteristics such as extremely long degradation time and hydrophobic nature of PCL which resulted in a lack of cell recognition sites for the assistance of cell adhesion and proliferation. Moreover, it also lacked mucoadhesive character which was required for the prolonged retention of nanofiber membrane in periodontal pockets. To overcome the abovementioned drawbacks, a blend of PCL with a mucoadhesive polymer like GE may prove to be a superior biomaterial which would exhibit the desired attributes of excellent biocompatibility, improved mucoadhesive property and hydrophilicity.

Electrospinning technique was employed for the preparation of GE/PCL nanofiber as this method is a simple, continuous and reproducible. Hexafluoro-2-propanol was selected as the solvent as it produced a clear homogenous solution of drug and polymer as well as an optimum conductivity for electrospinning process. The Formulation (TNZ-PGHNF) was optimized by using "Quality by Design" approach in order to meet the critical quality attributes of the final product.

5.3.1 Experimental design

A total of 17 batches of TNZ-PGHNF membrane were fabricated in accordance with the design matrix of BBD generated by Design-Expert software, by altering the independent variables, i.e. GE/PCL ratio (X_1), drug concentration (X_2), and applied voltage (X_3) in three defined levels. Two dependent responses were analysed, i.e. nanofiber diameter (Y_1) and EE (Y_2). The results for different experimental runs are summarized in Table 5.11. The useful results obtained by statistical analysis of data as shown in Table 5.12 reaffirmed the utility of "Quality by Design" approach in performing experiments.

Table 5.11 Box–Behnken experimental design representing experimental runs with independent variables and dependent responses of TNZ-PGHNF membrane[a]

Run No.	Independent variables			Dependent variables	
	X_1	X_2	X_3	Y_1	Y_2
Factorial Points					
1	-1	-1	0	219.7±12.4	88.8±0.8
2	1	-1	0	121.6±10.5	76.2± 1.2
3	-1	1	0	208±11.9	86.8±2.4
4	1	1	0	110.5±9.25	68.4±1.8
5	-1	0	-1	215.6±10.4	82.7±0.9
6	1	0	-1	120.3±12.2	70.5±0.6
7	-1	0	1	210.2±8.5	84.2±1.3
8	1	0	1	113.9±9.8	69.6±0.8
9	0	-1	-1	180.4±11.6	82.8±0.7
10	0	1	-1	176.3±11.2	74.5±1.4
11	0	-1	1	177.4±9.3	81.6±0.6
12	0	1	1	172.2±14.7	73.4±1.2
Centre Points					
13	0	0	0	172.6±12.5	79.4±0.9
14	0	0	0	170.7±10.8	80.3±0.7
15	0	0	0	172.2±13.4	81.2±1.0
16	0	0	0	171.6±10.7	80.8±0.8
17	0	0	0	170.3±11.4	82.4±1.4

[a]All data are shown as mean±S.D.; n = 3

In the polynomial equation, a direct relationship between the independent variables and dependent responses is denoted by a positive coefficient, whereas negative coefficient denotes an inverse relation. Figure 5.22 shows three-dimensional surface plots, which delineate the interaction of any two independent variables on the dependent variable, by keeping the third a constant level. Further, the utility of "Quality by Design" approach in performing experiments was confirmed by the statistical data analysis and statistical optimization.

Table 5.12 Statistical analysis results of lack of fit test and model summary for diameter and entrapment efficiency of TNZ-PGHNF membrane

Model	Lack of fit test					Model summary statistics					Remark
	SS	df	MS	F-Value	p-Value prob >F	SD	R^2	Adjusted R^2	Predicted R^2	PRESS	
Diameter											
Linear	422.50	9	46.94	49.57	0.001	5.73	0.9781	0.9730	0.9552	870.44	
2FI	416.67	6	69.45	73.33	0.0005	6.48	0.9784	0.9654	0.8936	2069.25	
Quadratic	17.50	3	5.83	6.16	0.0557	1.74	0.9989	0.9975	0.9853	286.00	Suggested
Cubic	0.000	0	-	-	-	0.97	0.9998	0.9992	-	+	Aliased
Pure error	3.79	4	0.95	-	-	-	-	-	-	-	-
Entrapment Efficiency											
Linear	30.24	9	3.36	2.73	0.1734	1.64	0.9418	0.9283	0.9114	53.51	
2FI	28.39	6	4.73	3.84	0.1068	1.83	0.9448	0.9117	0.8550	87.58	
Quadratic	2.17	3	0.72	0.59	0.6553	1.01	0.9883	0.9731	0.9298	42.38	Suggested
Cubic	0.000	0	-	-	-	1.11	0.9918	0.9674		+	Aliased
Pure error	1.59	4	1.23	-	-						

SS: sum of squares, df: degree of freedom, MS: mean square, SD: standard deviation, PRESS: Predicted Residual Error Sum of Squares; 2FI: two factor interaction, +: PRESS statistic not defined, p-value < 0.05 was considered as statistically significant.

5.3.1.1 Influence of independent variables on diameter (Y_1)

The diameter plays a crucial role in achieving the desired release profile from the nanofiber-based drug delivery systems. In order to gain effective mass transfer, the smaller diameter of nanofibers is preferred as it provides shorter diffusion passage length along with greater surface area. The diameter of the fabricated nanofibers was found to be in the range of 110.5±9.25 nm to 219.7±12.4 nm for different factor level combinations. The relationship between the diameter of nanofibers and independent variables was found to be in accordance with the following polynomial equation.

$$\text{Diameter} = Y_1 = 171.48 - 48.58X_1 - 3.80X_2 - 1.73X_3 + 0.57X_1X_2 + 1.03X_1X_3 - 0.28X_2X_3 - 9.23X_{12} - 2.68X_{22} + 1.97X_{32}$$

The quadratic model was found to be significant as it had F value of 709.38 ($p < 0.0001$) and best suited for establishing a relation between the diameter of nanofibers and independent variables. The higher value of R^2 coefficient (0.9989) indicated the existence of a good correlation between predicted values and experimental values. The difference between the predicted R^2 (0.9853) value and adjusted R^2 (0.9975) value was very less, which indicated the suitability of the selected model for prediction of responses. The lack of fit data was found to be non-significant with F-value 4.37 and p values 0.0589, inferring the adequate fitting of data. Moreover, a lower value for the coefficient of variation (0.82%) confirmed the reliability of the quadratic model with a higher degree of precision. On the basis of this analysis, the selected quadratic model proved to be suitable to navigate generated design space for nanofibers [Patel et al. 2015].

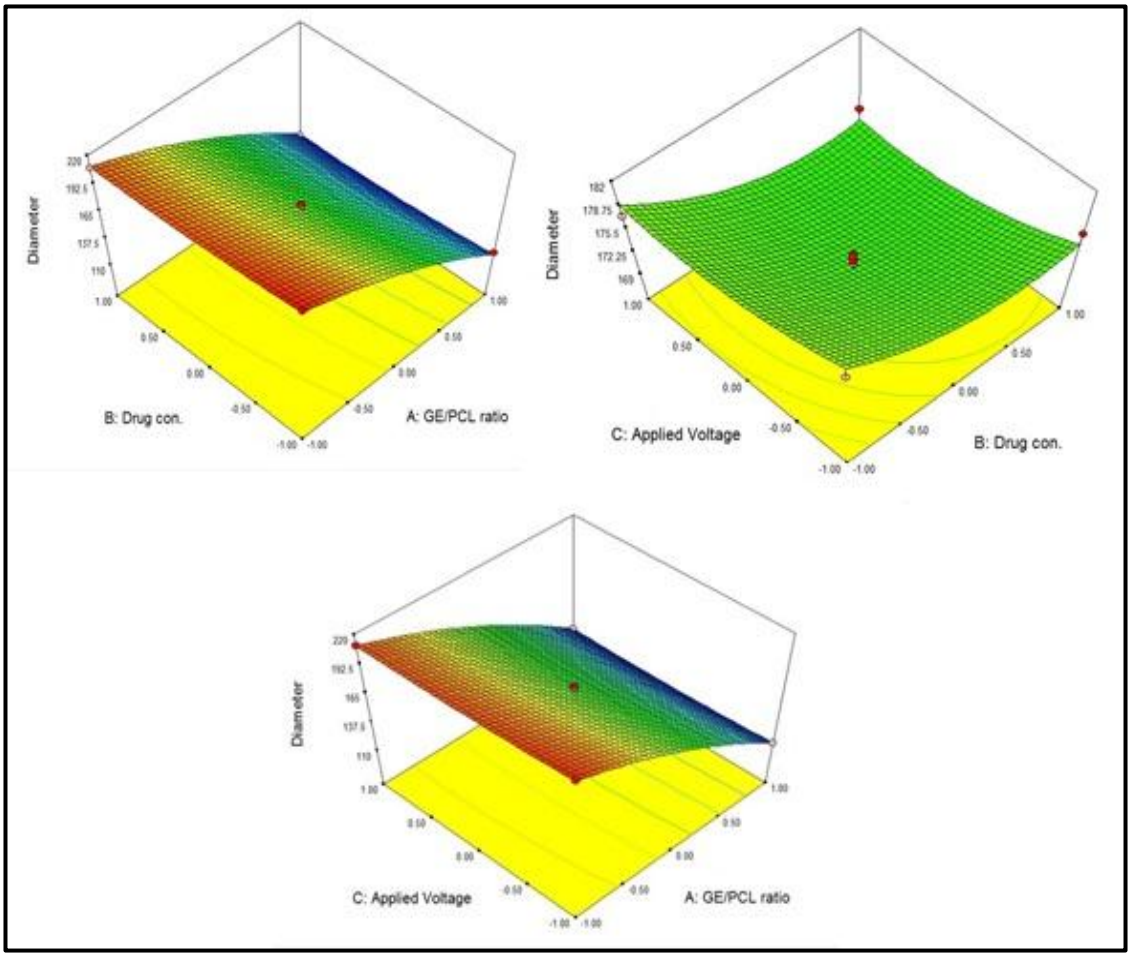

Figure 5.22 Response surface 3D plots showing the effect of independent variables on diameter of nanofiber

As indicated in Figure 5.22, GE/PCL ratio (X_1) exhibited an inverse relationship with the diameter of TNZ-PGHNF membrane owing to its direct impact on the viscosity. At higher GE/PCL ratio, the viscosity of the electrospinning solution decreased leading to reduced resistance of jet. This ultimately leads to the formation of thinner fibres due to bending instability and rapid solidification of the polymer jet [Jacobs et al. 2010]. Similarly, the drug concentration and the applied voltage also presented an inverse impact on the diameter as depicted in Figure 5.22. A notable reduction in viscosity was observed at a higher amount of TNZ, which might be due to TNZ molecules acting as a plasticizer for GE/PCL chains. Simultaneously, a rise in the conductivity of electrospinning solution was observed as a consequence of the enhanced polarity. Thus,

the combined effect of reduced viscosity along with increased conductivity might have resulted in decreased diameter of nanofibers. Likewise, an increase in the applied voltage (X_3) leads to a rise in the electric charges being carried by the electrospinning jet, which in turn enforces generation of higher elongation forces to the jet under applied electrical field [Zamani et al. 2010]. Higher solution conductivity leads to enhanced bending instability and thereby, ultimately causing elongated jet path with higher stretching of the solution, leading to reduced nanofiber diameter.

5.3.1.2 Influence of independent variables on entrapment efficiency (Y_2)

The Entrapment Efficiency of TNZ-PGHNF membrane was found to be varying between a minimum of 68.4% to a maximum of 90.8% for different experimental runs. The second order polynomial equation which depicted the effect of independent variable on EE (Y_2) can be written in terms of coded significant model terms as:

$$EE = 80.82 - 7.22X_1 - 4.29X_2 - 0.71X_3 + 0.55X_1X_2 - 0.40X_1X_3 + 0.025X_2X_3 - 1.05X_{12} - 0.72X_{22} - 2.02X_{32}$$

The quadratic model was analysed to be significant with the Model F value of 65.42 ($p < 0.0001$) as indicated by model summary statistics. A good correlation between the predicted and the experimental values was indicated by the high value of R^2 coefficient (0.9883). The model also revealed an adequate fitting to the data which was indicated by a non-significant lack of fit, having p values of 0.6553 ($p < 0.05$). The difference between predicted R^2 (0.9298) and adjusted R^2 (0.9731) value is very less, which indicated the adequacy of the selected model for prediction of responses. Thus, this model was selected for the analysis of the effect of independent variables on EE. ANOVA analysis depicted X_1, X_2, X_3, X_1X_2, X_1X_3, X_2X_3, X_{12}, X_{22}, X_{32} as the significant model terms.

The ratio of GE/PCL (X_1), drug concentration and applied voltage have a negative impact on EE as depicted in Figure 5.23. Also, higher coefficient value (7.22) of the ratio of GE/PCL (X_1) in the polynomial equation is indicative of the fact that ratio GE/PCL (X_1) has more significant effect on EE as compared, followed by the concentration of drug (X_2) and applied voltage (X_3). Though, the effect of independent variables on EE was lower as compared to their effect on the diameter of the nanofiber. This can be concluded by observing the lower coefficient value of the main effects and interactive terms in the polynomial equation of EE as compared to that of nanofiber diameter.

A significant increase in the EE of formulated TNZ-PGHNF membrane was observed with a decrease in the GE/PCL ratio. The lower GE/PCL ratio conferred a diffusional barrier due to increased viscosity of the solution and hence hindered the outward movement of TNZ, ultimately enhancing the EE. Increased diffusional path length owing to increased diameter at a lower GE/PCL ratio might also be one of the plausible reasons for higher EE [Budhian et al. 2007]. Conversely, a significant reduction in the EE was observed at higher concentrations of the drug. The probable reason might be the presence of the solubilized drug in the polymeric solution, which might have enhanced the migration of dissolved drug towards the surface of the nanofiber membrane during the electrospinning process. Likewise, a decrease in the EE was achieved with a substantial increase in applied voltage (X_3) as a result of a consequential reduction in the diameter of the nanofiber.

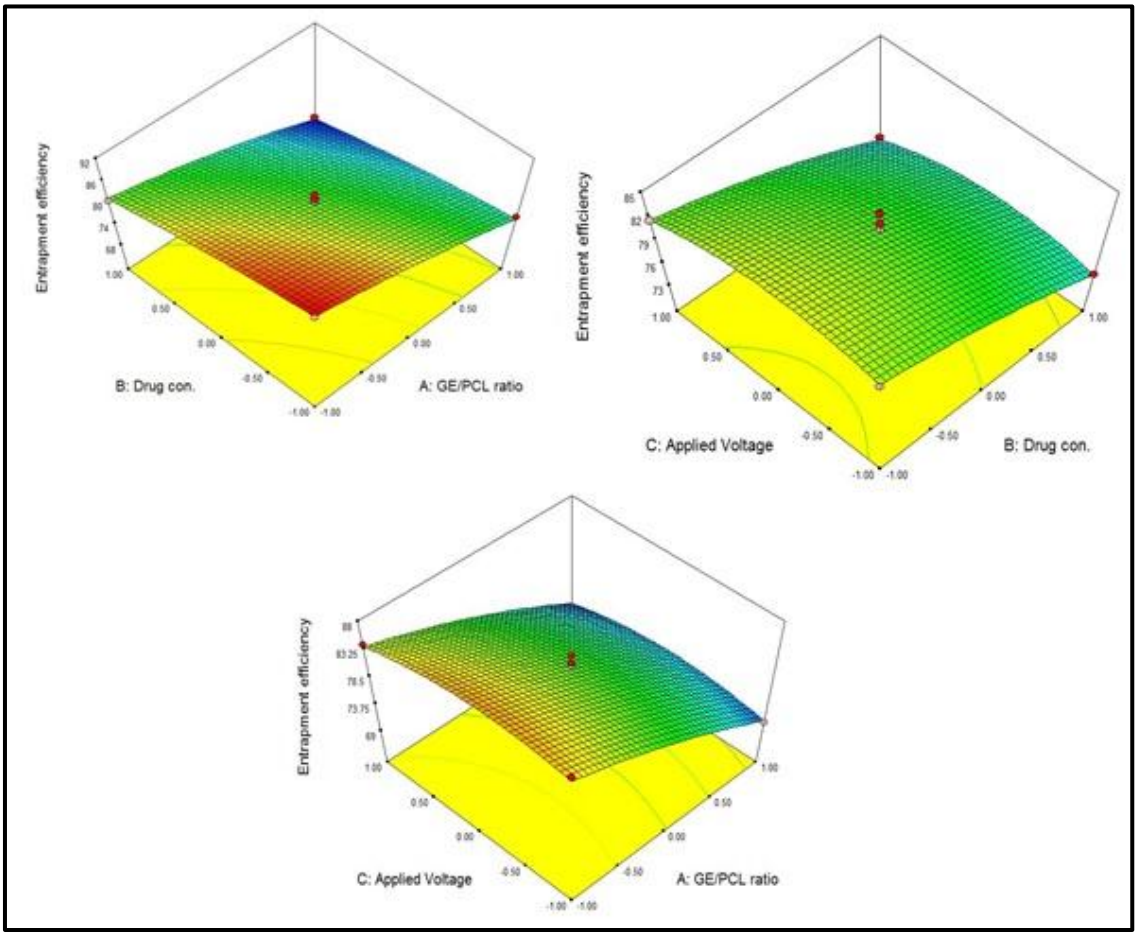

Figure 5.23 Response surface 3D plots showing the effect of independent variables on entrapment efficiency of nanofiber.

5.3.1.3 Optimization of TNZ-PGHNF membrane

The formulation was statistically optimized by using the desirability based numerical optimization technique. Different constraints were fixed for all three independent variables in the Design Expert® Software to achieve maximized EE with minimum diameter. Predicted levels of independent variables X_1, X_2 and X_3 were found to be 0.42, 10% w/w and 12 kV, respectively, with a diameter of 162.54 nm, EE of 81.93% and desirability of 0.856. After that, the optimized TNZ-PGHNF membrane was formulated with predicted levels of independent variables in order to establish the validity as well as the predictability of BBD. The optimized experimental TNZ-PGHNF membrane exhibited a diameter of 160.54±11.8 nm and EE of 82.75±1.6. The lower value of bias between the predicted values and the experimental values indicated that

results were in good agreement with observed values and thereby, confirmed the reliability of BBD for statistical optimization so as to develop nanofiber system for TNZ delivery aimed towards the treatment of periodontitis.

5.3.2 Solid-state characterization of TNZ-PGHNF by FT-IR, DSC and PXRD

5.3.2.1 Fourier transform infrared spectroscopy (FTIR) study

FTIR studies were performed to confirm the compatibility between drugs and polymer as well as to analyse any possible effect of the electrospinning process on the functional group of drug present in the formulation. FTIR spectra of TNZ, GE, PCL and optimized nanofiber membrane are depicted in Figure 5.24. TNZ exhibited characteristic peaks at 1265 cm^{-1} (C-O stretching), 1301 cm^{-1} (asymmetric stretching vibration of S=O) and 1367 cm^{-1} (symmetric stretching vibration of N=O) in the spectrum. Moreover, FTIR peaks appeared at 1521 cm^{-1}, 1492 cm^{-1} and 2914-3001 cm^{-1} which were attributed to the asymmetric stretching vibration of C=N (imidazole ring), N=O (NO_2), and C-H, respectively. FTIR spectra corresponding to GE showed characteristic band at approximately 1650 cm^{-1} (amide I) and 1540 cm^{-1} (amide II), whereas PCL showed characteristic peak at 1733 cm^{-1} (C=O stretching), 2853 cm^{-1} (symmetric CH_2-stretching) and 2948 cm^{-1} (asymmetric CH_2 stretching) [Shalumon et al. 2010]. The FTIR spectrum of nanofiber membrane exhibited all characteristics peak corresponding to TNZ, GE and PCL with slight variation in frequencies as compared to its pure form. This indicates the compatibility between the drug and polymer and absence of any possible interaction between them. Also, the conclusion can be made that electrospinning process did not impair the molecular structure of TNZ present in the nanofiber membrane. Thus, it can be speculated that the drugs and polymers are compatible with one another and can be formulated into nanofiber membrane.

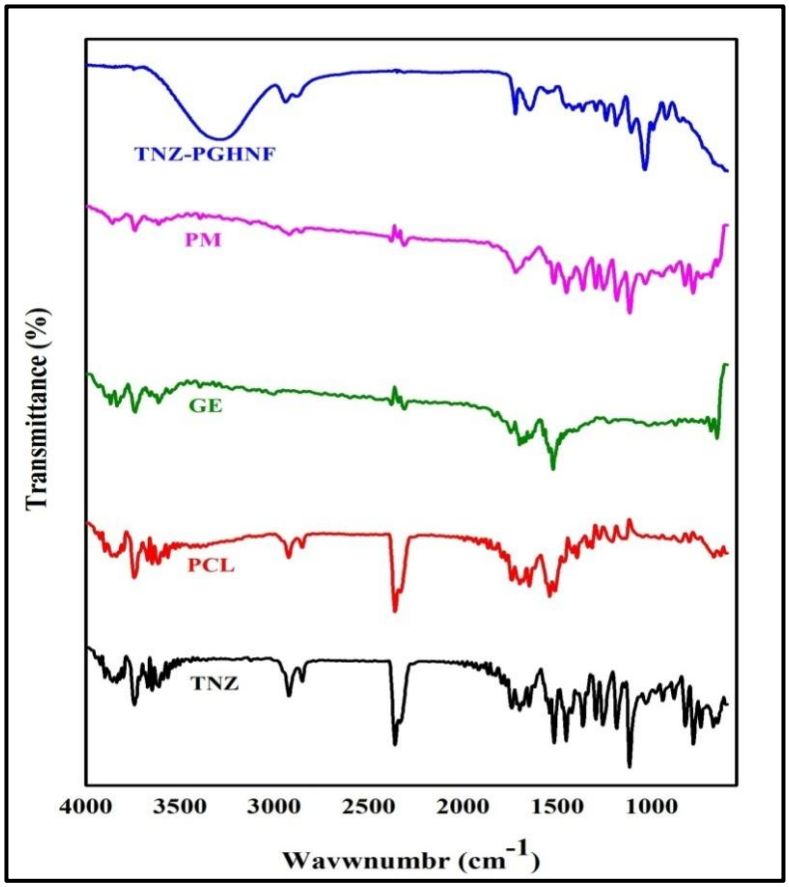

Figure 5.24 FTIR spectra of TNZ, PCL, GE, PM of TNZ with excipients and optimized formulation (TNZ-PGHNF)

5.3.2.2 Differential scanning calorimetry (DSC) study

DSC studies were performed to characterize the solid state of drugs and polymers. Moreover, the compatibility between drug and excipients was also evaluated by observing the thermal behaviour of compounds such as appearance or disappearance of an endothermic or exothermic peak. If all the peaks remain the same, we can conclude that drug and excipients are compatible to one another. DSC thermogram of TNZ, GE, PCL and optimized nanofiber membrane are depicted in Figure 5.25. DSC thermogram of TNZ showed a sharp endothermic peak at 128.5 ºC which represented its melting point. The sharp melting peaks exhibited by TNZ confirmed the existence of drug in crystalline form. GE exhibited three endothermic peaks at diffraction angles of 82.4 °C, 215.6 °C and 283.7 °C. Thermogram of PCL exhibited a characteristic peak at 60 ºC

representing its semi-crystalline nature. The optimized TNZ-PGHNF membrane exhibited flat curve without the presence of any sharp endothermic or exothermic peaks of the drug. This indicated that crystalline state were transformed to the amorphous state during the formulation process [Patel et al. 2015]. This might have occurred due to the shear stress offered by the stirrer and electrospinning process during the fabrication of nanofiber preventing the recrystallization of TNZ, leaving TNZ in molecular dispersion form inside the TNZ-PGHNF membrane.

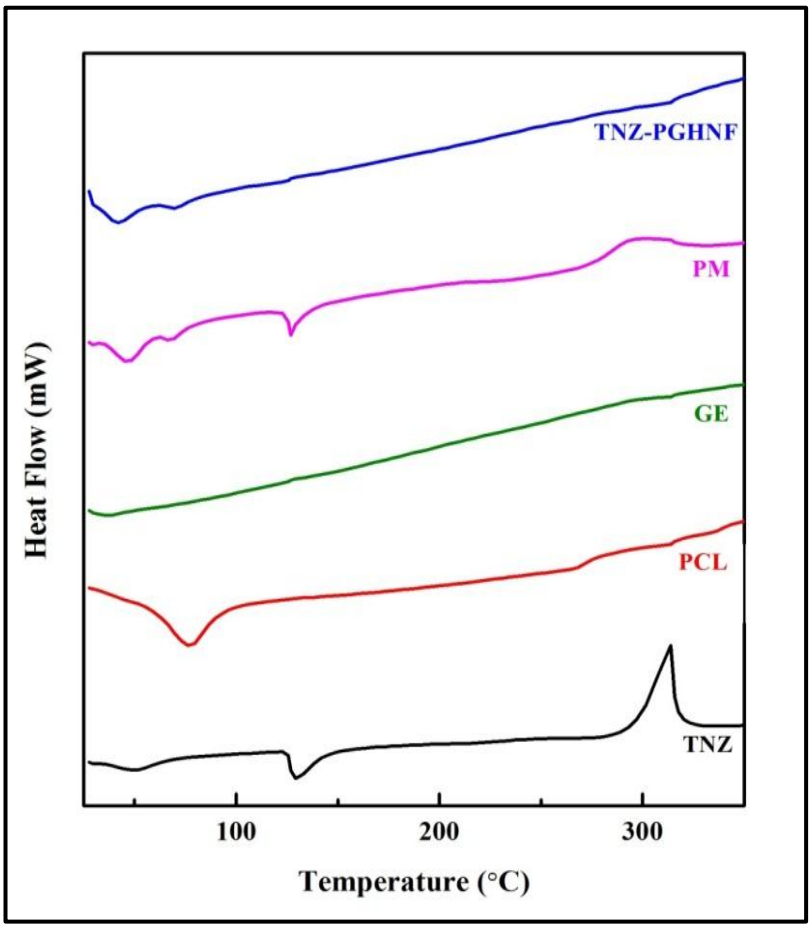

Figure 5.25 DSC Thermograms of TNZ, PCL, GE, PM of TNZ with excipients and optimized formulation (TNZ-PGHNF)

5.3.2.3 Powder X-ray diffractometry (PXRD) study

PXRD pattern of pure drug, GE, PCL and TNZ-PGHNF membrane were recorded and analysed in order to understand the crystallinity of the drug in the nanofiber membrane.

(Figure 5.26). TNZ exhibited four characteristic peaks at 2θ of 12.2º, 17.9º, 22.7º and 33.8º which demonstrated the crystalline nature of the drug. Two peaks were exhibited by PCL in the diffractogram at a diffraction angle of 22.4º and 24.6º indicating the semi-crystalline nature of PCL while two broad peaks were present in the diffractogram of GE at a diffraction angle of 20.9° and 31.5°. Whereas, PXRD pattern of TNZ-PGHNF membrane demonstrated more of an amorphous nature as compared to pure TNZ which was due to shifting of the diffraction intensity. This hereby conformed that the physical state of TNZ transformed from crystalline to amorphous while being entrapped in the nanofiber membrane.

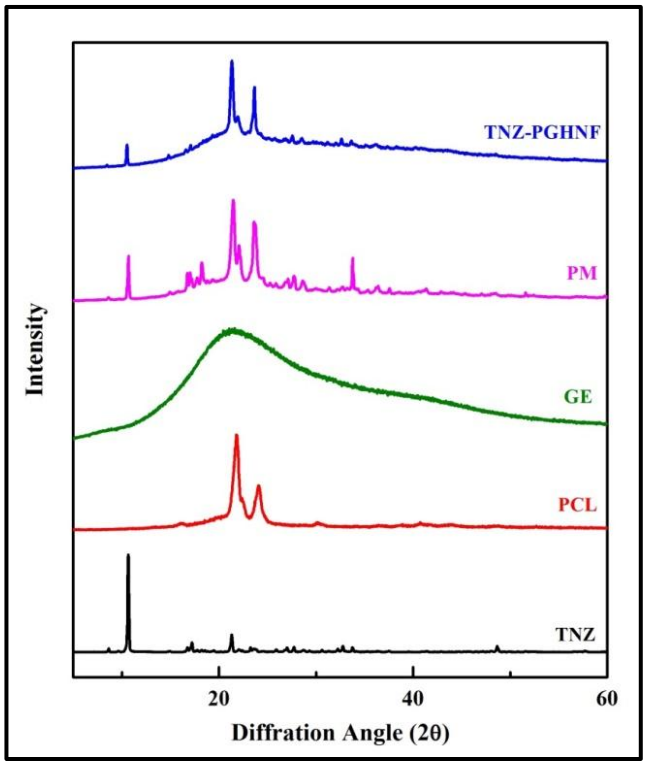

Figure 5.26 Overlay PXRD patterns of TNZ, PCL, GE, PM of TNZ with excipients and optimized formulation (TNZ-PGHNF)

5.3.3 Shape and surface morphology

Figure 5.27 depicts SEM micrographs of the optimized TNZ-PGHNF membrane and placebo nanofiber membrane at different magnification. As evident from the Image, nanofibers with smooth and uniform characteristics were formed without any bead

defects. The diameters of the nanofiber with different concentration of the drug are in the range of a minimum of 110.5±9.25 nm to a maximum of 219.7±12.4 nm and shown in the Table 5.11. The porosities of the nanofiber membranes were found in the range of 53-75%.

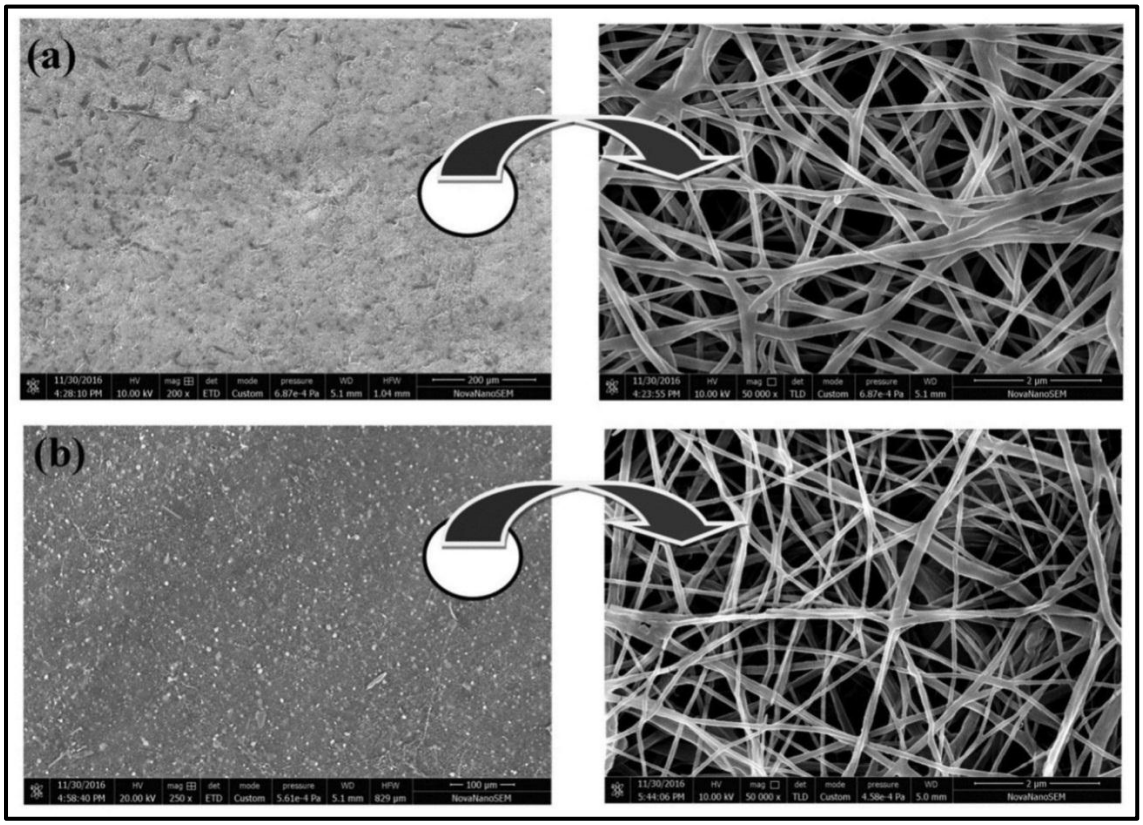

Figure 5.27 HR-SEM images of optimized electrospun TNZ-PGHNF membrane at different magnification (a) Placebo nanofiber (b) TNZ loaded nanofiber membrane

AFM study was performed to get detailed idea about the structure, surface morphology and diameter of electrospun nanofiber membrane. The topographic and 3D AFM images generated by the atomic level interaction between surfaces of electrospun nanofiber and the sharp tip of the scanner are depicted in Figure 5.28. The fiber diameters were measured from the height and were found in accordance with the SEM study. AFM micrographs presented an arbitrarily interconnected structure, smooth morphology and uniform distribution of electrospun nanofiber with rare bead defect.

Uniform mixing of drug and polymer in the solvent could be the possible reason for the smooth surface.

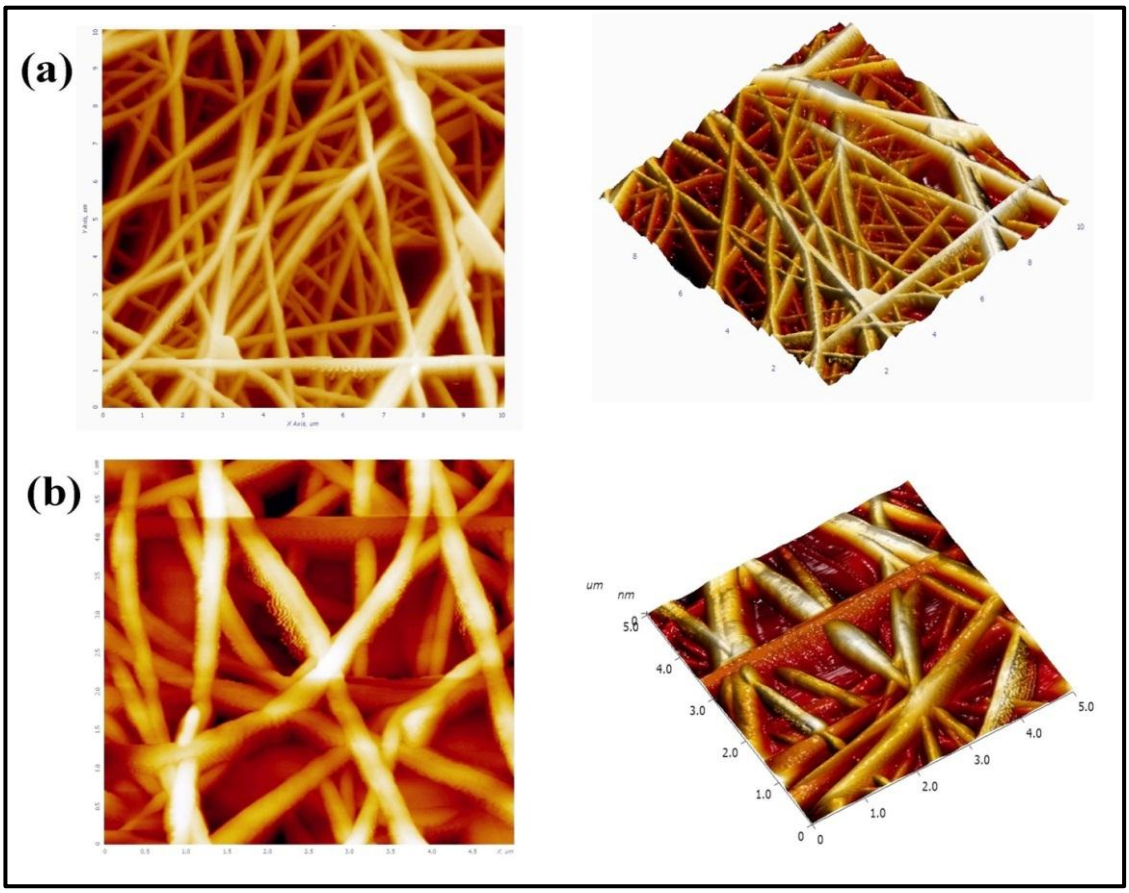

Figure 5.28 Surface morphology of optimized nanofiber membrane at different resolutions: 2D and 3D-atomic force microscopic images showing smooth and bead free surface of nanofiber membrane

5.3.4 Surface pH and Drug Content Uniformity

Highly acidic or highly basic pH of nanofiber membrane adversely affects the area of application and causes irritation to oral mucosal membrane leading to patient incompatibility [Ahuja et al. 2006]. Moreover, acidic pH also leads to the dissolution of enamel and demineralization of the teeth. To overcome these challenges, the pH of the nanofiber membrane must be taken into consideration and must be assured to be closer to pH of the GCF (pH 6.6). Surface pH of all the batches was found to be ranging from 6 to 7.5 indicating the suitability of the formulation for pocket insertion. In fact, formulations with pH 6.5 to 7 are preferred over others as the closeness of pH values to

neutrality. The content uniformity studies of the nanofiber showed that the drug was uniformly distributed and all the batches showed recovery in the range of 83.5% to 87.0%.

Table 5.13 Physicochemical characteristics of different batches of TNZ-PGHNF membrane

Run No.	Mucoadhesive strength* (gm/cm^2)	Total drug Content* (%)	Surface pH
1	121±1.42	86.2±2.45	6.5
2	120±1.25	87.0±2.87	6.5
3	112±1.60	83.6±3.25	7.5
4	114±1.45	84.8±2.45	7.5
5	116±1.32	85.4±3.77	7.0
6	117±0.75	86.0±2.25	6.5
7	115±1.22	85.5±2.67	6.0
8	113±1.32	84.3±2.65	7.5
9	116±1.20	86.7±2.58	6.5
10	112±1.35	83.5±3.45	7.5
11	117±1.37	86.5±2.47	7.5
12	115±1.42	84.2±3.67	7.5
13	114±1.25	86.4±3.27	7.0
14	114±1.30	85.2±2.55	7.0
15	116±1.12	86.5±2.25	7.0
16	115±1.52	86.3±2.70	7.0
17	116±1.42	86.0±2.35	7.0
Optimized TNZ-PGHNF	120±1.25	85.6±2.32	6.5

*Result are presented as mean ±SD, (n=3)

5.3.5 Contact angle

Contact angle represents the wettability or hydrophilicity of the nanofiber membrane, which directly influences the attachment and proliferation of cells. In spite of the excellent biocompatibility of PCL, the problem associated with this material is its

hydrophobicity. Hence, contact angle estimations were evaluated to explore the impacts of GE content on the hydrophilicity of the nanofiber membrane.

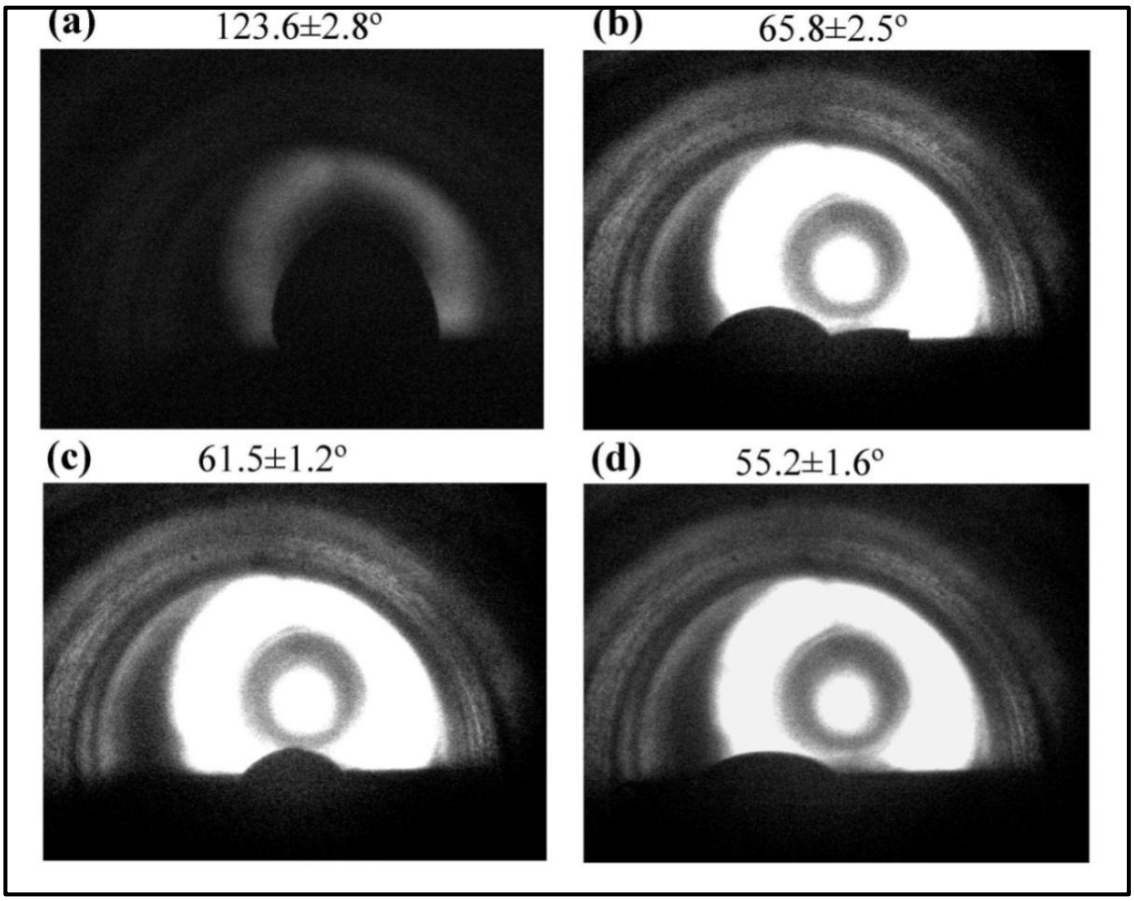

Figure 5.29 Contact angle of TNZ-PGHNF membrane containing different proportion of GE/PCL: (a) 0%; (b) 10.0%; (c) 20.0%; (d) 30.0%. Images suggesting that with the increase of GE content, water contact angle of the nanofiber membranes decreases, indicating increase in hydrophilicity of nanofiber membrane.

The outcomes are represented in Figure 5.29. It was observed that PCL nanofiber membrane exhibited the highest contact angle (123.4±2.5º). As the concentration of GE increased, water contact angle of the membrane was found to be reduced whereas hydrophilicity and wettability of the nanofiber membrane increased. This change could be ascribed to the presence of carbonyl and polar amine functional group in the GE molecule. This increase in the hydrophilicity will be expected to increase the cell adhesion at the site of action and enhanced proliferation of cells, tissue recovery and the biodegradation of the nanofiber membrane [Jing et al. 2015].

5.3.6 *In vitro* mucoadhesion studies

One of the essential properties of nanofiber is mucoadhesion to the gingival mucosa. The nanofiber membrane is required to possess characteristics mucoadhesive property so that it can be retained in the periodontal pocket up to several days and it should not ooze out during movement of jaws. The mucoadhesive strength of the polymer depends upon the degree of hydration of polymer chains. Hydration helps in expanding the polymer chain, hence exposing more available sites for bond formation and creating channels for diffusion of the polymer chain. The bioadhesion property of the polymer results due to the inter-diffusion and entanglement of expanded polymer chains as well as the formation of secondary bonds which can further be enhanced by increasing contact time and applied force [Mayet et al. 2014, Sharma et al. 2016]. The mucoadhesive detachment force for optimized drug-loaded nanofibers and blank nanofibers was found to be 120 gm/cm^2 and 131 gm/cm^2, respectively. The reduced value of mucoadhesive force in case of drug-loaded nanofibers can be attributed to the decreased specific area associated with a wider diameter of drug-loaded nanofibers as compared to that of the blank nanofibers.

5.3.7 Entrapment efficiency

The EE of different batches of TNZ-PGHNF membrane was found to be in the range of 68.4±1.7% to 90.8±2.5% which is presented in Table 5.11. The outcomes revealed a precise dependence of the entrapment efficiency on the concentration of the incorporated drug. It was observed that EE decreased at higher drug concentration; which might be due to the inclination of the dissolved drug molecules in the polymer solution to relocate to the surface or close to the surface of nanofiber during electrospinning procedure. Another reason could be the loss of a part of the aggregated drug, which might not have been entrapped into the nanofiber membrane. Moreover,

the entrapment of TNZ into nanofiber membrane also depends on the factors such as effective hydrogen bonding of TNZ with PCL and homogenous mixing of TNZ and GE/PCL in the solvent.

5.3.8 *In vitro* release study

In vitro drug release study of TNZ from nanofiber membrane and pure drug, suspension was performed in McIlvaine buffer (pH 6.6) and release data are shown in Table 5.14 and

Table 5.15. As illustrated in the Figure 5.30, the drug was released from the nanofiber membrane in a biphasic mode, with an initial burst release followed by a sustained release. The nanofiber membrane exhibited a significant release of 27% of the drug within 8 hr of release studies whereas almost 90% TNZ was released within first 8 hr from TNZ drug suspension. Therefore, TNZ-PGHNF membrane can be said to greatly reduce the burst effect and produce sustained release of TNZ over 15 days. The immediate burst release was observed due to the leaching of free drug particles on the superficial layer of the nanofiber membrane, in immediate access to the dissolution media. The burst release of antibiotics is essential for the antimicrobial therapy to combat the presence of the bacterial load in the periodontal pockets, provide immediate effect and achieve MIC [Khan et al. 2016b]. The drug release mechanism and release kinetics were further determined by substituting the drug release data to different release kinetic models. The release kinetic data of the optimized batch with obtained r^2 values for different models are represented in Table 5.16. The modelling confirmed that the drug release pattern from TNZ-PGHNF membrane was best explained by Korsmeyer-Peppas equation with the highest value of linearity ($r^2 > 0.994$) in comparison to other models. Moreover, the diffusion coefficient (n) value for Korsemeyer-Peppas equation for all batches was found to be less than 0.5 which reveals

that the drug release from the nanofiber membrane followed diffusion mechanism [Costa and Lobo 2001].

Table 5.14 *In vitro* drug release data of the optimized TNZ-PGHNF membrane in McIlvaine buffer pH 6.6

Time (hr)	Cumulative % drug release
1	13.6±4.33
2	17.8±3.67
4	24.5±3.26
6	27.2±3.44
8	31.2±2.77
12	37.7±4.22
24	46.6±4.5
48	54.5±3.24
72	60.9±4.25
96	65.7±3.78
120	69.4±3.25
144	72.2±2.76
168	74.8±3.28
192	79.2±2.85
216	81.7±3.85
240	84.6±2.72
264	86.5±2.64
288	89.3±2.25
312	91.5±4.2
336	93.4±2.78
360	94.3±2.35

Results are shown as mean ±S.D.; n = 3

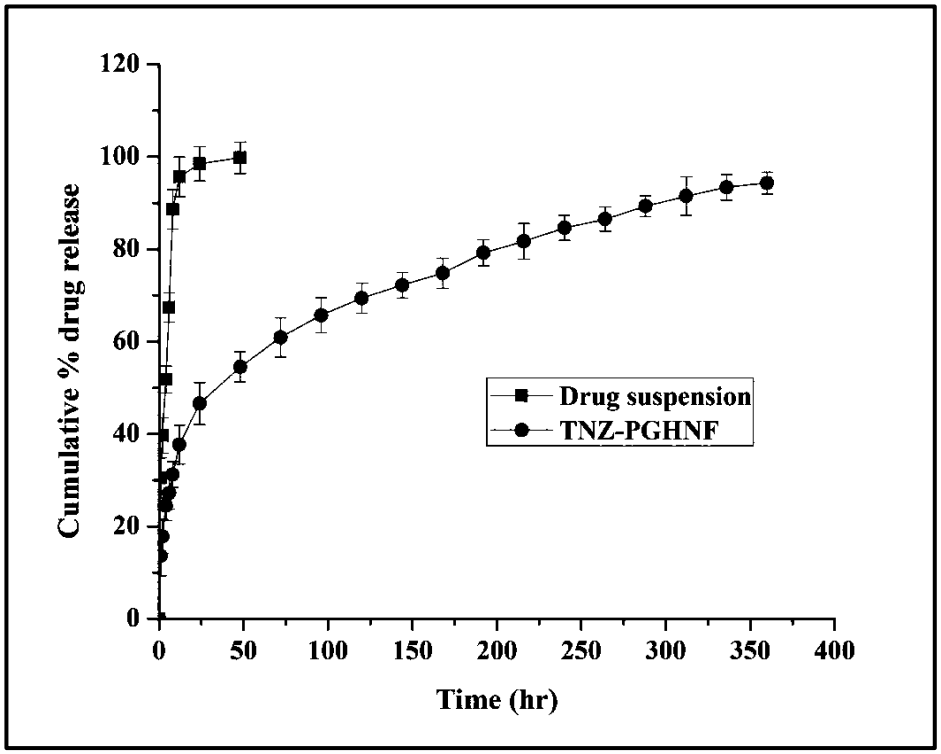

Figure 5.30 *In vitro* drug release profile of optimized TNZ-PGH nanofiber and drug suspension in McIlvaine buffer pH 6.6 (vertical bars represent the SD, results are shown as mean ±S.D.; n = 3)

Table 5.15 *In vitro* drug release data of the TNZ suspension in McIlvaine buffer pH 6.6

Time (hr)	Cumulative % drug release
1	29.3±3.30
2	37.5±3.54
4	52.7±4.25
6	66.4±2.55
8	85.5±3.65
12	96.6±2.35
24	97.4±4.46
48	98.7±2.65

Results are shown as mean ±S.D.; n = 3

Table 5.16 Release kinetic modelling for optimized batch of TNZ-PGHNF in McIlvaine buffer pH 6.6

Batch	Zero order	First order	Higuchi model	Korsmeyer-Peppas model
TNZ-PGHNF	$r^2 = 0.816$	$r^2 = 0.512$	$r^2 = 0.946$	$r^2 = 0.960$ $n = 0.271$

5.3.9 *In vitro* antibacterial study

The *In vitro* antibacterial activity of the electrospun nanofiber membrane was evaluated using well diffusion method in which the zone of inhibition against *S. aureus* was measured (MTCC1303). Figure 5.31 shows the result of the antibacterial activity of nanofiber membrane against *S. aureus*. It was observed that all the drug-loaded nanofiber membranes exhibited a prolonged antibacterial activity over a period of 21 days, whereas placebo membrane showed non-significant antibacterial activity. The mean inhibition zone was observed to be 39.40±0.65 mm, 42.8±1.5 mm and 45.8±1.25 mm on the first day for TNZ-PGHNF (10%), TNZ-PGHNF (20%) and TNZ-PGHNF (30%) membrane, respectively. After that, the inhibition zone slowly decreased to 10.2±0.55 mm, 12.25±1.2 mm and 14.5±0.85 mm at the end of 21 days of incubation, which was calculated to be equivalent to 3.4, 4.10, and 5.25 µg/ml of TNZ. Since the MIC of TNZ against periodontal pathogen was reported as 2.4 µg/ml. Therefore, we can come to the conclusion that TNZ is released from nanofiber membrane at a constant rate and is effective against these bacterial strains over 21 days [Kassem et al. 2015]. Furthermore, loading of TNZ into the nanofiber membrane using electrospinning did not change the antibacterial activity of the drug.

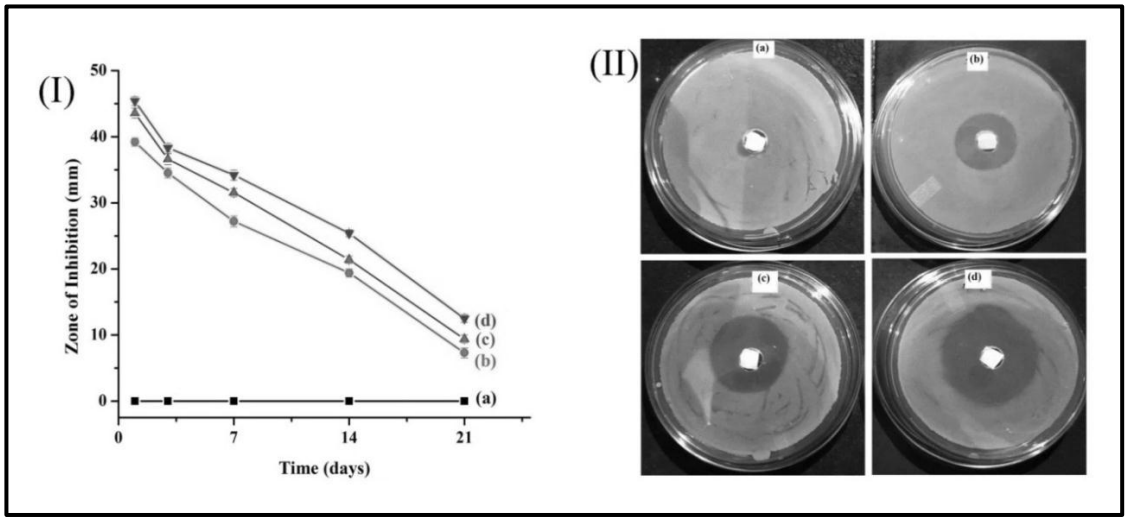

Figure 5.31 Graphical illustration representing inhibition zone diameter versus incubation time for TNZ-PGHNF membrane containing w/w percentages of TNZ (a) 0%; (b) 10% (c) 20% and (d) 30% against *S. aureus.* (II) Inhibition of bacterial growth on agar plate against *S. aureus.*

5.3.10 Cytocompatibility study

Using MTT test, cell viabilities of mouse fibroblast (L-929 cell lines) treated with different aliquots of DMEM taken from media incubated with nanofiber from 1-21 days was determined by comparing with the number of living cells of a negative control depicted in Figure 5.32. It was evident that none of the TNZ-PGHNF membranes impairs cell viability more than 10%, indicated that the DMEM aliquots of nanofiber membrane were not cytotoxic to the cells. Figure 5.33 shows the images obtained from the microscopic analysis of the L-929 cells that were exposed directly on the surface of the medicated nanofiber membrane with different concentrations of TNZ and coloured with FDA and EtBr. The fibroblasts were observed as green coloured due to staining by FDA and exhibited their specific structures related to the cell motility of fibroblasts-filopodia and lamellipodia [Xue et al. 2014c]. This clearly suggested the cytocompatibility of nanofiber membrane to the cells. From the results, it was concluded that the TNZ-PGHNF membrane would not cause any toxicity to the periodontal tissues during its application. Reise et al also reported similar results while

studying the release of metronidazole from electrospun poly (l-lactide-co-d/l-lactide) nanofiber for the treatment of periodontitis [Reise et al. 2012].

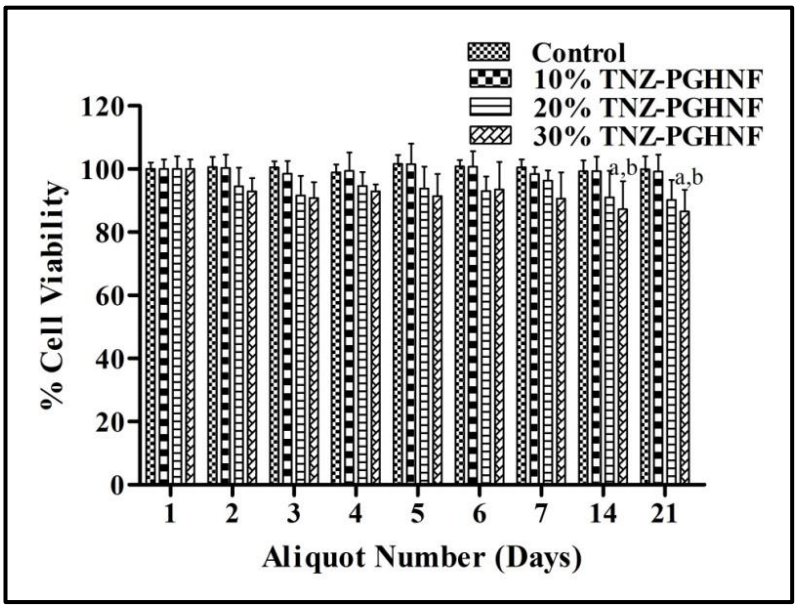

Figure 5.32 Graphics illustrating L-929 cell viability (%), measured by MTT assay, after exposure to aliquots of DMEM media. DMEM aliquots were taken from the nanofiber membrane on successive days (1–7) and then for a week (days 14-21).

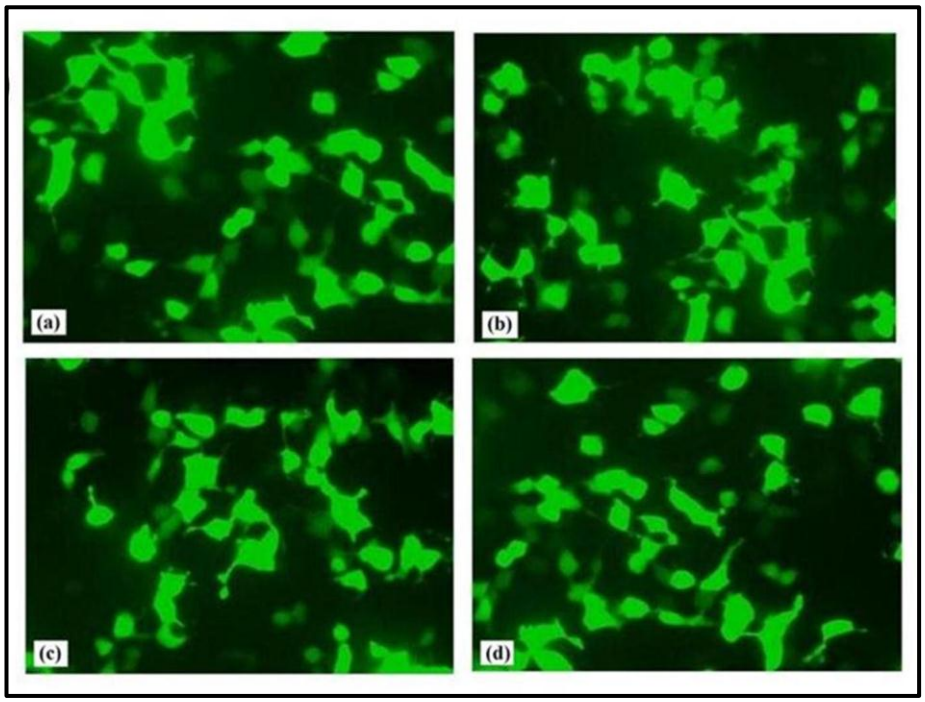

Figure 5.33 Images shows cytocompatibility of nanofiber membrane with mouse fibroblasts (L-929 cell lines) after direct exposure to the surface of TNZ-PGHNF membrane containing w/w percentages of TNZ: (A) 0%; (B) 10.0%; (C) 20.0%; (D) 30.0%; typical healthy structures are apparent in all cases

5.3.11 Haemocompatibility of TNZ-PGHNF membrane

Assessing the biocompatibility of developed nanofiber membrane is essential as the polymer in contact with the living body tissue may cause several critical reactions, such as thrombosis. Thus, the haemocompatibility of developed TNZ-PGHNF membrane was evaluated by haemolysis method. The proportion of red blood cells damaged by the test sample in contact with blood is denoted as haemolysis percentage (HP). Figure 5.34 exhibits the HP of nanofiber membrane loaded with different concentration of TNZ (0%, 10%, 20%, and 30%) with ACD blood. The results presented that the HP was under 3% for 0%,10% and 20% TNZ loaded nanofiber membrane, demonstrating a good anti haemolysis character among all the TNZ-PGHNF membrane [Dey and Ray 2003]. However, nanofiber membrane loaded with 30% TNZ showed maximum HP viz. 3.9±0.35%.

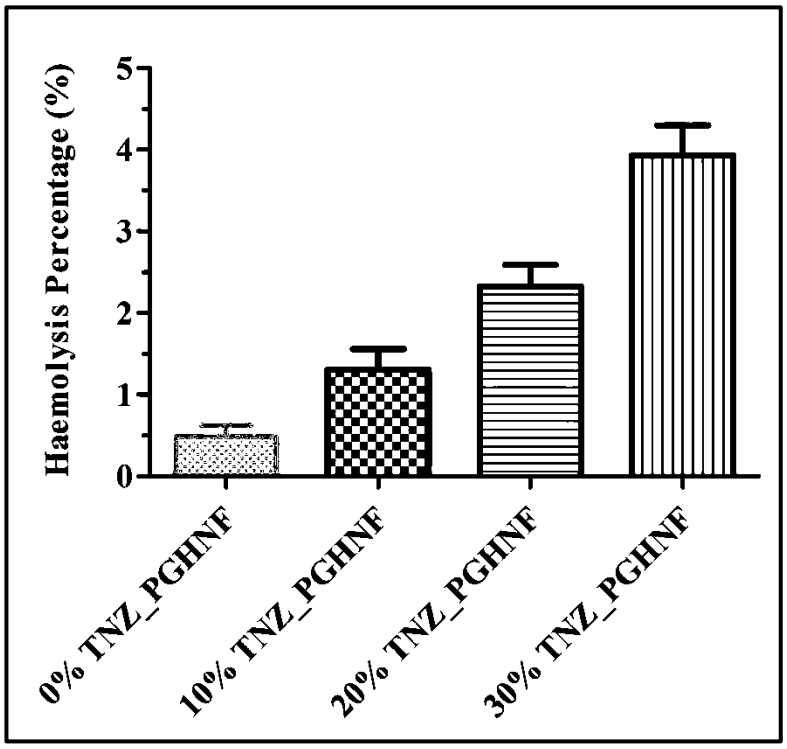

Figure 5.34 Haemolysis percentage of electrospun TNZ-PGHNF membranes containing w/w percentages of TNZ: (a) 0%; (b) 10.0%; (c) 20.0%; (d) 30.0%. Vertical bars in figure represents SD, results are shown as mean±S.D.; (n = 3).

This high value of HP might be attributed to the increased surface roughness of TNZ-PGHNF (30%) membrane owing to higher drug concentration. Thus, a shear stress is produced when RBCs come in contact with the rough surface of nanofiber inducing the cracking of red blood cells, ultimately leading to haemolysis [Meng et al. 2010].

5.3.12 Storage stability study

In order to ensure the final *in vivo* performance of the nanofiber membrane, assuring the stability of nanofiber against environmental changes is of prime importance. The change in the properties of TNZ-PGHNF like diameter and EE during stability studies performed over a period of 6 months in different study conditions such as room temperature (30±2 ºC), refrigerated condition (4±1 ºC), and accelerated condition (40±2 ºC/75±5% RH) is depicted in Figure 5.35. No significant change was observed in the physical appearance (i.e. colour change and change in pH) at different environmental condition during the study. Similarly, an insignificant ($p > 0.05$) change in the diameter and EE of TNZ-PGHNF was observed in the product stored at room temperature (30±2 ºC) and refrigerated condition (4±1 ºC). Whereas, a significant change in the diameter and EE was noticed at accelerated condition (40±2 ºC/75±5% RH) which indicated the instability which might have occurred due to biodegradation of polymer leading to expelled drug molecules from the nanofibers. Hence, it is strongly recommended that the nanofiber membrane should be stored at room temperature (30±2 ºC) as well as refrigerated condition (4±1 ºC), to maintain the stability of the product and the pharmaceutical properties essential for safe and effective long-term use.

The shelf-life of optimized nanofiber membrane was found to be 16.02, 14.12 and 9.46 months when stored at refrigeration, room temperature and high-temperature

conditions, respectively (Figure 5.36). This indicated the high stability of the nanofiber membrane at refrigerated storage and room temperature for a long period.

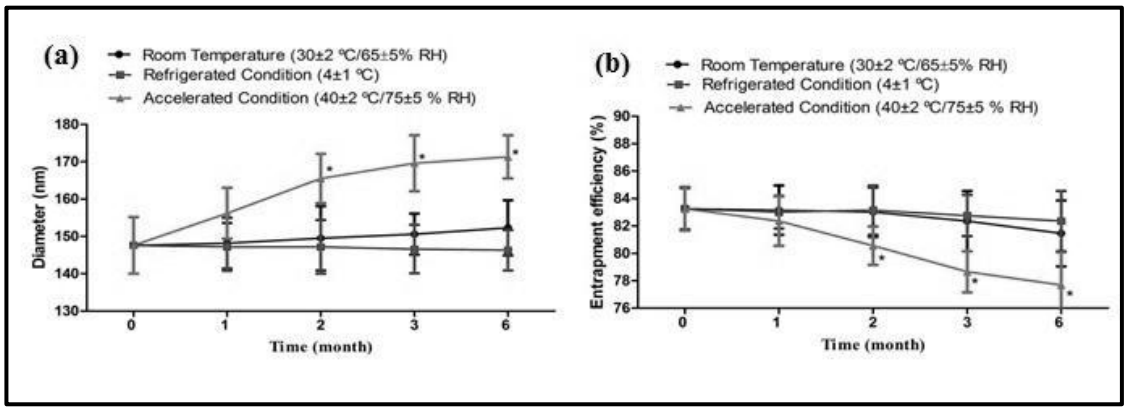

Figure 5.35 Effect on (a) diameter and (b) entrapment efficiency of TNZ-PGHNF stored at different environmental conditions over different time interval (vertical bars represent SD; n = 3). *significant values at $p < 0.05$ compared with 0 time (One-way ANOVA; Dunnett's multiple comparison test).

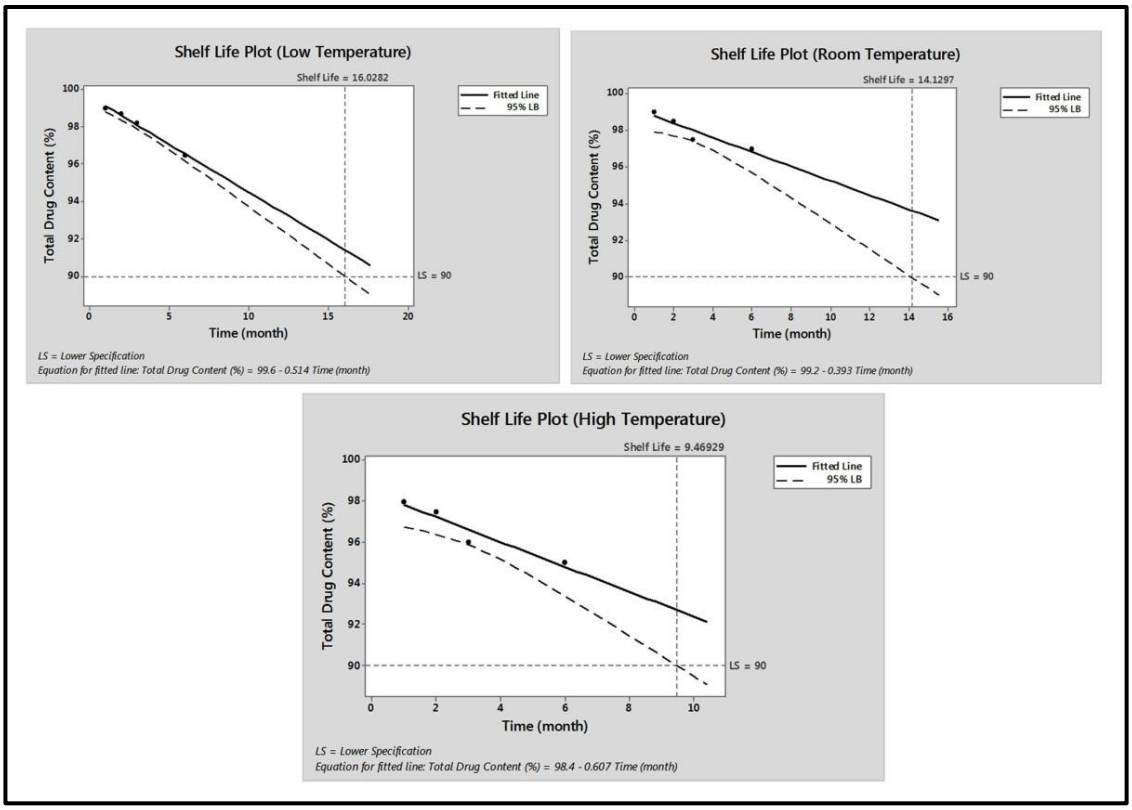

Figure 5.36 Shelf-life plots of optimized batch of TNZ-PGHNF membrane at different storage conditions, viz. Storage 1 (low temperature), Storage 2 (room temperature) and Storage 3 (high temperature) LS: lower specification (90%).

5.3.13 *In vivo* study

Ligature-induced periodontitis model in rats was employed to study the progression of periodontitis and to evaluate the *in vivo* activity of developed TNZ-PGHNF membrane. Figure 5.37(a) represents the graded response for continuity of epithelium and Figure 5.37(b) represents graded response for continuity of transseptal fibers of the Interdental papilla. A significant improvement in the continuity of the epithelium of the Interdental papilla was observed in the rats of Group C as compared to that of group A and group B ($p < 0.05$). The continuity of epithelium of the Interdental papilla was retained by the rats of Group C, up to a large extent. The response of group B regarding the continuity of epithelium was non-significant while compared to group A ($p > 0.05$). Moreover, significant improvement was also noticed in the continuity of transseptal fibers of Interdental papilla in group C as compared to group A and group B ($p < 0.05$).

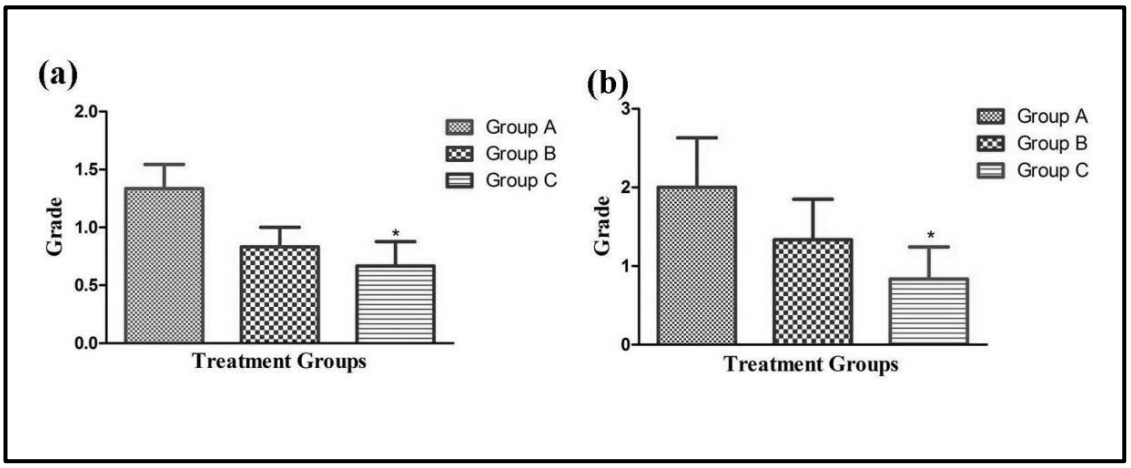

Figure 5.37 Graph represents (a) Graded response for continuity of epithelium in the interdental papilla and (b) Graded response for continuity of transseptal fibers in the interdental papilla. *$p < 0.05$, n.s. = not significant, compared to control group by one-way (ANOVA) followed by Tukey's multiple comparison test, $n = 6$.

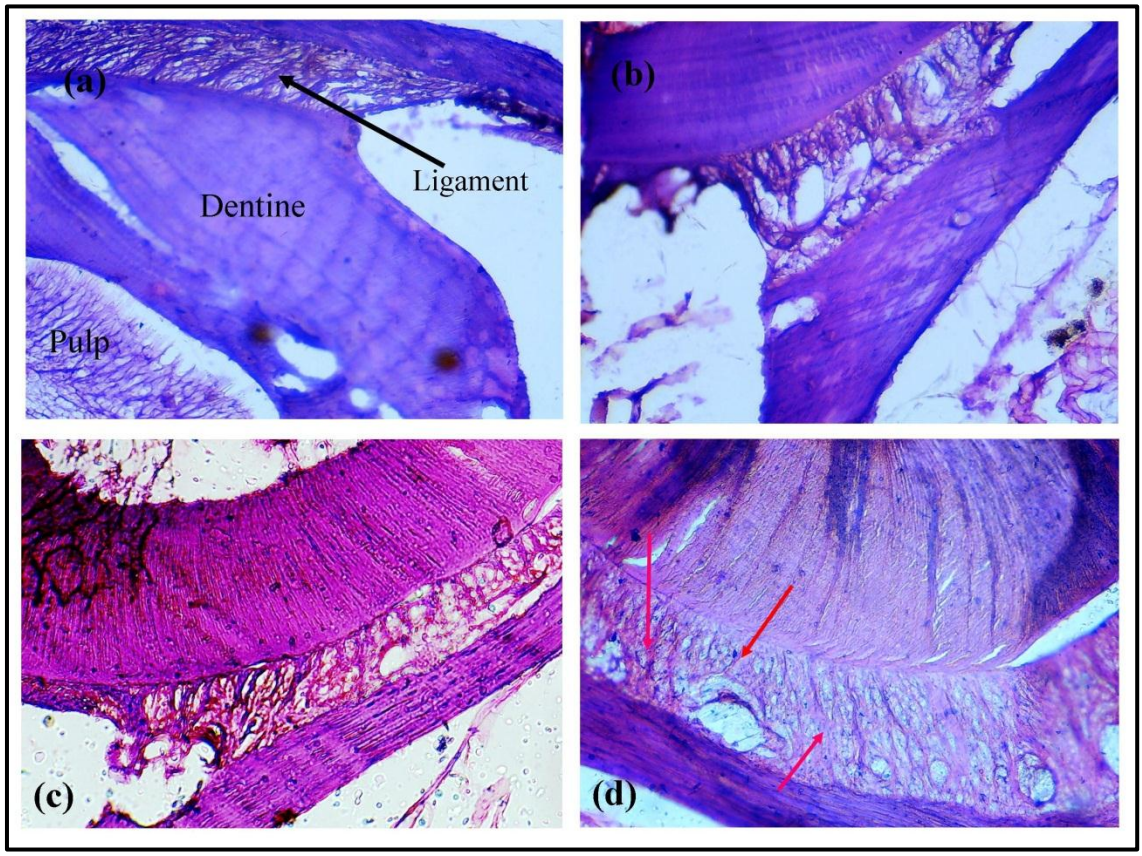

Figure 5.38 Histological results of the periodontium of rats in different treatment groups subjected to ligature-induced periodontitis (a) healthy periodontium (b) periodontitis induced periodontium showing disrupted ligament tissue structure and (c & d) treated with TNZ gel and TNZ-PGH nanofiber membrane, respectively and red arrow indicate formation of ligament tissue.

Figure 5.38 delineates the histo-micrograph of the rat's periodontium of different groups subjected to ligature-induced periodontitis. Certain criteria such as cementoenamel junction (CEJ)-bone distance, alveolar bone resorption as well as periodontal ligament degeneration are generally used to evaluate periodontitis [Xie et al. 2011]. It can be clearly observed from the Figure 5.38, that different groups exhibit a clear demarcation of degeneration of ligament tissue. It was evident from the histo-micrographs that the group treated with TNZ loaded nanofiber showed minimal degeneration of periodontal ligament and cementoenamel junction (CEJ) - bone distance as compared to that of the group treated with TNZ gel.

5.4 Preparation, optimization, *in vitro* and *in vivo* characterization as well as clinical evaluation of TNZ encapsulated CH/PCL hybrid nanofiber membrane (TNZ-PCHNF)

In this part, we had use CH/PCL polymer blend in place of GE/PCL for improvement of mucoadhesive property, hydrophilicity as well as the homogeneous distribution of diameter of developed nanofiber membrane.

CH/PCL nanofiber membrane was prepared by electrospinning technique and optimized by "Quality by Design" approach in order to meet the critical quality attributes of the final product.

5.4.1 Experimental design

A total of 17 batches of TNZ-PCHNF membrane were engineered as per the design matrix of BBD generated by Design-Expert software, by changing the independent variables, i.e. CH/PCL ratio (X_1), drug concentration (X_2), and formic acid/acetic acid ratio (X_3) in their three levels. The selected dependent responses were nanofiber diameter (Y_1) and EE (Y_2). The results for different experimental runs are summarized in Table 5.17. In the polynomial equation, the positive coefficient indicates the existence of a direct relationship between the independent variables and dependent responses, whereas negative coefficient denotes the inverse relation. Figure 5.39 shows three-dimensional surface plots, which delineate the interaction of any two independent variables on the dependent variable, by keeping third one at a constant level. Further, the usefulness of "Quality by Design" approach in performing experiments was confirmed by the results obtained by statistical analysis of data and statistical optimization given in Table 5.18.

Table 5.17 Box–Behnken experimental design representing experimental runs with independent variables and dependent response of TNZ-PCHNF[a]

Run No.	Independent Variables			Dependent Variables	
	X_1	X_2	X_3	Y_1	Y_2
Factorial Points					
1	-1	-1	0	141.3± 11.2	81.2± 0.9
2	1	-1	0	173±10.8	89.2± 1.5
3	-1	1	0	140±10.9	70.9± 2.2
4	1	1	0	171.2± 12.5	71.8± 1.6
5	-1	0	-1	175.6± 10.4	74.8± 1.1
6	1	0	-1	199.5± 9.2	84± 0.8
7	-1	0	1	136.4± 9.8	74.6± 1.2
8	1	0	1	176.2± 8.6	74.6± 0.6
9	0	-1	-1	179.2± 11.5	87.2± 0.9
10	0	1	-1	177.2± 10.2	73.7± 1.5
11	0	-1	1	147.4± 11.3	84.6±1.0
12	0	1	1	140.4± 13.5	68.5± 1.4
Centre Points					
13	0	0	0	149.6± 11.5	79.2±0.8
14	0	0	0	148.4± 10.4	77.8± 0.9
15	0	0	0	148.2±11.6	77.9± 1.2
16	0	0	0	147.8± 12.4	79± 0.9
17	0	0	0	149.6± 10.2	78.5± 1.0

[a]All data are shown as mean±S.D.; n = 3

Table 5.18 Statistical analysis results of lack of fit test and model summary for diameter and entrapment efficiency of TNZ-PCHNF membrane

Model	Lack of fit test					Model summary statistics					Remark
	SS	df	MS	F-Value	p-Value prob >F	SD	R^2	Adjusted R^2	Predicted R^2	PRESS	
Diameter											
Linear	1315.29	9	146.14	225.53	< 0.0001	10.07	0.7599	0.7044	0.5880	2260.97	
2FI	1245.77	6	207.63	320.42	< 0.0001	11.17	0.7725	0.6360	0.2083	4344.88	
Quadratic	9.08	3	3.03	4.67	0.0853	1.29	0.9979	0.9951	0.9728	149.37	Suggested
Cubic	0.000	0	-	-	-	0.80	0.9995	0.9981	-	+	Aliased
Pure error	2.59	4	0.65	-	-	-	-	-	-	-	-
Entrapment Efficiency											
Linear	42.64	9	4.74	11.93	0.0147	1.84	0.9171	0.8980	0.8307	156.01	
2FI	7.19	6	1.20	3.02	0.1522	0.94	0.9835	0.9737	0.9332	35.66	
Quadratic	0.87	3	0.29	0.73	0.5863	0.59	0.9954	0.9895	0.9693	16.36	Suggested
Cubic	0.000	0	-	-	-	0.63	0.9970	0.9881		+	Aliased
Pure error	1.59	4	0.40	-	-						

SS: sum of squares, df: degree of freedom, MS: mean square, SD: standard deviation, PRESS: Predicted Residual Error Sum of Squares; 2FI: two-factor interaction, +: PRESS statistic not defined, p-value < 0.05 was considered as statistically significant.

5.4.1.1 Influence of independent variables on diameter (Y_1)

Diameter is one of the critical factors for achieving desired drug release profile from nanofiber-based drug delivery systems. The Smaller diameter is preferable for nanofibers as it provides shorter diffusion passage length for effective mass transfer along with greater surface area. The diameter of prepared nanofibers was obtained in the range of 136.4±9.8 nm to 199.5±9.2 nm for different factor level combinations. The relationship between the diameter of nanofibers and independent variables was derived by following polynomial equation.

$$\text{Diameter} = 148.72 + 15.83X_1 - 1.51X_2 - 16.39X_3 - 0.13X_1X_2 + 3.97X_1X_3 - 1.25X_2X_3 + 9.26X_{12} - 1.61X_{22} + 13.94X_{32}$$

The quadratic model was found to be significant as it had F value of 359.69 ($p < 0.0001$) and best suited for establishing a relation between the diameter of nanofibers and independent variables. The higher value of R^2 coefficient (0.9978) indicated the existence of a good correlation between predicted values and experimental values. The least difference between predicted R^2 (0.9728) and adjusted R^2 (0.9951) value also indicated the adequacy of the selected model for prediction of response. The lack of fit data was found to be non-significant with F-value 4.37 and p values 0.0939, inferring the adequate fitting of data. Moreover, a lower value for the coefficient of variation (0.82%) confirmed the reliability of the quadratic model with a higher degree of precision. Hence, the selected quadratic model can be used to navigate generated design space for nanofibers [Patel et al. 2015].

As indicated in Figure 5.39(a), CH/PCL concentration (X_1) affects positively on the diameter of TNZ-PCHNF membrane due to its direct impact on the viscosity. At higher CH/PCL concentration, the viscosity of the electrospinning solution increases, which

ultimately impacted resistance of jet. This in turn forms thicker fibres due to bending instability and a faster solidification of the polymer jet [Jacobs et al. 2010]. Contrarily, drug concentration and FA/AA ratio had an inverse impact on the diameter as depicted in Figure 5.39(b,c).

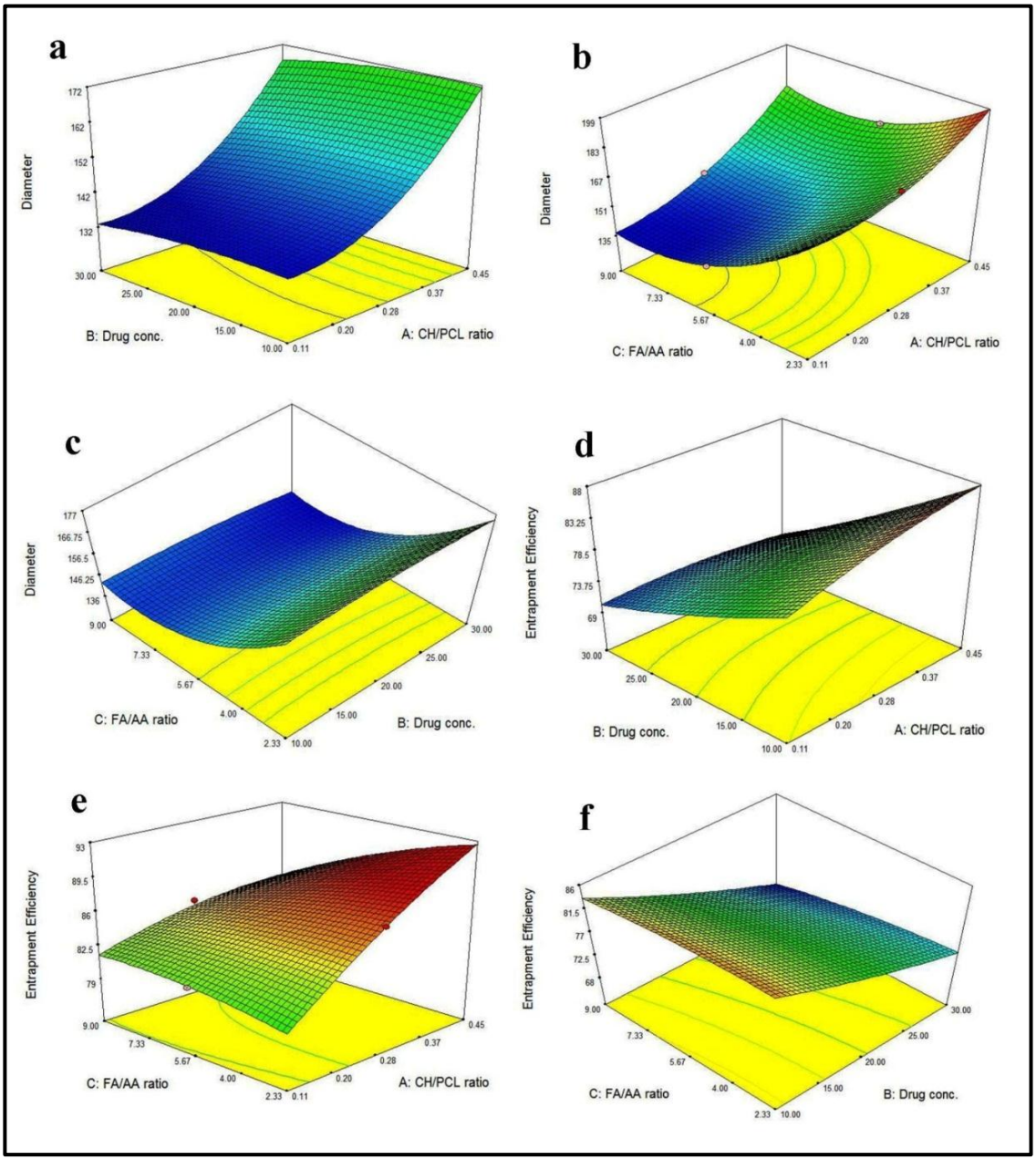

Figure 5.39 Three-dimensional response surface plots showing the effect of independent variables (concentration of CH/PCL ratio, concentration of drug and FA/AA ratio on dependent response variables: diameter of nanofiber (a-c) and entrapment efficiency (d-f).

Reduction in viscosity was found at a higher amount of TNZ, which might be due to TNZ molecules acting as a plasticizer for CH/PCL chains. Simultaneously, conductivity of electrospinning solution was increased as a consequence of the enhanced polarity. Therefore, both reduced viscosity with an increase in conductivity would have decreased diameter of nanofibers. Likewise, on increasing the FA/AA ratio (X_3) conductivity of the electrospinning solution increased (dielectric constant 57.2 for FA and 6.2 for AA at 25 ºC) and thereby, the diameter of nanofiber decreases. When the conductivity of solution increases, the electric charges carried by the electrospinning jet also increases, this, in turn, enforces generation of higher elongation forces to the jet under applied electrical field [Zamani et al. 2010]. Bending instability also increases at higher solution conductivity and thereby, causes elongation of the jet path with higher stretching of the solution, leading to a reduction in nanofiber diameter.

5.4.1.2 Influence of independent variables on entrapment efficiency (Y_2)

Entrapment efficiency of TNZ-PCHNF membrane varied from a minimum of 68.5% to maximum of 89.2% for different experimental runs. The second order polynomial equation relating to the effect of independent variable on EE (Y_2) can be given as follow in terms of coded significant model terms:

$$EE = 78.48 + 2.26X_1 - 7.16X_2 - 2.18X_3 - 1.78X_1X_2 - 2.30X_1X_3 - 0.65X_2X_3 - 0.85X_{12} + 0.65X_{22} - 0.63X_{32}$$

The quadratic model was found significant with Model F value of 168.19 ($p < 0.0001$) as indicated by model summary statistics. The higher value of R^2 coefficient (0.9954) indicates the existence of a good correlation between predicted values and experimental values. The model showed an adequate fitting to data as indicated by non-significant lack of fit, having p values of 0.5863 ($p < 0.05$). The least difference between predicted

R^2 (0.9693) and adjusted R^2 (0.9895) value also indicated adequacy of a selected model for prediction of response. Therefore, this model was selected for analysis of independent variable on EE. ANOVA analysis showed that X_1, X_2, X_3, X_1X_2, X_1X_3, X_2X_3, X_{12}, X_{22}, X_{32} were the significant model term.

The concentration of CH/PCL (X_1) had a positive effect whereas drug concentration, and FA/AA ratio have a negative effect on EE as depicted in Figure 5.39(d,e). Also, higher coefficient value (7.16) of the concentration of drug (X_2) in the polynomial equation indicated that it had more significant effect on EE followed by the ratio of CH/PCL (X_1) and FA/AA ratio (X_3). Though, the effect of independent variables on EE was lower than the effect on the diameter of the nanofiber. This was as a result of the lower coefficient value of the main effects and interactive terms in the polynomial equation of EE compared to the nanofiber diameter.

The significant increment in the EE of the developed TNZ-PCHNF membrane was observed with an increase in the CH/PCL ratio. The higher CH/PCL ratio conferred a diffusional barrier by increasing viscosity of the solution and thereby, hindered the outward movement of TNZ and enhanced the EE. Additionally, increased diffusional path length as a result of increased diameter at a higher CH/PCL ratio, also might be one of the plausible reasons for higher EE [Budhian et al. 2007]. Inversely, a significant reduction in the EE was observed at higher drug concentration. The probable reason was the existence of solubilized drug in the polymeric solution, which would have enhanced migration of dissolved drug towards the surface of the nanofiber membrane during the electrospinning process. Likewise, lowering of EE was achieved with an increase in FA/AA ratio (X_3) as a result of a substantial reduction in the diameter of nanofiber.

5.4.1.3 Optimization of TNZ-PCHNF membrane

The statistical optimization of the formulation was performed by using the desirability based numerical optimization technique. The constraints were fixed for all three independent variables in the Design Expert® Software in order to achieve maximized EE with minimum diameter. Predicted level of independent variables X_1, X_2 and X_3 were found 0.24, 10% w/w and 6.77, respectively, with diameter of 141.71 nm, EE of 84.99% and having desirability of 0.853. Therefore, the optimized TNZ-PCHNF membrane was prepared with predicted levels of independent variables in order to confirm validity as well as predictive capability of BBD. The optimized experimental TNZ-PCHNF membrane exhibited a diameter of 143.55±8.5 nm and EE of 83.25±1.8%. The lower value of bias between the predicted values and the experimental values indicated that results were in good agreement with observed values and thereby, confirmed the reliability of BBD for statistical optimization in order to develop nanofiber system for delivery of TNZ for treatment of periodontitis.

5.4.2 Solid-state characterization of TNZ-PGHNF by FTIR, DSC and PXRD

5.4.2.1 Fourier transform infrared spectroscopy (FTIR) study

FTIR was performed to confirm compatibility between drugs and polymer as well as to ensure the effect of the electrospinning on the functional group of drug present in the formulation. FTIR spectra of TNZ, CH, PCL and optimized nanofiber membrane are depicted in Figure 5.40. TNZ spectrum showed characteristic peaks at 1265 cm^{-1} (C-O stretching), 1301 cm^{-1} (asymmetric stretching vibration of S=O) and 1367 cm^{-1} was assigned symmetric stretching vibration of N=O. Moreover, FTIR peaks appeared at 1521 cm^{-1}, 1492 cm^{-1} and 2914-3001 cm^{-1} attributed to asymmetric stretching vibration of C=N (imidazole ring), N=O (NO_2), and C-H, respectively. CH related FTIR spectra showed the characteristic band at 1652 cm^{-1} and 3450 cm^{-1} which is attributed to the

presence of amide group, $-NH_2$ and –OH groups, respectively. PCL showed characteristic peak at 1733 cm^{-1} (C=O stretching), 2853 cm^{-1} (symmetric CH_2 stretching) and 2948 cm^{-1} (asymmetric CH_2 stretching) [Shalumon et al. 2010]. FTIR spectrum of nanofiber membrane exhibited all the characteristic peaks of TNZ, CH and PCL with slight variation in frequencies similar to its pure form which indicated compatibility between the drug and polymer and absence of any possible interaction between them and also confirmed that electrospinning process does not impair the molecular structure of TNZ present in the nanofiber membrane. Therefore, it could be speculated that the drugs and polymers were compatible and could be formulated into nanofiber membrane.

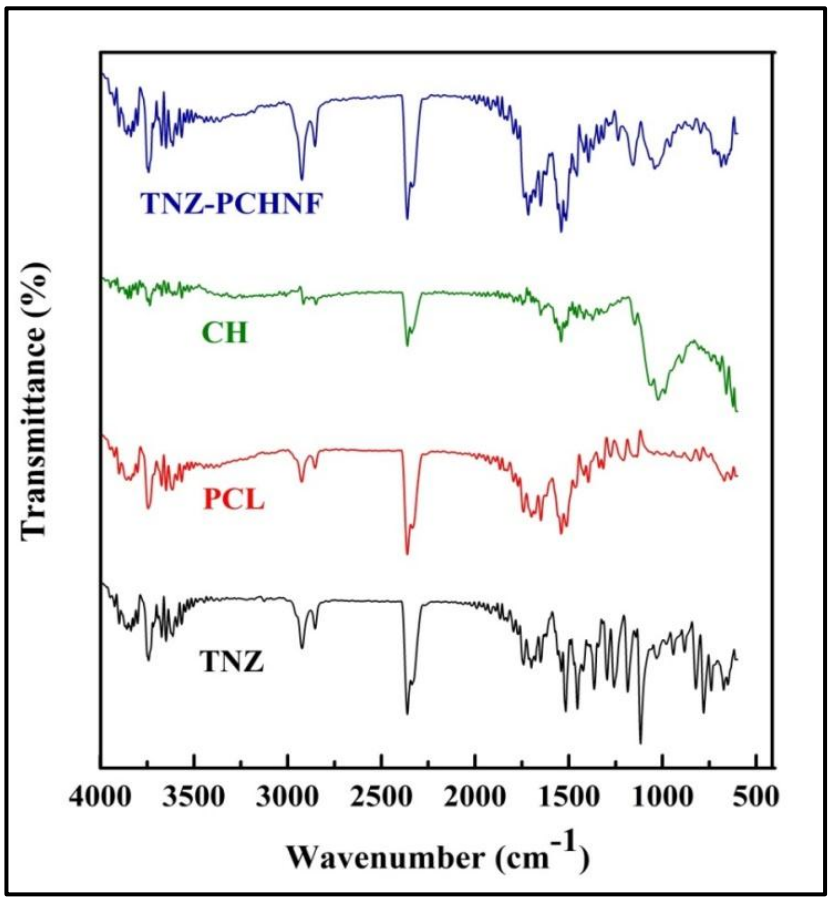

Figure 5.40 FTIR spectra of TNZ, PCL, CH and optimized formulation (TNZ-PCHNF)

5.4.2.2 Differential scanning calorimetry (DSC) study

DSC studies were performed to characterize the solid state of drugs and polymers. Further, compatibility between drug and excipients can be evaluated by observing the thermal behaviour of compounds such as appearance or disappearance of an endothermic or exothermic peak. If all the peaks remain the same, compatibility can be expected. DSC thermogram of TNZ, CH, PCL and optimized nanofiber membrane are depicted in Figure 5.41.

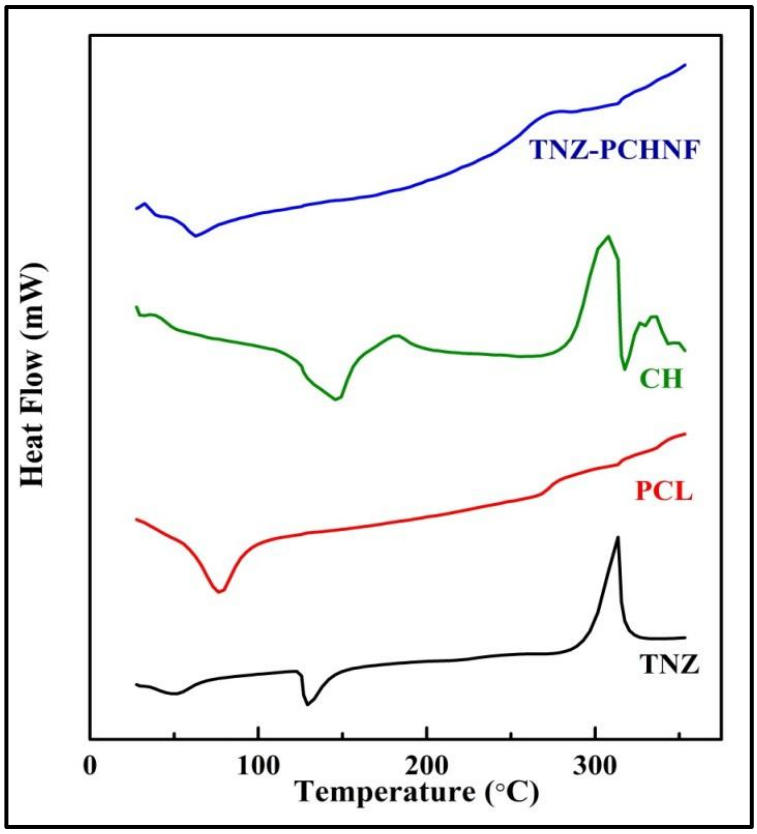

Figure 5.41 DSC Thermograms of TNZ, PCL, CH, and optimized formulation (TNZ-PCHNF)

DSC thermogram of TNZ showed a sharp endothermic peak at 128.5 ºC which was attributed to its melting point. The sharp melting peaks exhibited by TNZ confirmed their existence as a crystalline form. CH showed a flat curve due to its amorphous nature. Thermogram of PCL exhibited a characteristic peak at 60 ºC due to its semi-crystalline nature. Whereas, optimized TNZ-PCHNF membrane showed flat curve

without sharp endothermic or exothermic peaks of the drug. This indicated that transformation of phase, i.e. crystalline state to amorphous state had taken place, during the entrapment process [Patel et al. 2015]. This might be due to shear stress provided by the stirrer and electrospinning during the fabrication process of nanofiber which might prevent the recrystallization of TNZ, leaving TNZ in molecular dispersion form inside the TNZ-PCHNF membrane.

5.4.2.3 Powder X-ray diffractometry (PXRD) study

To understand the crystallinity of the drug in the nanofiber membrane, PXRD pattern of pure drug, CH, PCL and TNZ-PCHNF membrane were recorded (Figure 5.42).

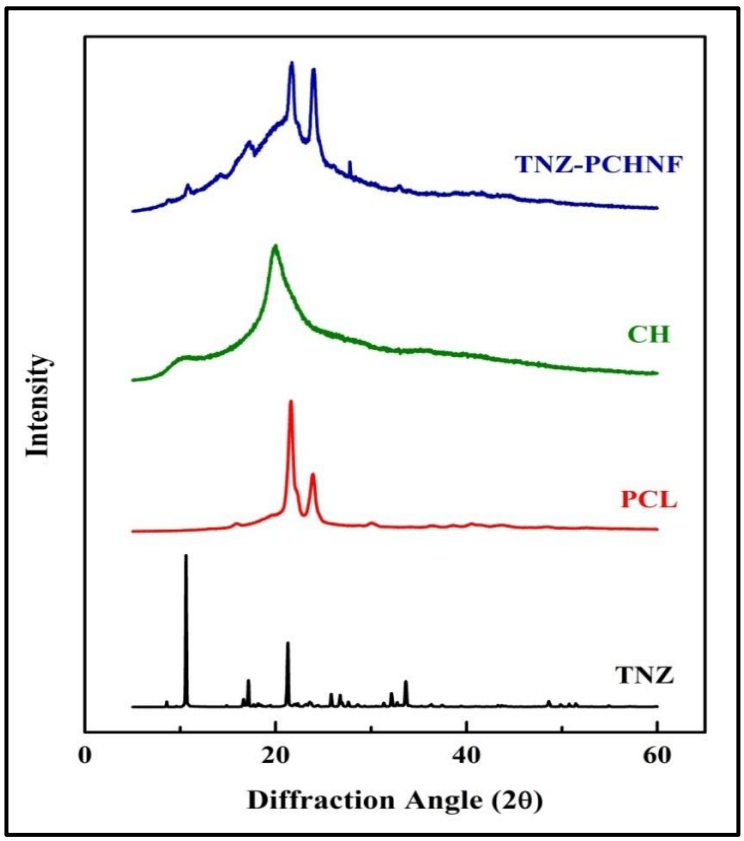

Figure 5.42 Overlay PXRD patterns of TNZ, PCL, CH, and optimized formulation (TNZ-PCHNF)

TNZ exhibited four characteristic peaks at 2θ of 12.2º, 17.9º, 22.7º and 33.8º which demonstrated crystalline nature of the drug. PCL showed two peaks in the diffractogram at a diffraction angle of 22.4º and 24.6º indicates semi-crystalline nature

of PCL while two broad peaks in the diffractogram of CH at a diffraction angle of 9-10º and 20-21º indicates amorphous nature of CH. Whereas, PXRD pattern of TNZ-PCHNF membrane exhibited more of an amorphous nature as compared to pure TNZ due to shifting of its diffraction intensity, conforming TNZ physical state transformed from crystalline state to amorphous state during the entrapment process in the nanofiber membrane.

5.4.3 Shape and surface morphology

Figure 5.43(a-d) shows SEM micrographs of TNZ-PCHNF membrane of the optimized batch at different magnification before and after *in vitro* release of TNZ. As can be seen from the figure, uniform and smooth nanofibers were formed with rare bead defects. The diameter of nanofiber membranes containing different concentrations of drug ranging from 136.4±9.8 nm to 199.5±9.2 nm is shown in the

Table 5.17. Porosities of the nanofiber membranes were found in the range of 68% to 85%. It had been reported by Chong et al., that porosities within the range of 60-90% are essential for the exchange of gas and nutrient. Moreover, the smaller pore size of membrane than the size of fibroblast is beneficial because it prevents ingrowths of fibroblasts into the tissue defect. Hence, we successfully fabricated TNZ loaded mucoadhesive nanofiber membrane [Chong et al. 2007].

EDXA was used to determine the elemental composition of the nanofiber membrane. TNZ-PCHNF membrane exhibited large peaks for carbon, oxygen and a small peak for nitrogen, indicating three of the major components of CH and PCL whereas, sulphur peak indicating the presence of TNZ (Figure 5.43(e)). Moreover, the elemental dispersion maps, presented uniform distribution of sulphur (Figure 5.43(f)) within the nanofiber membrane.

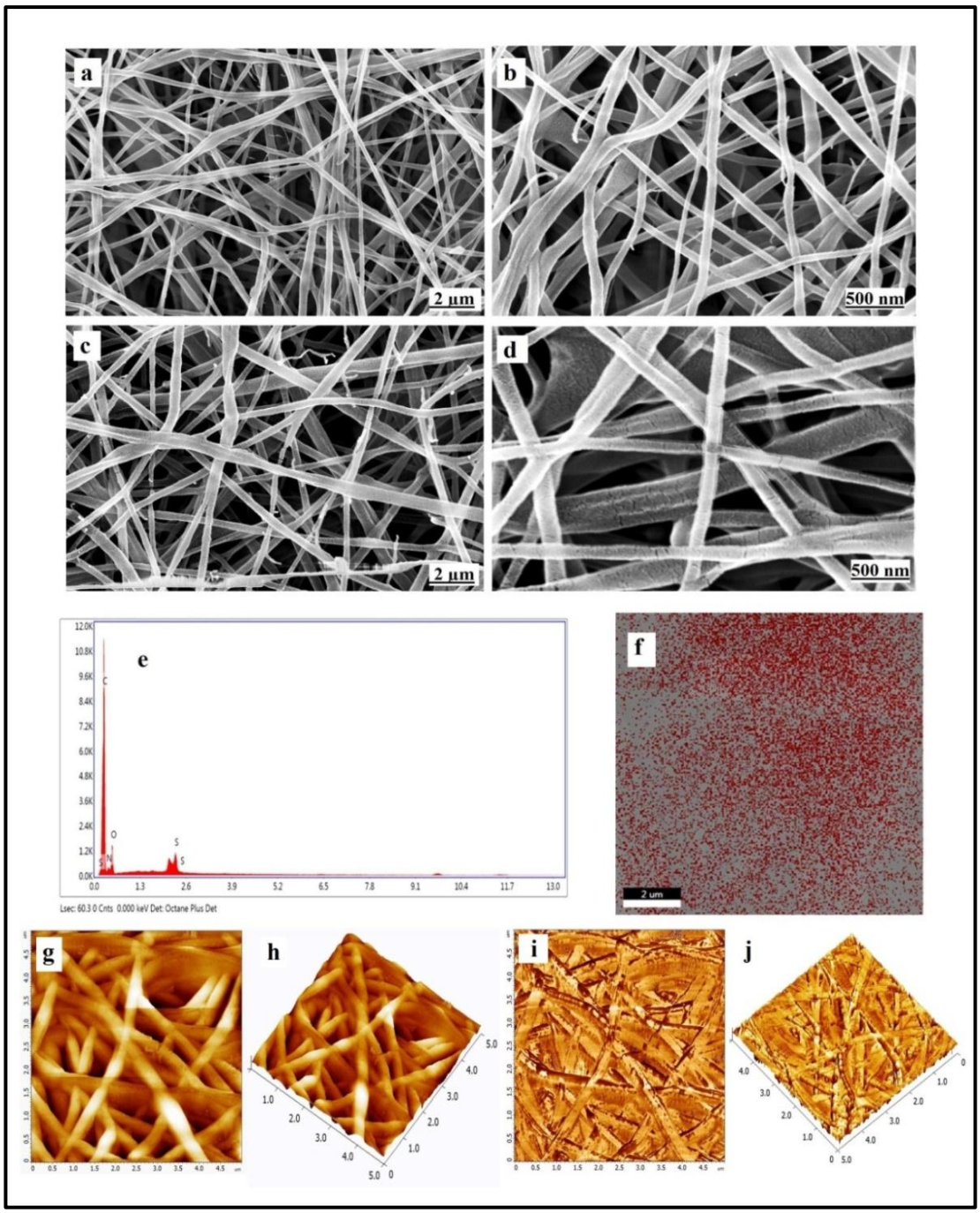

Figure 5.43 Representative HR-SEM images of optimized electrospun TNZ-PCHNF membrane at different magnification (a & b) before and (c & d) after 18 days in McIlvaine buffer. (e) EDXA, analysis of optimized nanofiber membrane. EDXA spectrum shows peaks of carbon, nitrogen, oxygen and sulphur. (f) Dot-analysis represents uniform distribution of sulphur within the nanofiber membrane. 2D and 3D-atomic force microscopic height image (g & h) and corresponding phase image (i & j) showing smooth and bead free surface of nanofiber membrane

AFM study was further used to study more detailed structure, surface morphology and diameter of electrospun nanofiber membrane. The topographic as well as 3D AFM

images of nanofiber membrane were generated by the atomic level interaction between surfaces of electrospun nanofiber and the sharp tip of the scanner and are depicted in Figure 5.43(g-j). The fiber diameters were measured from the height and were found in accordance to SEM study. AFM micrographs showed an arbitrarily interconnected structure, smooth morphology and uniform distribution of electrospun nanofiber with rare bead defect. The possible reason for smooth surface could be attributed to uniform mixing of drug and polymer in the combined solvent system of FA/AA.

5.4.4 Surface pH and Drug Content Uniformity

Surface pH of nanofiber membrane was taken into consideration because too much acidic or basic pH affects the area of application and causes irritation to oral mucosal membrane leading to patient discomfort [Ahuja et al. 2006]. Also, acidic pH leads to the dissolution of enamel and demineralisation of teeth. To overcome these problems, the pH of the nanofiber membrane must be closer to pH of the GCF (pH 6.6). Surface pH of all batches ranged from 6 to 7.5 indicating acceptability of formulation for pocket insertion. In fact, formulations with pH 6.5 to 7 are more preferred due to the closeness of pH values to neutrality. Further, content uniformity studies of the nanofiber showed that the drug was uniformly distributed and recovery was found to be in the range of 83.5% to 87.3% for all the batches as indicated in Table 5.19.

Table 5.19 Physicochemical characteristics of different batches of TNZ-PCHNF membrane

Run No.	Mucoadhesive strength* (gm/cm^2)	Total drug Content* (%)	Surface pH
1	160±1.22	83.5±2.32	6.0
2	163±1.15	84.8±2.26	6.5
3	161±1.30	83.5±3.63	7.5
4	163±1.25	87.3±2.27	7.5
5	164±1.32	85.3±3.23	7.0
6	166±1.15	86.4±2.44	6.5
7	165±1.22	84.6±2.62	6.0
8	162±1.32	85.5±2.25	7.0
9	165±1.30	87.0±2.42	6.5
10	161±1.35	83.8±3.24	7.0
11	166±1.37	85.7±2.22	7.5
12	165±1.22	84.5±3.44	7.5
13	166±1.15	86.4±3.36	7.0
14	169±1.50	84.6±2.43	7.0
15	168±1.22	86.2±2.34	7.0
16	171±1.42	85.5±2.55	7.0
17	170±1.32	86.0±2.25	7.0
Optimized TNZ-PCHNF	175±1.25	87.5±2.22	7.0

*Result are presented as mean±SD, (n = 3)

5.4.5 Contact angle

Contact angle impersonates the wettability or hydrophilicity of the nanofiber membrane, which influences attachment and proliferation of cells. In spite of the excellent biocompatibility of PCL, the real confinement of this material is its hydrophobicity. Subsequently, contact angle estimations were done to explore the impacts of CH content on the hydrophilicity of the nanofiber membrane. The outcomes are represented in Figure 5.44.

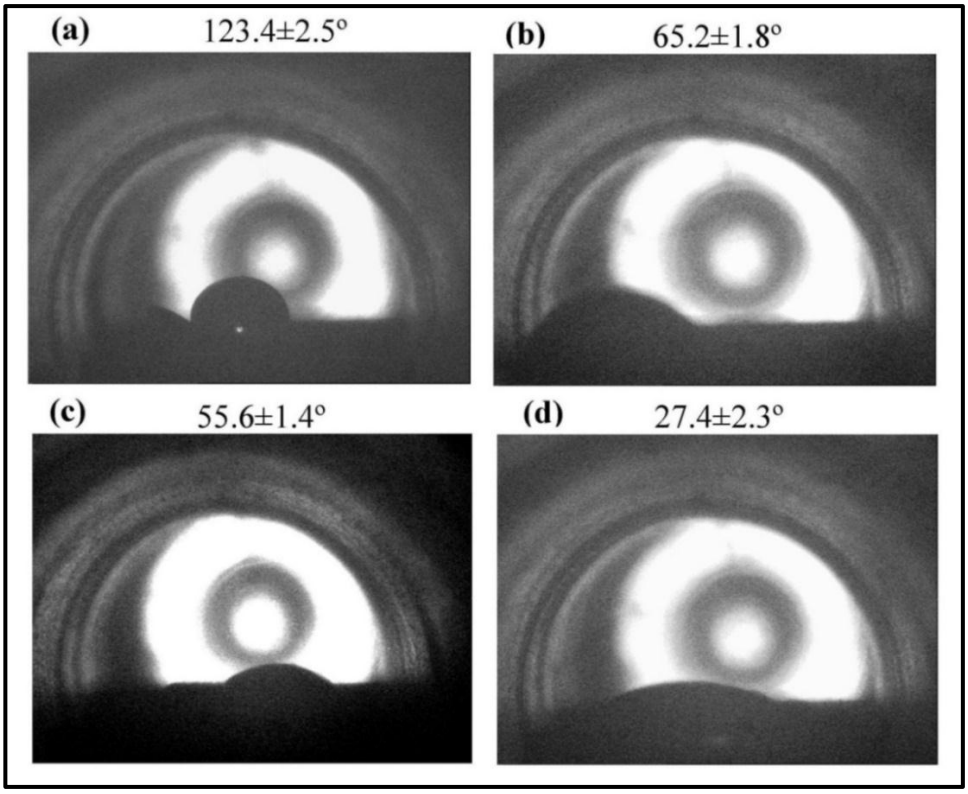

Figure 5.44 Contact angle of TNZ-PCHNF membrane containing different proportion of CH/PCL: (a) 0%; (b) 10.0%; (c) 20.0%; (d) 30.0%. Images suggesting that with the increase of CH content, water contact angle of the nanofiber membranes decreases, indicating increase in hydrophilicity of nanofiber membrane.

It was shown that PCL nanofiber membrane had the highest contact angle (123.4±2.5º). With the increase of CH concentration, water contact angle of the membrane diminished while hydrophilicity as well as wettability of the nanofiber membrane increases. This change was ascribed to the presence of hydroxyl and polar amine functional group in the CH molecule. Such a change in hydrophilicity will increase cell adhesion at the site of action and start a proliferation of cells, tissue recovery and the biodegradation of the nanofiber membrane [Jing et al. 2015].

5.4.6 *In vitro* mucoadhesion studies

Mucoadhesion of nanofiber to the gingival mucosa is an important property to retain the nanofiber membrane in the periodontal pocket up to several days, and it should not ooze out during movement of jaws. Mucoadhesive strength of polymer depends on the

degree of hydration of polymer chains. Hydration helps in expanding polymer chain exposing more available sites for bond formation and creating channels for diffusion of the polymer chain. The interdiffusion and entanglement of expanded polymer chains, as well as formation of secondary bonds, confers bioadhesion property to the polymer which can be enhanced by increasing contact time and applied force [Mayet et al. 2014, Sharma et al. 2016]. The mucoadhesive detachment force for optimized TNZ-PCHNF membrane and blank nanofiber membrane was found to be 175 gm/cm^2, and 190 gm/cm^2, respectively (Table 5.19). The lower value of mucoadhesive force in the case of drug-loaded nanofibers can be attributed to the decrease in the specific area associated with a wider diameter of drug-loaded nanofibers than that of the blank nanofibers. Furthermore, it was observed that TNZ-PCHNF membrane showed the higher mucoadhesive property as compared to previous one (TNZ-PGHNF membrane) was due to cationic nature of CS having a high affinity for negatively charged mucus membranes. Moreover, it was mentioned that high proportions of cationic CH chains could react with sialic acid and sulphate parts of mucus glycoproteins, which have a negative charge in the oral cavity [Davoudi et al. 2017]. Thus, the mucoadhesive force in CH/PCL nanofiber membrane is the result of this reaction.

5.4.7 Entrapment efficiency

The EE of TNZ-PCHNF membrane was found in the range of 68.5 to 89.2% for various batches which was shown in Table 5.17. The outcomes showed a precise dependence of the entrapment efficiency on the concentration of drug incorporated. EE decreased at higher drug concentration; this might be due to the dissolved drug in the polymer solution, which had more inclinations to relocate to the surface or close to the surface of nanofiber during electrospinning procedure or it may be because of loss of small part of aggregated drug, which cannot be entrapped into the nanofiber membrane. Further,

entrapment of TNZ into nanofiber membrane depends on the concept of its effective hydrogen bonding with PCL as well as the homogenous mixing of TNZ and CH/PCL in the solvent [Xue et al. 2014c].

5.4.8 *In vitro* release study

In vitro drug release of TNZ from nanofiber membrane and pure drug, suspension was evaluated in McIlvaine buffer (pH 6.6) and release data are shown in Table 5.20 and Results are shown as mean±S.D.; n = 3

Table 5.21.

Table 5.20 *In vitro* drug release data of the optimized TNZ-PCHNF membrane in McIlvaine buffer pH 6.6.

Time (hr)	Cumulative % drug release
1	13.6±4.33
2	17.8±3.67
4	24.5±3.26
6	27.2±3.44
8	31.2±2.77
12	37.7±4.22
24	46.6±4.5
48	54.5±3.24
72	60.9±4.25
96	65.7±3.78
120	69.4±3.25
144	72.2±2.76
168	74.8±3.28
192	78.2±3.28
216	80.7±3.85
240	83.6±2.72
264	86.5±2.64
288	89.3±2.25
312	91.5±4.2
336	93.4±2.78
360	94.3±2.35
384	95.2±2.28
408	96.5±3.24
432	97.4±2.56

Results are shown as mean±S.D.; n = 3

Table 5.21 *In vitro* drug release data of the TNZ suspension in McIlvaine buffer pH 6.6.

Time (hr)	Cumulative % drug release
1	30.5±2.50
2	36.2±5.34
4	53.4±3.25
6	68.2±4.25
8	83.6±3.35
12	94.4±2.45
24	95.46±2.56
48	99.3±3.35

Results are shown as mean±S.D.; n = 3

As illustrated in the Figure 5.45, nanofiber membrane released the drug in a biphasic mode with an initial burst release followed by sustained release. The nanofiber membrane exhibited a significant 31% burst within 8 hr of release whereas almost 90% TNZ release within first 8 hr from TNZ drug suspension. Therefore, TNZ-PCHNF membrane can greatly reduce burst effect and achieve sustained release of TNZ over 18 days. The immediate burst release is contributed by the leaching of free drug particles on the superficial layer of the nanofiber membrane which was in immediate access to the dissolution media. On account of the presence of the bacterial load in the periodontal pockets and to provide immediate effect as well as to achieve MIC, burst release of antibiotics is useful for antimicrobial therapy [Khan et al. 2016b]. Further, drug release mechanism and kinetics were determined by means of substituting the drug release data to the different release kinetic models. The release kinetic data of the optimized batch with r^2 values obtained for different models are represented in Table 5.22.

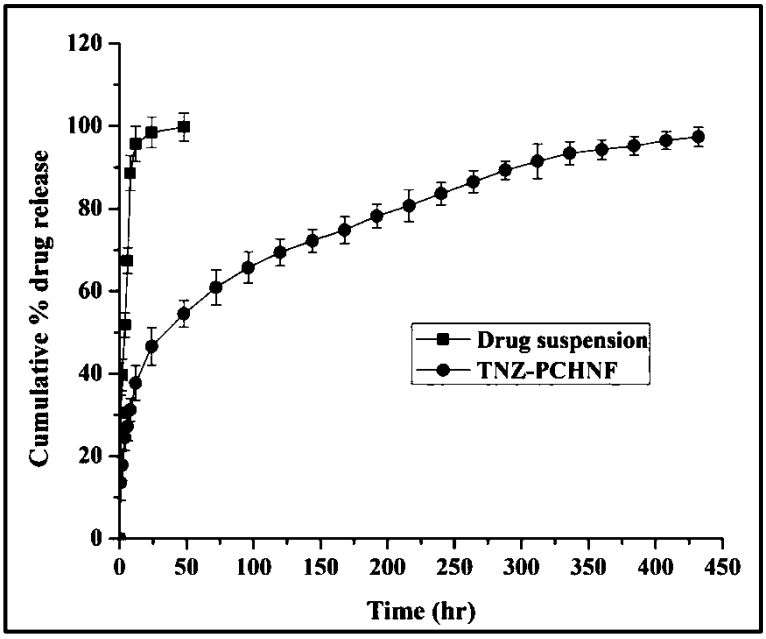

Figure 5.45 *In vitro* drug release profiles of optimized TNZ-PCHNF membrane and drug suspension in McIlvaine buffer pH 6.6 (vertical bars represent the SD, results are shown as mean±S.D.; n = 3).

Table 5.22 Release kinetic modelling for optimized batch of TNZ-PCHNF membrane in McIlvaine buffer pH 6.6

Batch	Zero order	First order	Higuchi model	Korsmeyer-Peppas model
TNZ-PCHNF	$r^2 = 0.828$	$r^2 = 0.422$	$r^2 = 0.959$	$r^2 = 0.991$ $n = 0.309$

The release kinetic modelling confirmed that the drug release pattern from TNZ-PCHNF membrane was best explained by Korsmeyer-Peppas equation with the highest value of linearity ($r^2 > 0.991$) in comparison to other models. Moreover, the diffusion coefficient (n) value for Korsemeyer-Peppas equation for all batches was less than 0.5 which showed drug release from the nanofiber membrane followed the diffusion mechanism [Costa and Lobo 2001].

5.4.9 *In vitro* antibacterial study

In vitro antibacterial activity of electrospun nanofiber membrane was tested using well diffusion method by measuring zone of inhibition against *S. aureus* (MTCC1303). Figure 5.46 shows the result of the antibacterial activity against *S. aureus;* it was

observed that all the drug-loaded nanofiber membrane exhibited a prolonged antibacterial activity over a period of 21 days, whereas placebo membrane showed non-significant antibacterial activity. The mean inhibition zone was found to be 40.20±0.65 mm, 43.5±1.5 mm and 45.4±1.25 mm on the first day for TNZ-PCHNF (10%), TNZ-PCHNF (20%) and TNZ-PCHNF (30%) membrane, respectively. After that, it slowly decreased to 7.3±0.55 mm, 9.25±1.2 mm and 12.5±0.85 mm at the end of 21 days of incubation, which were equivalent to 2.5, 3.0, and 4.25 µg/ml of TNZ. Since the MIC of TNZ against the *S.aureus* was found to be 1.0 µg/ml. Therefore, it can be concluded that TNZ is released from nanofiber membrane uniformly and it is effective against these bacterial strains over 21 days [Kassem et al. 2015]. Furthermore, loading of TNZ into the nanofiber membrane by using electrospinning did not alter the antibacterial activity of the drug.

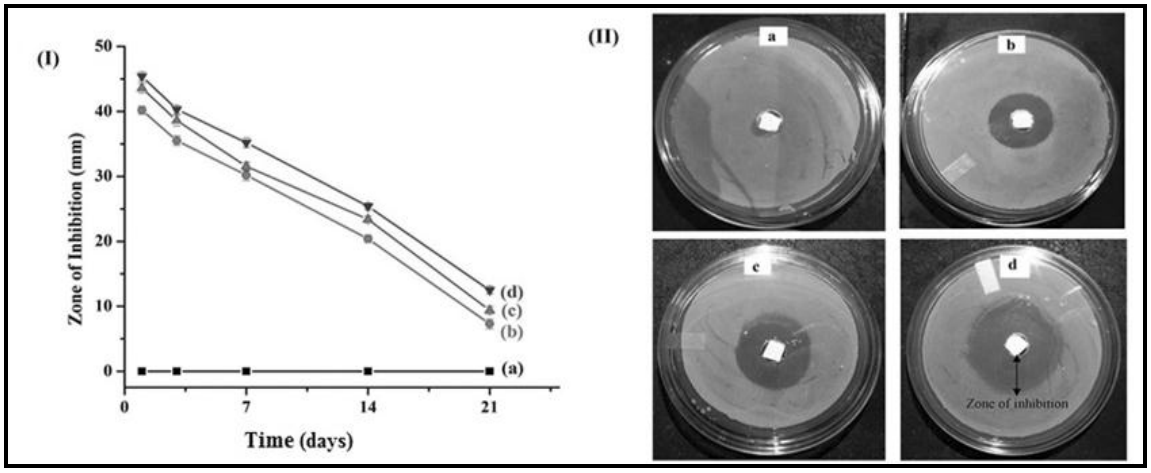

Figure 5.46 (I) Graphical outline representing inhibition zone diameter versus incubation time for TNZ-PCHNF membrane containing different proportion (w/w) of TNZ: (a) 0%; (b) 10% (c) 20% and (d) 30% against *S. aureus*. (II) Inhibition of bacterial growth on agar plate against *S. aureus*. Vertical bars in Figure represents SD, results are shown as mean±S.D. (n = 3).

5.4.10 Cytocompatibility study

Using MTT test, cell viabilities of mouse fibroblast (L-929 cell lines) treated with different aliquots of DMEM taken from media incubated with nanofiber from 1-21 days

was determined by comparing with the number of living cells of a negative control depicted in Figure 5.47(I). It was evident that none of the TNZ-PCHNF membranes impairs cell viability more than 10%, indicated that the DMEM aliquots of nanofiber membrane were not cytotoxic to the cells. Figure 5.47(II) shows images obtained from the microscopic analysis of the L-929 cells that were exposed directly on the surface of the medicated nanofiber membrane with different concentrations of TNZ and coloured with FDA and EtBr. The fibroblasts were observed as green coloured due to staining by FDA and exhibited their specific structures related to the cell motility of fibroblasts-filopodia and lamellipodia [Xue et al. 2014c]. This clearly suggested the cytocompatibility of nanofiber membrane to the cells. From the results, it was concluded that the TNZ-PCHNF membrane would not cause any toxicity to the periodontal tissues during its application. Similar results was also reported by Reise et al. while studying the release of metronidazole from electrospun poly (l-lactide-co-d/l-lactide) nanofiber for the treatment of periodontitis [Reise et al. 2012].

5.4.11 Haemocompatibility of TNZ-PCHNF membrane

Biocompatibility of drug delivery device is essential since some polymer in contact with the tissue from a living body, prompt various critical reactions, such as thrombosis. Along these lines, haemocompatibility of TNZ-PCHNF membrane was assessed by haemolysis method. The haemolysis percentage (HP) denotes the degree of red blood cells broken by the test sample in contact with blood. HP consequences of ACD blood with nanofiber membrane containing a different concentration of TNZ (0%, 10%, 20%, and 30%) are shown in Figure 5.47[III]). Results revealed that the HP was under 3% for nanofiber membrane loaded with 0%,10% and 20% TNZ, demonstrating the good character of anti-haemolysis among all the TNZ-PCHNF membrane [Dey and Ray 2003]. However, TNZ-PCHNF membrane containing 30% drug indicated maximum

HP viz. 4.54±0.43%. This might be ascribed to the expanded surface roughness of TNZ-PCHNF (30%) membrane because of higher concentration of TNZ, so a shear stress prompt the red blood cells crack and bringing about haemolysis when blood contact with the rough surface of materials [Meng et al. 2010].

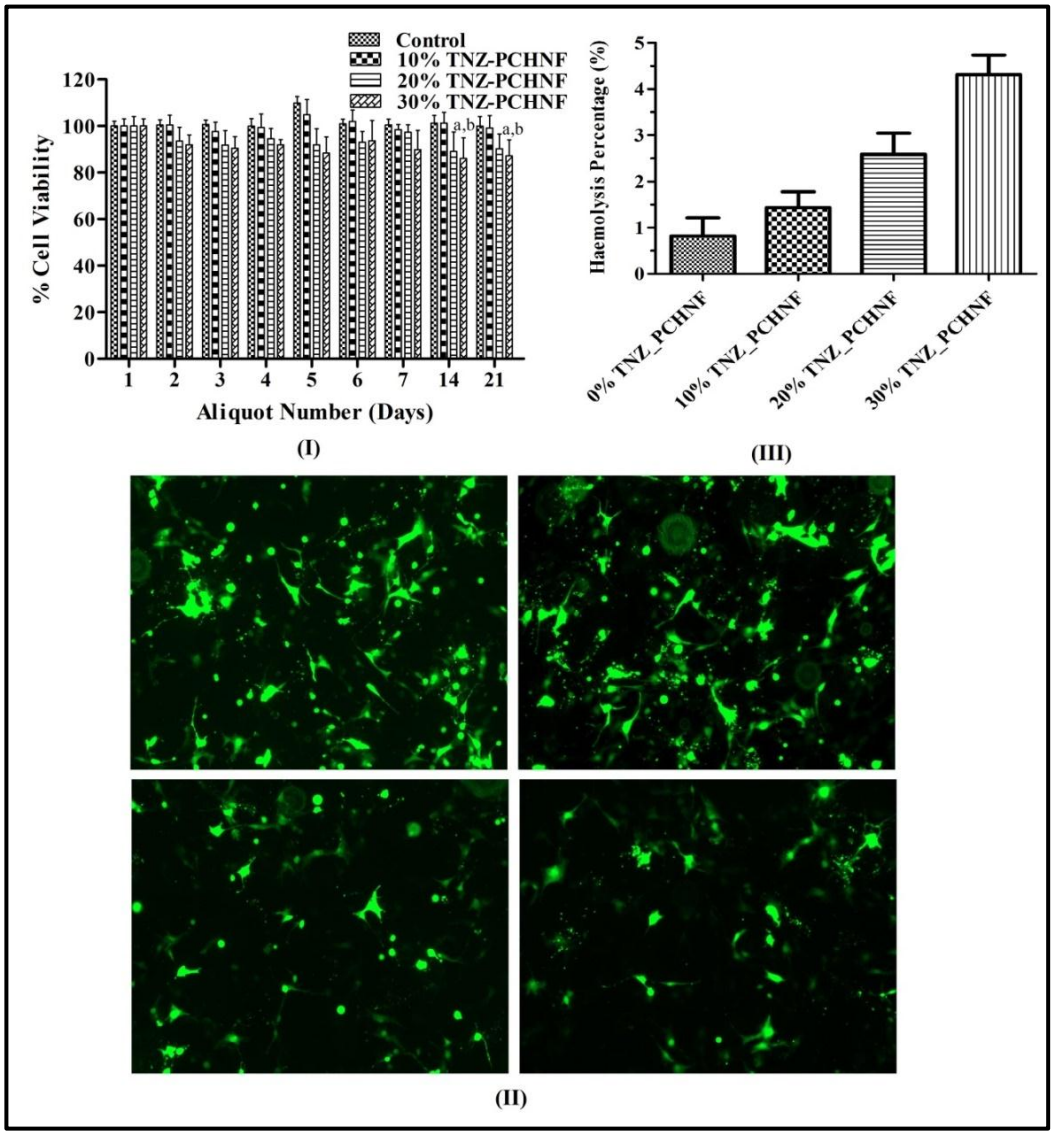

Figure 5.47 (I) Graphics illustrating L-929 cell viability (%), measured by means of MTT assay, after exposure to aliquots of DMEM media. DMEM aliquots were taken from the nanofiber membrane on successive days (1–7) after which for a week (days 14-21). (II) Figure shows cytocompatibility of nanofiber membrane with mouse fibroblasts (L-929 cell lines) after direct exposure to the surface of medicated nanofiber membrane containing different concentration of TNZ: (A) 0%; (B) 10.0%; (C) 20.0%; (D) 30.0%; typical healthy structures are apparent in all cases. (III) Haemolysis percentage of electrospun TNZ-PCHNF membranes containing w/w percentages of TNZ: (a) 0%; (b) 10.0%; (c) 20.0%; (d) 30.0%. Vertical bars in Figure represents SD, results are shown as mean±S.D.; (n = 3).

5.4.12 Storage stability study

The ability of nanofiber membrane to remain stable against environmental changes is of the prime requirement to ensure its final *in vivo* performance. The change in properties of TNZ-PCHNF like diameter and EE during stability study over 6 months at room temperature (30±2 ºC), refrigerated condition (4±1 ºC), and accelerated condition (40±2 ºC/75±5% RH) is depicted in Figure 5.48. There was no any significant noticeable change in the physical appearance (i.e., colour change and change in pH) observed at different environmental condition during the study. Similarly, insignificant ($p > 0.05$) change in the diameter and EE of TNZ-PGHNF was observed during the storage at room temperature (30±2 ºC) and refrigerated condition (4±1 ºC). Whereas, a significant change was observed at accelerated condition (40±2 ºC/75±5% RH) suggesting instability due to biodegradation of polymer which would have expelled the drug molecule from nanofiber hence, it is strongly recommended that the nanofiber membrane should be stored at room temperature (30±2 ºC) as well as refrigerated condition (4±1 ºC), to hold the pharmaceutical properties for safe and effective long-term use.

The shelf-life of optimized nanofiber membrane was found to be 19.79, 18.5 and 10.93 months when stored at refrigeration, room temperature and high-temperature storage, respectively (Figure 5.49). This indicated high stability of nanofiber membrane for a long period especially at refrigerated storage and room temperature.

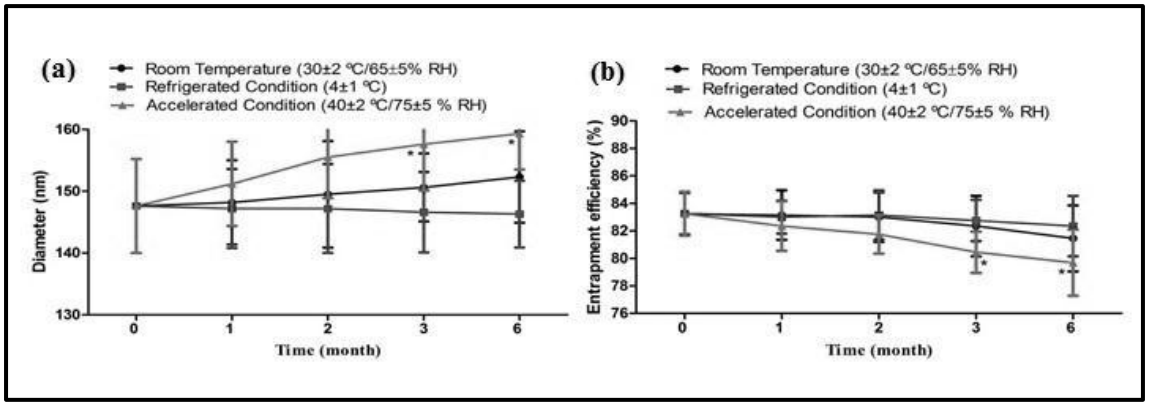

Figure 5.48 Effect on (a) diameter and (b) encapsulation efficiency of TNZ-PCHNF stored at different environmental conditions over different time interval (vertical bars represent±SD; n = 3); *significant values at $p < 0.05$ compared with 0 time (One-way ANOVA; Dunnett's multiple comparison test).

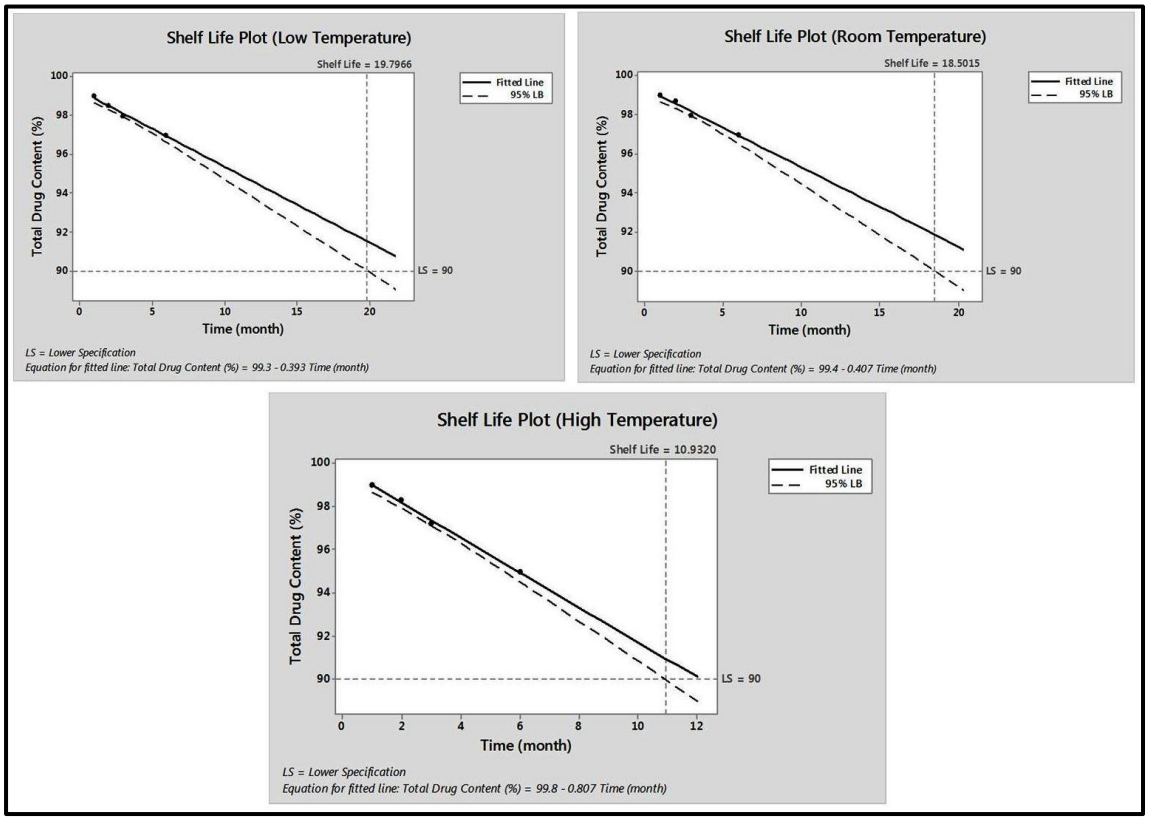

Figure 5.49 Shelf-life plots of optimized batch of TNZ-PCHNF membrane at different storage conditions, viz. Storage 1 (refrigeration), Storage 2 (room temperature) and Storage 3 (high temperature) LS: lower specification (90%).

5.4.13 *In vivo* study

Ligature-induced periodontitis model in rats was employed to study the progression of periodontitis and to evaluate the *in vivo* activity of developed TNZ-PCHNF membrane. Figure 5.50(a) represents the graded response for continuity of epithelium and Figure 5.50(b) represents graded response for continuity of transseptal fibers of the Interdental papilla. A significant improvement in the continuity of the epithelium of the Interdental papilla was observed in the rats of Group C as compared to that of group A and group B ($p < 0.05$). The continuity of epithelium of the Interdental papilla was retained by the rats of Group C, up to a large extent. The response of group B in terms of the continuity of epithelium was non-significant while compared to group A ($p > 0.05$). Moreover, significant improvement was also noticed in the continuity of transseptal fibers of Interdental papilla in group C as compared to group A and group B ($p < 0.05$).

Figure 5.51 depicts the histo-micrograph of the periodontium of rats subjected to ligature-induced periodontitis belonging to different groups. Various parameters such as cementoenamel junction (CEJ)-bone distance, alveolar bone resorption and periodontal ligament degeneration are used to assess periodontitis [Xie et al. 2011]. It can be observed from the Figure 5.51, that different groups exhibit a clear demarcation of degeneration of ligament tissue. It is evident from the histo-micrographs that the group treated with TNZ loaded nanofiber showed minimal degeneration of periodontal ligament and cementoenamel junction (CEJ)-bone distance as compared to that of the group treated with TNZ gel.

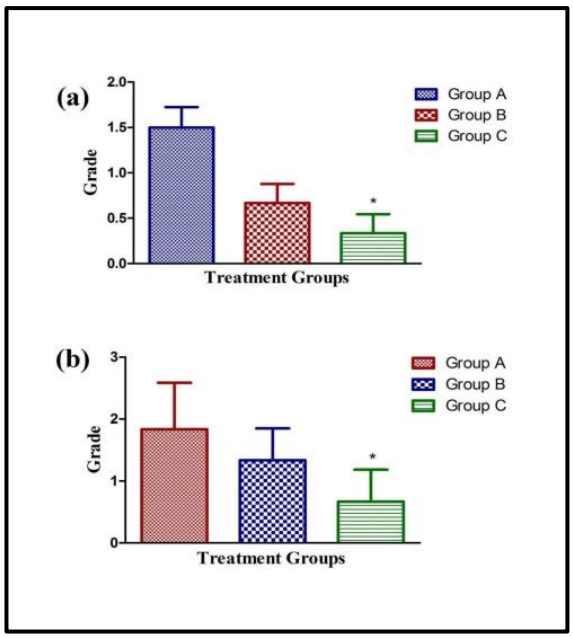

Figure 5.50 Graph represents (a) Graded response for continuity of epithelium in the interdental papilla and (b) Graded response for continuity of transseptal fibers in the interdental papilla. *$p < 0.05$, n.s. = not significant, compared to control group by one-way (ANOVA) followed by Tukey's multiple comparison test, $n = 6$.

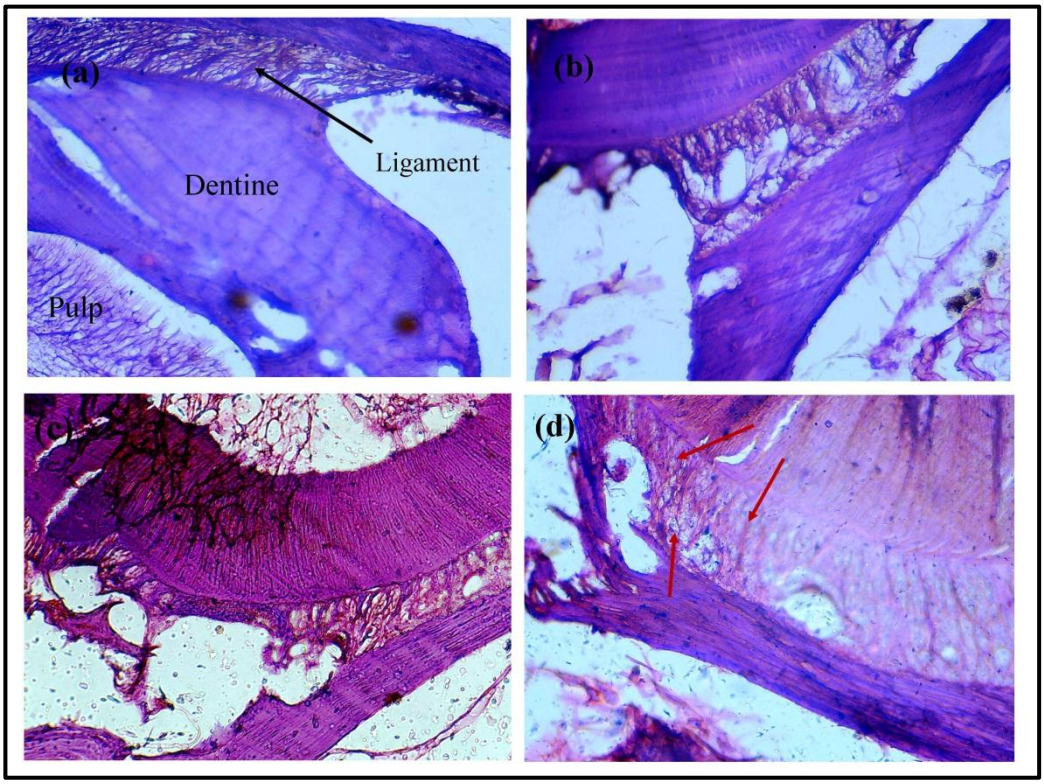

Figure 5.51 Histological results of the periodontium of rats in different treatment groups subjected to ligature-induced periodontitis (a) healthy periodontium (b) periodontitis induced periodontium showing disrupted ligament tissue structure and (c & d) treated with TNZ gel and TNZ-PCH nanofiber membrane respectively, red arrow indicate formation of ligament tissue.

After developing and comparing all three types of nanofiber based drug delivery systems, our results suggest that TNZ-PCHNF has a better potential to deliver TNZ locally into the periodontal pockets, based on homogenous distribution of diameter, hydrophilic nature of nanofiber, entrapment efficiency, mucoadhesive strength and drug release performance further, clinical study was also conducted in patients suffering from periodontitis to assess the efficacy and therapeutic potential.

5.4.14 Clinical study

The preliminary clinical study was conducted to assess the efficacy and therapeutic potential of TNZ-PCHNF membrane in the patients suffering from the periodontitis. Further, its potential was compared with group 1 and group 2 treated with only SRP and SRP+Placebo nanofiber membrane respectively. All treatments were given to the same patient having at least three infected sites to lessen the influence of the risk factors related to the periodontal disease on the outcomes of the treatment provided. The nanofiber membranes were inserted into the periodontal pockets of the patients after SRP, i.e. at the baseline (Figure 5.52). The patients were recalled every week for a check-up during the study period of 8 weeks.

The results of the study showed that the PPD reduction was 1.9±0.52 mm, 2.8±0.69 mm, and 3.6±0.51 mm and gain in CAL was 1.7±0.42 mm, 2.3±0.84 mm, and 3.4±0.42 mm for group-1, group-2 and group-3, respectively. The significant reduction ($p < 0.05$) in the PPD (Figure 5.52) was observed for the drug-treated groups (group-3) from the baseline value compared to group-1. Similarly, CAL also showed significant improvement during the study span (Figure 5.52). Amongst all, group-3 showed significant ($p < 0.05$ and $p < 0.001$) improvement in CAL from fourth week onwards. Furthermore, the reduction in PPD and improvement in CAL for group-3 was higher

than group-2 and group-1 after 8 weeks, which confirms the therapeutic efficacy of medicated nanofiber membrane due to the strong antimicrobial effect of TNZ on the periodontal pathogens as reported earlier in a similar study [Salvi et al. 2002].

The GI which indicates the compliance of the patient towards the periodontal therapy was recorded at the regular predefined interval (Figure 5.52). The GI was found to be 0.8±0.051, 0.4±0.52, and 0.2±0.48 for group-1, group-2 and group-3 respectively at the end of treatment. The reduction in GI values for group-3 was statistically significant from the baseline value as compared to group-1, at second, fourth and eighth week except at the first week. At the end of the study (after eight weeks), group-3 showed a maximum reduction in GI amongst all other treated groups, indicating the regaining of oral hygiene in patients treated with TNZ-PCHNF membrane.

After 8 weeks of study, BoP was found to be 0.6±0.42, 0.3±0.45, and 0.2±0.37 for group-1, group-2 and group-3 respectively. The findings of BoP revealed significant ($p < 0.05$) reduction in the BoP of group-3, from the second week onward compared to group-1(Figure 5.52) which establishes the therapeutic potential of the developed medicated nanofiber membrane.

At the end of the study, it was observed that a significant reduction in PPD, GI, BOP and a significant gain in CAL of periodontal ligament was observed in group-3 patients in comparison to group-1. This consequence may be attributed to the presence of TNZ in the formulation which has strong antimicrobial activity against the periodontal pathogen. Whereas, group-2 also exhibited statistically insignificant improvement in clinical outcomes compared to group-1. The reason for this finding is attributed to the antimicrobial activity of CH against the Porphyromonas gingivalis microorganism, a causative agent in the progression of periodontal tissue destruction in chronic

periodontitis [Ikinci et al. 2002]. Furthermore, the obtained results showed that the treatment period had a significant effect on the mean values of the tested clinical parameters for the treated group from the baseline.

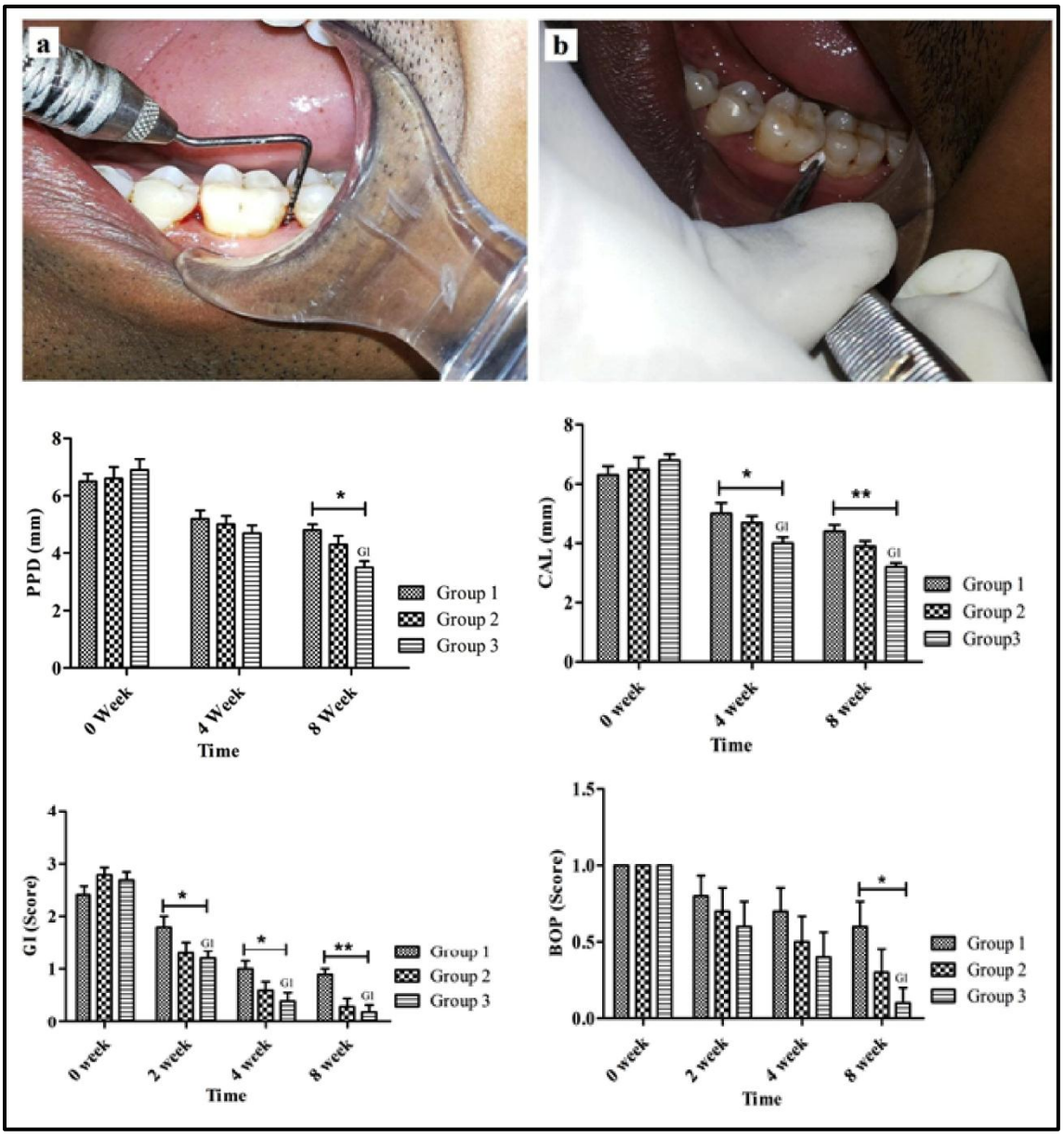

Figure 5.52 Image illustrating (a) pocket depth measurement (b) placement of nanofiber membrane and results of clinical evaluation of following clinical markers obtained after 8 weeks. (c) Probing pocket depth (PPD), (d) Clinical attachment level (CAL), (e) Score of gingival index (GI) and (f) Score of bleeding on probing (BOP). *$p < 0.05$, and **$p < 0.01$ compared to group 1 by two-way (ANOVA) followed by Bonferroni post-tests, (vertical bars represent the SEM, results are shown as mean±SEM.; $n = 10$).

From the clinical study, therefore it could be concluded that the nanofiber membranes were well tolerated, without showing any sign of irritation at the place of treatment. Although the traditional technique, SRP, applied for the treatment of periodontitis is effective as being previously reported but group-3 treated with SRP along with the medicated nanofiber membrane confirmed significant improvement compared to the group-1 treated with SRP alone [Cobb 1996].